

(2)

# AIR DEFENSE INITIATIVE
# AIR-TO-AIR ENGAGEMENT ANALYSIS

## VOLUME 2: ERROR MODELS AND SIMULATION FOR CASE I: PRE-LAUNCH COORDINATION WITHOUT POST-LAUNCH UPDATES

8 March 1991

Ac

**Synetics**



Synetics

TR-535-2

# AIR DEFENSE INITIATIVE
# AIR-TO-AIR ENGAGEMENT ANALYSIS

## VOLUME 2: ERROR MODELS AND SIMULATION FOR CASE I: PRE-LAUNCH COORDINATION WITHOUT POST-LAUNCH UPDATES

**8 March 1991**

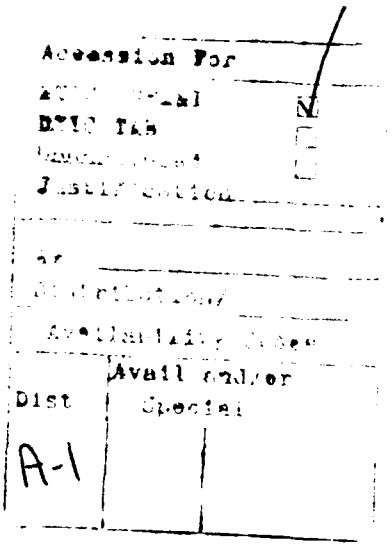


**Covering the period:**

**31 January 1990 - 8 March 1991**

**Prepared under Contract No. DCA100-90-C-0031**
**for the Defense Communications Agency**

**Prepared by:**

**Jorge I. Galdos**

540 Edgewater Drive • Wakefield, MA 01880 • (617) 245-9090 • Fax (617) 245-6311

# REPORT DOCUMENTATION PAGE

Form Approved
OMB No. 0704-0188



| 1. AGENCY USE ONLY (Leave blank) | 2. REPORT DATE | 3. REPORT TYPE AND DATES COVERED |
|---|---|---|
| | 8 March 1991 | Final 31 Jan 90 - 8 March 91 |

**4. TITLE AND SUBTITLE**
Air Defense Initiative Air-to-Air Engagement Analysis
Volume 2: Error Models and Simulation for Case I:
Pre-Launch Coordination without Post-Launch Upates

**5. FUNDING NUMBERS**
(C) DCA100-90-C-0031

**6. AUTHOR(S)**
Jorge I. Galdos

**7. PERFORMING ORGANIZATION NAME(S) AND ADDRESS(ES)**
*SYNETICS* Corporation
540 Edgewater Drive
Wakefield, MA 01880

**8. PERFORMING ORGANIZATION REPORT NUMBER**
TR-535-2

**9. SPONSORING / MONITORING AGENCY NAME(S) AND ADDRESS(ES)**
JDSSC/JNSV
Defense Communications Agency
Washington, DC 20305-2000

**10. SPONSORING / MONITORING AGENCY REPORT NUMBER**

**11. SUPPLEMENTARY NOTES**
This is volume two of a three volume final report

**12a. DISTRIBUTION / AVAILABILITY STATEMENT**
Unclassified/Unlimited

**12b. DISTRIBUTION CODE**

**13. ABSTRACT** (Maximum 200 words)

This report formulates an error model for analyzing a cooperative engagement cruise missile defense scenario in which a surveillance platform transmits the location of a target to an air interceptor missile only once, just prior to launch. Included in this model is a description of the three relevant inertial navigation systems (aboard the surveillance platform, the launch platform, and the missile), the guidance system of the missile, the surveillance platform radar, and the motion of the target. Detailed equations for each of these components are provided along with numerical values for the error parameters assumed for the various instruments.

**14. SUBJECT TERMS**
Cooperative Engagement; Modelling
Inertial Navigation System; Simulation

**15. NUMBER OF PAGES**
118

**16. PRICE CODE**

| 17. SECURITY CLASSIFICATION OF REPORT | 18. SECURITY CLASSIFICATION OF THIS PAGE | 19. SECURITY CLASSIFICATION OF ABSTRACT | 20. LIMITATION OF ABSTRACT |
|---|---|---|---|
| UNCLASSIFIED | UNCLASSIFIED | UNCLASSIFIED | UL |

# ACKNOWLEDGEMENT

This report was prepared under the direction of the Deputy Director, NMCS ADP by *SYNETICS* Corporation under Contract Number DCA100-90-C-0031 to the Defense Communications Agency.

(This page is intentionally left blank)

## ABSTRACT

This report formulates an error model for analyzing a cooperative engagement cruise missile defense scenario in which a surveillance platform transmits the location of a target to an air interceptor missile only once, just prior to launch. Included in this model is a description of the three relevant inertial navigation systems (aboard the surveillance platform, the launch platform, and the missile), the guidance system of the missile, the surveillance platform radar, and the motion of the target. Detailed equations for each of these components are provided along with numerical values for the error parameters assumed for the various instruments.

This report is the second volume of the final report of an analysis of the effectiveness of a U.S. interceptor long-range defense force to defend against the cruise missile threat in the 2005 time frame, conducted by *SYNETICS* Corporation, and its subcontractors, Vitro Corporation and Veda Inc., under Contract Number DCA100-90-C-0031 with the Defense Communications Agency. Contract effort focused on two related issues: formulation of the problem to permit examination of advanced surveillance and communication technology potentially defining a "cooperative engagement" concept, and a bottoms-up approach to detailed modeling of the current and emerging generation of air-to-air missiles.

The other volumes of this report include:

**Volume I:** Problem Definition, Solution Formulation, Illustrative Results and Recommendations

**Volume II:** Error Models and Simulation Formulation for Case I: Pre-Launch Coordination without Post-Launch Updates

**Volume III:** Simulation Tools: Current Status and Recommendations for Future Development.

(This page is intentionally left blank)

# Contents

# List of Figures

(This page is intentionally left blank)

# List of Tables

# Chapter 1

# INTRODUCTION

## 1.1 Background

This memo contains a description of the error models developed for Case I of an engagement involving four entities:

- A Target, abbreviated by "T"
- A Missile, abbreviated by "M"
- A Surveillance Platform, abbreviated by "SP"
- A Launch Platform, abbreviated by "LP".

Case I, illustrated in Figure 1.1, represents the simplest cooperative engagement scenario under consideration: the SP transmits the location of T to M only once, just prior to launch. This scenario is advantageous because after launch the SP can devote its resources to tracking other targets and also because communications equipment aboard M is unnecessary resulting in a lighter and less expensive M.

Other scenarios under consideration are:

- Case II: During flyout the SP tracks T and transmits the location estimates to M (possibly through the LP). This case requires M to have a receiver and additional data processing equipment.
- Case III: Same as Case II but in addition the SP tracks M. This case requires M to have a transponder.
- Case IV: Tracking with more than one SP operating in a multistatic mode. This configuration is particularly effective for detecting and tracking low-observable targets ([Foster, 1987]).

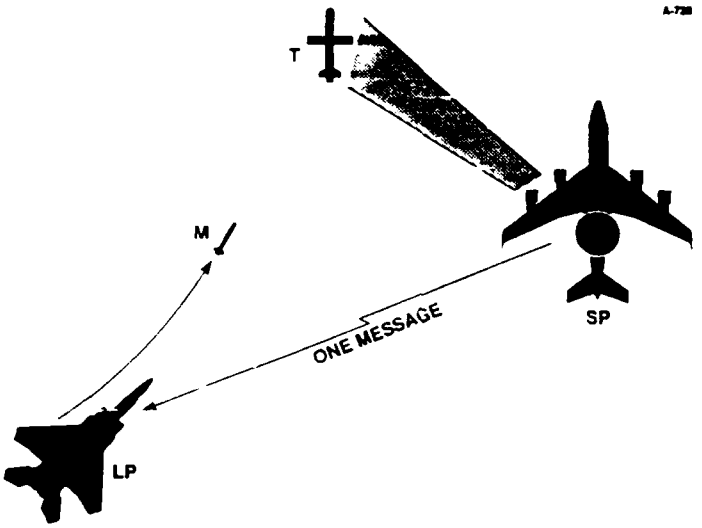


Figure 1.1: Case 1 Scenario

## 1.2 Organization

This memo is organized into three parts:

- The first part is a description of the top-level of a simulation that implements the pre-launch to handover error model. This part is contained in Section 2.
- The second part describes each of the components of the top-level model at a qualitative (without equations) level. This part is contained in Section 3.
- The third part provides detailed equations for each of the components described in Section 3 including numerical values for the errors of the assumed instruments. This part is contained in Appendix A (which makes reference to derivations contained in Appendix B).

# Chapter 2

# TOP-LEVEL MODEL

## 2.1 Model Objective

The objective of the model developed herein is to compute four quantities:

- M mean position and velocity at handover
- T mean position and velocity at handover
- M position and velocity covariance at handover
- T position and velocity covariance at handover .

The model is a *linearized* model suitable for analysis with a covariance simulation ([Gelb, 1974]).

The procedure followed by the model is as summarized in Figure 2.1:

1. The mean and covariance of the estimated T location (position and velocity) at launch is computed based on the measurements provided by the radar and INS of the SP
2. The mean and covariance of the predicted T location at handover is computed. A sample of this prediction is illustrated by the straight-line in the figure
3. The mean and covariance of the estimated M location at launch is computed
4. From items **2** and **3** an acceleration command for the M is computed so that an intercept would result in the absence of errors. In the figure, an (erroneous) predicted M trajectory is illustrated by a solid curve, whereas the resulting M trajectory is illustrated by a dashed curve
5. From item **4**, the mean and covariance of the M location at handover is computed
6. Finally, the mean and covariance of the T location at handover is computed.

This sequence of steps can be divided into three top-level steps: the first two steps are pre-launch initializations while the third step simulates the launch to handover flight. These three steps are described in the subsections that follow.

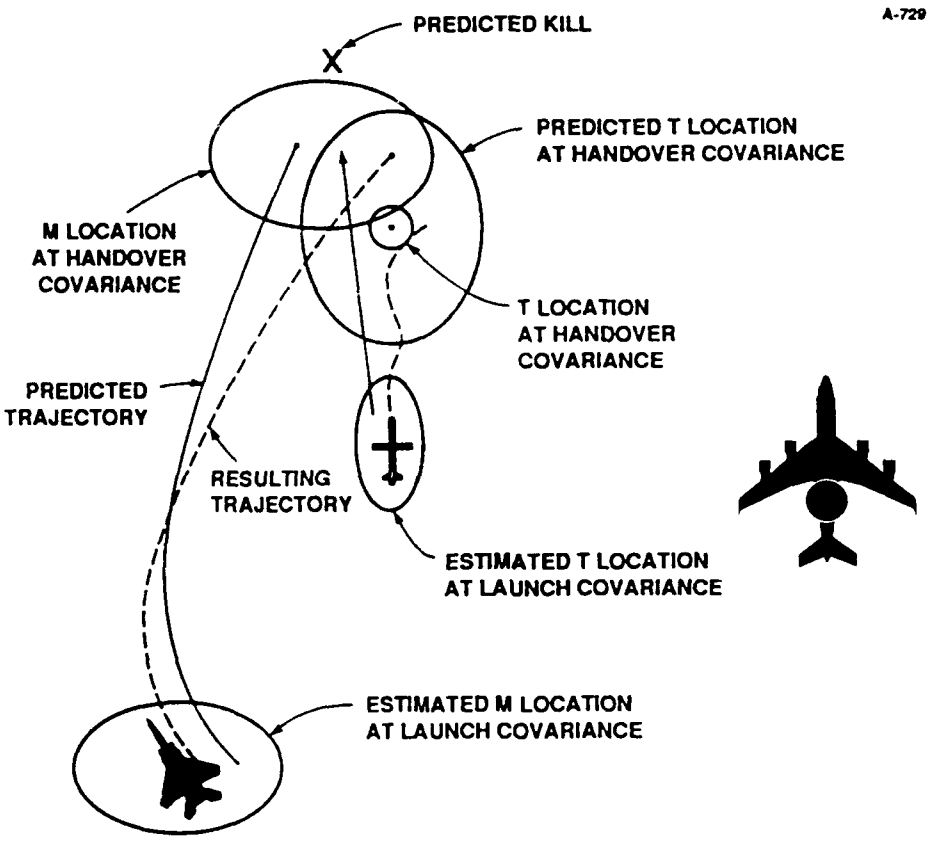


Figure 2.1: Procedure Overview

## 2.2 Step 1: Compute T Location Covariance

Assumptions:

- The SP has a "better quality" platform INS ("better" meaning better than 1 nm/hr) which undergoes a ground align procedure prior to takeoff
- The SP has a radar that measures range, azimuth, elevation, and range-rate
- The SP is travelling in a constant velocity trajectory
- The T is also travelling in a constant velocity trajectory just prior to launch.

Inputs:

- SP nominal (deterministic) position and velocity at launch
- T nominal position and velocity at launch
- RCS of T
- Error model for the INS of the SP
- Error model for the radar of the SP.

Outputs: The output of Step 1 is the error covariance matrix of the target's position and velocity at the moment of launch. This covariance matrix is computed based on the geometry of the engagement and the error models for the INS and the radar of the SP.

Sequence of events within Step 1: Figure 2.2 summarizes the following sequence of events:

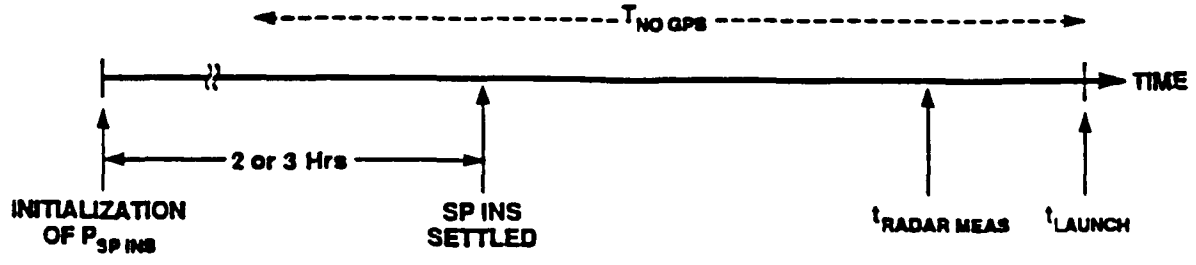


Figure 2.2: Step 1 Timeline

1. Set $P_{\text{SP INS}}$ to a diagonal matrix. $P_{\text{SP INS}}$ is the covariance matrix of a local-level INS (9 states plus error sources).

2. Simulate a ground-align procedure by solving the Riccatti equation for $P_{\text{SP INS}}$ with measurements of position, velocity, and heading as specified in the ground-align model. Ground align lasts for 10 min.

3. Propagate $P_{\text{SP INS}}$ for 2 or 3 hours by solving the Riccatti equation assuming GPS fixes every 10 sec until time $t_{\text{LAUNCH}} - T_{\text{NO GPS}}$, where $T_{\text{NO GPS}}$ is the interval of time prior to launch during which GPS is assumed to be unavailable (possibly $T_{\text{NO GPS}} = 0$).

4. If $T_{\text{NO GPS}} \neq 0$, propagate $P_{\text{SP INS}}$ to $t_{\text{LAUNCH}}$ without GPS fixes.

5. Set the tracking filter covariance matrix, $P_{\text{SP TRACK}}(t^-_{\text{RADAR MEAS}})$ equal to a block-diagonal matrix with two blocks: $P_{\text{SP INS}}(t^-_{\text{RADAR MEAS}})$ and $P_{\text{TARGET}}(t^-_{\text{RADAR MEAS}})$ where $t_{\text{RADAR MEAS}} \triangleq t_{\text{LAUNCH}} - \delta$, with $\delta$ a small number, is the time at which the radar measurement is taken just prior to launch. $P_{\text{TARGET}}(t^-_{\text{RADAR MEAS}})$ is set to a large diagonal matrix.

6. Perform one optimal update on $P_{\text{SP TRACK}}$ modeling one radar measurement (which may represent several measurements). Alternatively, tracking over a period of time may be modeled by performing a number of optimal propagates and updates.

7. Do a $CPC^T$ transformation on $P_{\text{SP TRACK}}$ to obtain the covariance matrix of the target position and velocity at launch, $P_{\text{TARGET}}(t^-_{\text{LAUNCH}})$.

Model Components: Step 1 requires three component error models:

- SP INS[1] model (described in Subsection 3.8)
- Ground align model (described in Subsection 3.5)
- T motion model (described in Subsection 3.1)
- SP radar measurement model (described in Subsection 3.9).

## 2.3 Step 2: Initialization of the M INS

Assumptions: The LP is assumed to have a 1 nm/hr strapdown INS and the M is assumed to have also a strapdown INS of somewhat worse quality.

Inputs:

- LP nominal (deterministic) trajectory prior to launch
- Error models for the INS of the LP

[1] A full-order model is used for the INS in this step because (1) the covariance is propagated for many Schuler periods and (2) the step is run by itself so that plenty of RAM is available.

- Error models for the INS of the M
- Separation (lever arm) between the LP and M INS.

Outputs: The output of Step 2 is the error covariance matrix of the M INS model at the time of launch. This covariance matrix is computed based on the error models for (1) the INS of the LP and (2) the INS of the M.

Sequence of Steps within Step 2: The objective of Step 2 is to simulate a transfer alignment of the M INS. This simulation requires the simultaneous propagation prior to launch of (1) the INS aboard the LP and (2) the INS aboard the M.

The propagation of the INS aboard the LP proceeds as summarized by the timeline shown in Figure 2.3:

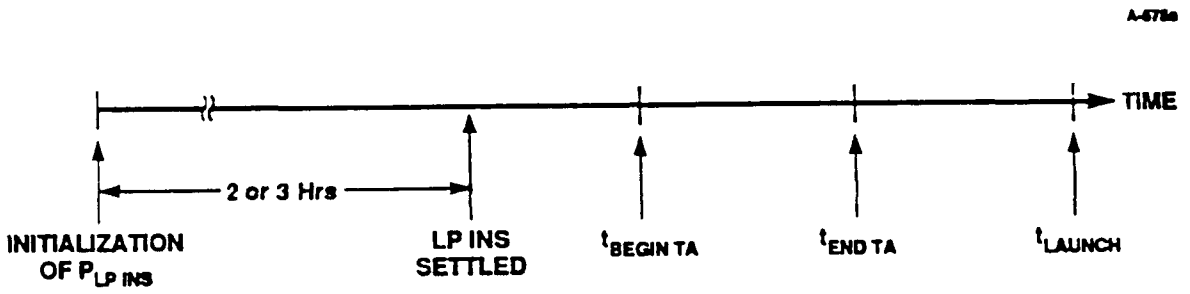


Figure 2.3: Step 2 Timeline

1. Set $P_{\text{LP INS}}$ to a diagonal matrix. $P_{\text{LP INS}}$ is the covariance matrix of a strapdown INS (9 states plus error sources).
2. Simulate a ground-align procedure by solving the Riccatti equation for $P_{\text{LP INS}}$ with measurements of position, velocity, and heading as specified in the ground-align model. Ground align lasts for 10 min.
3. Propagate $P_{\text{LP INS}}$ for 2 or 3 hours by solving the Riccatti equation assuming GPS fixes every 10 sec up until time $t_{\text{LAUNCH}} - T_{\text{NO GPS}}$. This propagation depends on the trajectory assumed for the LP as discussed below.
4. If $T_{\text{NO GPS}} \neq 0$, propagate $P_{\text{LP INS}}$ to $t_{\text{LAUNCH}}$ without GPS fixes.

The timeline for the propagation of the INS aboard the M, also summarized in Figure 2.3, proceeds as follows:

1. Set $P_{\text{M INS}}$ to a diagonal matrix and simulate a ground-align analogous to that of the SP and LP. $P_{\text{M INS}}$ is the covariance matrix of a strapdown INS (9 states plus error sources).

2. Propagate $P_{\text{M INS}}$ open-loop for 2 or 3 hours until the INS settles

3. Perform the transfer alignment during the interval $t_{\text{BEGIN TA}} \leq t \leq t_{\text{END TA}}$. During this interval:

   - The LP performs an S-maneuver
   - The Riccatti equation for the covariance of the concatenated M INS state and LP INS state is propagated with measurement of the difference in the output of the measurements provided by both INSs (taking into account the lever arm effect).

4. Set $P_{\text{M INS}}(t_{\text{END TA}})$ to the final covariance matrix computed from the Riccatti equation.

5. Propagate $P_{\text{M INS}}$ open-loop to $t_{\text{LAUNCH}}$. Note that the beneficial effect of the transfer alignment is diminished if the M in question is launched a long time after the transfer alignment (i.e., the length of the time interval $t_{\text{LAUNCH}} - t_{\text{END TA}}$ is a parameter of the engagement).

6. Initialize the covariance matrix for the M INS.[2]

Model Components: Step 2 requires three component error models:

- LP INS, model (described in Subsection 3.11)
- M INS, model (described in Subsection 3.4)
- LP deterministic trajectory model (described in Subsection 3.3).

## 2.4 Step 3: Launch to Handover Simulation

Assumptions:

- The transfer function of the M autopilot has no lags

Inputs:

- Acquisition range of M seeker (determines when the flyout ends)
- Parameters for the random T motion Singer model
- Parameters for the random M motion Singer model

[2]Instead of a full-order covariance, a reduced-order covariance can be used if necessary to accommodate the DOS 640K RAM limit. The reduced-order covariance can be then propagated during flyout using a reduced-order model for the M INS.

- Error models for the M INS
- T and M nominal (deterministic) position and velocity at launch
- Covariance of T location at launch (from Step 1)
- Covariance of M INS model at launch (from Step 2)

Outputs: The output of Step 3 is the mean and covariance of the M and T position and velocity at the end of flyout.

Sequence of Steps within Step 3: The following two steps are executed:

1. Compute mean and covariance of M-acceleration command. The acceleration command is computed from the (erroneous) position and velocity estimates of M and T so that an intercept is produced if (1) M and T do not maneuver during the endgame and (2) all estimates are error-free.
2. Propagate:
   - T position and velocity (from the Singer model and the nominal trajectory)
   - M INS (from the INS model and the mean acceleration command)
   - M position and velocity (from the Singer model and the commanded acceleration vector pointed in the erroneous direction indicated by the M INS).

This procedure is summarized in Figure 2.4.

Model Components: Step 3 requires four component error models:

- T random motion (Singer) model (described in Subsection 3.1)
- M random motion (Singer) model (described in Subsection 3.2)
- M INS model (described in Subsection 3.4)
- M mid-course guidance model (described in Subsection 3.7).

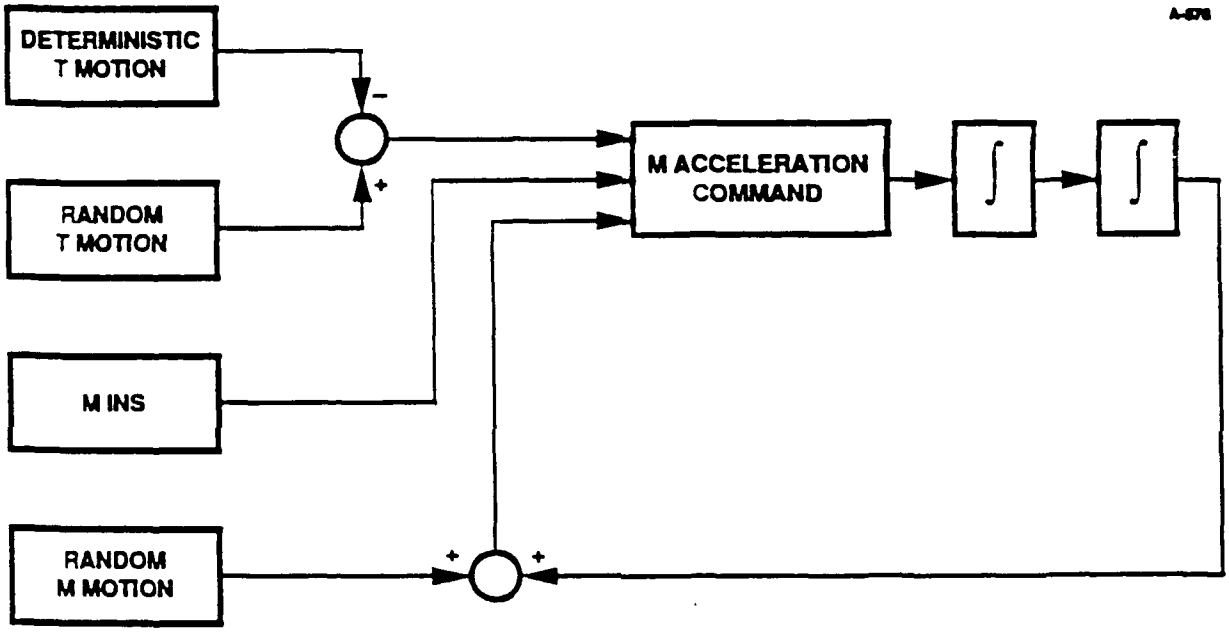


Figure 2.4: Step 3 Block Diagram

# Chapter 3

# COMPONENT MODELS

This section provides an overview of the thirteen component models required in the simulation of Case I:

- T:
  - T motion model (Subsection 3.1)
- M:
  - M random motion model (Subsection 3.2)
  - M INS model (Subsection 3.4)
  - M ground align (Subsection 3.5)
  - M transfer align (Subsection 3.6)
  - M mid-course guidance model (Subsection 3.7)
- SP:
  - SP INS model (Subsection 3.8)
  - SP ground align (Subsection 3.5)
  - SP radar model (Subsection 3.9)
  - SP tracking filter model (Subsection 3.10)
- LP:
  - LP deterministic trajectory model (Subsection 3.3)
  - LP INS model (Subsection 3.11)
  - LP ground align (Subsection 3.5)

## 3.1 T Motion Model

The T motion model is composed of two components: a nominal (deterministic) trajectory which is an input to the simulation; and a random component which models small deviations from the nominal trajectory. The deviations of the random component are a result of wind, turbulence, and random motion introduced by the guidance mechanism of the T. These random deviations are unpredictable and consequently contribute to the miss distance.

The random component is modeled by a Singer model ([Singer, 1969]). The Singer equations characterize acceleration as a band-limited random process with the bandwidth and power based on the anticipated motion of the target. The state variables of the Singer model are listed in Table 3.1 (position, velocity, and acceleration along the $x$-, $y$-, and $z$-axes). Subsection A.1 of Appendix A gives the detailed equations for the Singer model as well as the equations used in computing the power of the acceleration process.

Table 3.1: STATE VARIABLES OF TARGET MOTION MODEL

| SYMBOL | DEFINITION |
|---|---|
| $p_{Tx}$ | $x$-position |
| $v_{Tx}$ | $x$-velocity |
| $a_{Tx}$ | $x$-acceleration |
| $p_{Ty}$ | $y$-position |
| $v_{Ty}$ | $y$-velocity |
| $a_{Ty}$ | $y$-acceleration |
| $p_{Tz}$ | $z$-position |
| $v_{Tz}$ | $z$-velocity |
| $a_{Tz}$ | $z$-acceleration |

## 3.2 M Random Motion Model

M motion is the sum of two components: motion resulting from the guidance command (considered in Subsection 3.7); and an uncontrollable perturbation resulting from random effects analogous to those in the T Motion Model. Both of these components affect miss distance.

The uncontrollable perturbations are modeled by a Singer models with state variables as listed in Table 3.2. The equations describing this model are addressed in Subsection A.2 of Appendix A.

## 3.3 LP Deterministic Trajectory Model

The LP is assumed to follow a deterministic trajectory which affects the geometry of the engagement. The detailed shape of this trajectory is also important because the error statistics of the LP INS and the M INS prior to launch are a function of the acceleration and angular rates (produced by roll, pitch, and yaw motions) experienced by the LP.

Table 3.2: STATE VARIABLES OF MISSILE MOTION MODEL

| SYMBOL | DEFINITION |
|---|---|
| $p_{Mx}$ | $x$-position |
| $v_{Mx}$ | $x$-velocity |
| $a_{Mx}$ | $x$-acceleration |
| $p_{My}$ | $y$-position |
| $v_{My}$ | $y$-velocity |
| $a_{My}$ | $y$-acceleration |
| $p_{Mz}$ | $z$-position |
| $v_{Mz}$ | $z$-velocity |
| $a_{Mz}$ | $z$-acceleration |

The motion of the LP is assumed to be a sequence of events chosen from the following menu:

- Level flight at constant velocity
- Right-turn / Left-turn to a given heading
- Climb to a given altitude
- Descent to a given altitude
- Speed-up along a constant altitude
- Azimuth change while on the ground.

For each of these events, the variables listed in Table 3.3 are computed. These variables specify the relevant aspects of the motion of the LP (and the M) from the time of ground align, prior to take-off, to the time of M launch

A detailed description of the LP motion events and the algorithms required for the computation of the motion variables is provided in Section A.3 of Appendix A.

## 3.4 M INS Model

The M is assumed to have a strapdown INS. The INS errors are characterized by a state vector having six groups of entries as shown in Table 3.4:

- Errors in attitude (body to local-level angles)
- Errors in latitude, longitude, and altitude rates
- Errors in latitude, longitude, and altitude
- Gyro drift rate errors
- Accelerometer errors

Table 3.3: LP DETERMINISTIC TRAJECTORY MOTION VARIABLES

| MOTION VARIABLE | RELATIVE TO | REQUIRED FOR: |
|---|---|---|
| Position | Rotating Earth | • Trajectory specification |
| Velocity | // | • Guidance computations |
| Acceleration | // | |
| Acceleration | Inertial space | • INS error dynamics |
| | | • Accelerometer scale factor errors |
| Latitude | The Equator | • INS error dynamics |
| Longitude | Vernal Equinox | |
| Longitude | Greenwich | |
| Altitude | Reference Ellipsoid | |
| Lat., Lon., Alt. rates | — | |
| Lat., Lon. accelerations | — | |
| Bank angle | — | • INS error dynamics |
| Elevation angle | — | |
| Azimuth | — | |
| Roll rate | Inertial space | • Gyro scale factor errors |
| Pitch rate | // | • Transfer alignment model |
| Yaw rate | // | |

- Altimeter errors.

The state equations for these errors are provided in Subsection A.4 of Appendix A.

[INS Reduced-Order Model] Because flyout lasts for only a few minutes, the error equations given in the previous subsection can be approximated by a reduced-order model. This model approximates the error by polynomials in time with coefficients determined by error source models valid over short time intervals. Different polynomials are used for different trajectory segments.

Currently a reduced-order model appears to be unnecessary because a suitable software development environment which bypasses the DOS 640K RAM limit is available. Consequently a more detailed description of this model is not provided.

## 3.5 M, LP, and SP Ground Align Model

The ground align procedure has three objectives: to level, align, and calibrate the INS. The first two objectives determine the relationship between the platform frame and the frame where navigation computations (double integration of acceleration) are performed. For an INS with a local-level platform (such as that of the SP), leveling involves orienting the platform so that it is perpendicular to the gravity vector (North and East accelerometers read zero) and rotating the platform until it points North (gyrocompassing, [Farrell, 1976]). For a strapdown INS (such as those of the M and LP), leveling and alignment is implemented within the computer by initializing estimates of the INS state and associated transformations ([Farrell, 1976]).

The third objective of the ground align procedure is to calibrate (estimate) the gyro and accelerometer bias. This bias is often called the "repeatability" or "turn-on" bias

Table 3.4: STATE VARIABLES OF M INS MODEL

| SYMBOL | DEFINITION |
|---|---|
| $\delta\theta_{MN}$ | Attitude Error About N Axis |
| $\delta\theta_{ME}$ | Attitude Error About E Axis |
| $\delta\theta_{MD}$ | Attitude Error About D Axis |
| $\delta\dot{L}_M$ | Latitude Rate Error |
| $\delta\dot{\ell}_M$ | Longitude Rate Error |
| $\delta\dot{h}_M$ | Altitude Rate Error |
| $\delta L_M$ | Latitude Error |
| $\delta\ell_M$ | Longitude Error |
| $\delta h_M$ | Altitude Error |
| $\underline{\varepsilon}_M$ | Gyro Error Source Vector |
| $\underline{\alpha}_M$ | Accelerometer Error Source Vector |
| $\delta h_{MA}$ | Altimeter Error |

because a different value is obtained every time the INS is activated.

The ground align procedure is modeled here by assuming an initial covariance matrix for the INS state and simulating Kalman filter updates derived from position, velocity, and magnetic heading measurements on a stationary aircraft. Details of the ground align model are provided in Subsection A.7 of Appendix A.

## 3.6 M Transfer Align Model

The objective of the transfer-align procedure is to calibrate (i.e., estimate and correct) errors in the M INS by comparing its read-out with that of the more accurate LP INS. The errors that are calibrated fall into two categories: (1) instrument errors (specifically gyro and accelerometer errors); and (2) system errors (specifically errors in the M INS estimates of where the North and Down directions are). This procedure is performed in-flight and as near to the time of launch as possible because the beneficial effect of the transfer-alignment (the reduction of the error covariance of the state of the M INS) decays with time. Details of the transfer-align model are provided in Subsection A.8

## 3.7 M Mid-Course Guidance Model

The guidance model describes the propagation of errors through three cascaded "maps" (indicated by "$\longrightarrow$"):

1. Current estimated position and velocity of M and T $\longrightarrow$ Commanded (computed) acceleration. This map is the "guidance law."

2. Commanded acceleration $\longrightarrow$ Resulting M acceleration. This map, which models the autopilot, includes the effect of the misalignment of the M INS.

3. Resulting M acceleration $\longrightarrow$ Resulting M velocity $\longrightarrow$ Resulting M position. This map is modeled by two integrations which represent Newton's second law.

The state variables of the M Mid-Course Guidance Model are listed in Table 3.5. The table shows five groups of variables:

- The state error vector of the M INS, $\underline{x}_M$
- Errors in the position and velocity read-out of the M INS (computed from $\underline{x}_M$)
- Errors in the position and velocity estimates of the T position (computed from the tracking filter model discussed in Section 3.10)
- Errors in the computed guidance quantities (accelerations and duration of applied accelerations) due to the preceding two groups (i.e., due to $\delta p_M^t$, $\delta v_M^t$, $\delta p_T^t$, and $\delta v_T^t$)
- Errors in the resulting M acceleration arising from the misorientation of the M INS (computed from $\underline{x}_M$).

State equations for these errors are provided in Subsection A.9 of Appendix A.

Table 3.5: STATE VARIABLES OF MISSILE MID-COURSE GUIDANCE MODEL, $\underline{x}_G$

| SYMBOL[1] | DEFINITION |
|---|---|
| $\underline{x}_M$ | M INS state error vector (Table 3.4) |
| $\delta p_M^t$<br>$\delta v_M^t$ | Error in M INS position read-out<br>Error in M INS velocity read-out |
| $\delta p_T^t$<br>$\delta v_T^t$ | Error in T position estimate from the SP tracking filter<br>Error in T velocity estimate from the SP tracking filter |
| $\delta \tau_{a,c}$<br>$\delta \bar{a}_{l,c}$<br>$\delta a_{z,c}$ | Error in the computed duration of applied acceleration<br>Error in the computed level (North/East) acceleration<br>Error in the computed vertical (down) acceleration |
| $\underline{x}_d$ | Error produced by the drift of the M INS during flyout |

[1]The subscript $t$ indicates that the vector is expressed in the *tangential* frame define on page 24.

## 3.8 SP INS Model

The SP INS model differs in two respects from the M INS model described in Subsection 3.4:

- A local-level platform INS is modeled instead of a strapdown INS
- The quality of the instruments is superior to those of the M INS.

Both of these factor affect only the forcing function (right-hand side) of the differential error equations ([Britting, 1971]). Consequently the state variables for the SP INS model, listed in Table 3.6, are analogous to those of the M INS (listed in Table 3.4).

Table 3.6: STATE VARIABLES OF SP INS MODEL

| SYMBOL | DEFINITION |
|---|---|
| $\delta\theta_{SN}$ | Attitude Error About N Axis |
| $\delta\theta_{SE}$ | Attitude Error About E Axis |
| $\delta\theta_{SD}$ | Attitude Error About D Axis |
| $\delta\dot{L}_S$ | Latitude Rate Error |
| $\delta\dot{\ell}_S$ | Longitude Rate Error |
| $\delta\dot{h}_S$ | Altitude Rate Error |
| $\delta L_S$ | Latitude Error |
| $\delta\ell S$ | Longitude Error |
| $\delta h_S$ | Altitude Error |
| $\underline{\varepsilon}_S$ | Gyro Error Source Vector |
| $\underline{\alpha}_S$ | Accelerometer Error Source Vector |
| $\delta h_{SA}$ | Altimeter Error |

The state equations for the SP INS errors are included in Subsection A.6 of Appendix A.

## 3.9 SP Radar Model

Radar measurement errors are assumed to be modeled by an uncorrelated sequence with covariance computed from the radar equation. Consequently, state variables are unnecessary for modeling the radar errors.

The equations for computing the measurement error covariance ($R$-matrix) are provided in Subsection A.10 of Appendix A.

## 3.10 SP Tracking Filter Model

The SP tracking filter is a nominal-trajectory linearized Kalman filter. The $R$-matrix for this filter is specified by the SP Radar Model discussed in the previous section. The state equations are divided into three groups as indicated in Table 3.7:

- The errors in the estimates of the position, velocity, and azimuth of the SP as indicated by the SP INS
- The states of the random component of target motion.
- A group of position and velocity biases modeling the a priori uncertainty. The covariance of these states is large before the radar measurement is processed.

Table 3.7: STATE VARIABLES OF SP TRACKING FILTER

| SYMBOL | DEFINITION |
|---|---|
| $\delta p_{SP}$<br>$\delta v_{SP}$<br>$\delta\theta_{SP,az}$ | Position Error from SP INS Model (Table 3.6)<br>Velocity Error from SP INS Model<br>Azimuth Error from SP INS Model |
| $\underline{x}_T$ | T Motion Model in Table 3.1 |
| $\delta p_{\mathrm{Tx\ BIAS}}$<br>$\delta v_{\mathrm{Tx\ BIAS}}$<br>$\delta p_{\mathrm{Ty\ BIAS}}$<br>$\delta v_{\mathrm{Ty\ BIAS}}$<br>$\delta p_{\mathrm{Tz\ BIAS}}$<br>$\delta v_{\mathrm{Tz\ BIAS}}$ | Bias Error in T $x$-Position<br>Bias Error in T $x$-Velocity<br>Bias Error in T $y$-Position<br>Bias Error in T $y$-Velocity<br>Bias Error in T $z$-Position<br>Bias Error in T $z$-Velocity |

The state equation for the tracking filter are provided in Subsection A.11 of Appendix A.

## 3.11 LP INS Model

The state variable and equations of the LP INS error model are identical to those of the T INS (Subsection 3.4) except for the instrument error models which correspond to better-quality instruments. The state variables are listed in Table 3.8 and the equations are provided in Subsection A.5 of Appendix A.

Table 3.8: STATE VARIABLES OF LP INS MODEL

| SYMBOL | DEFINITION |
|---|---|
| $\delta\theta_{LN}$ | Attitude Error About N Axis |
| $\delta\theta_{LE}$ | Attitude Error About E Axis |
| $\delta\theta_{LD}$ | Attitude Error About D Axis |
| $\delta\dot{L}_L$ | Latitude Rate Error |
| $\delta\dot{\ell}_L$ | Longitude Rate Error |
| $\delta\dot{h}_L$ | Altitude Rate Error |
| $\delta L_L$ | Latitude Error |
| $\delta\ell$L | Longitude Error |
| $\delta h_L$ | Altitude Error |
| $\underline{\varepsilon}_L$ | Gyro Error Source Vector |
| $\underline{\alpha}_L$ | Accelerometer Error Source Vector |
| $\delta h_{LA}$ | Altimeter Error |

(This page is intentionally left blank)

# Appendix A

# DETAILED COMPONENT MODEL

This appendix provides detailed equations for each of the component models described in Section 2.

## A.1 T Motion Model

The T motion model is composed of two components: deterministic and random. These two components are described in Subsections A.1.1 and A.1.2.

### A.1.1 T Deterministic Motion Model

The deterministic motion of the T is approximated by polynomials in the $x$-, $y$-, and $z$-axes of the tangential frame defined in Section A.3. Motion in the $x$-direction is specified in the interval $t_i \leq t \leq t_{i+1}$ by

$$p_{Tx,\mathrm{det}}(t) = p_{Tx,\mathrm{det},i} + v_{Tx,\mathrm{det},i}(t - t_i) + \frac{1}{2}a_{Tx,\mathrm{det},i}(t - t_i)^2, \tag{A.1}$$

and similarly for the $y$- and $z$-axes. Consequently, the deterministic motion of the target is specified by an array of the form shown in Table A.1. For most cases the acceleration term in Equation A.1 is set to zero to obtain a piece-wise linear T trajectory.

### A.1.2 T Random Motion Model

The random component of the T Motion Model is composed of three Singer models which specify motion along each of the three axes of the tangential frame defined in Section A.3. The model corresponding to the $x$-axis is given by state-space equations of the form ([Gelb, 1974])

$$\dot{\underline{x}}_{Tx} = \underline{F}_{Tx}\,\underline{x}_{Tx} + \underline{w}_{Tx} \ . \tag{A.2}$$

Table A.1: T DETERMINISTIC MODEL INPUT TABLE

| BEGIN TIME | END TIME | $x$-MOTION COEFFICIENTS | $y$-MOTION COEFFICIENTS | $z$-MOTION COEFFICIENTS |
|---|---|---|---|---|
| $\vdots$ | $\vdots$ | $\vdots$ | $\vdots$ | $\vdots$ |
| $t_i$ | $t_{i+1}$ | $p_{Tx,\mathrm{det},i}$, $p_{Tx,\mathrm{det},i}$, $p_{Tx,\mathrm{det},i}$ | $v_{Tx,\mathrm{det},i}$, $v_{Tx,\mathrm{det},i}$, $v_{Tx,\mathrm{det},i}$ | $a_{Tx,\mathrm{det},i}$, $a_{Tx,\mathrm{det},i}$, $a_{Tx,\mathrm{det},i}$ |
| $\vdots$ | $\vdots$ | $\vdots$ | $\vdots$ | $\vdots$ |

The $F$-matrix, the white noise vector, and its spectral matrix ([Gelb, 1974]) are given by ([Singer, 1969])

$$\underline{F}_{Tx} = \begin{bmatrix} 0 & 1 & 0 \\ 0 & 0 & 1 \\ 0 & 0 & -\alpha_{Tx} \end{bmatrix} \tag{A.3}$$

$$\underline{w}_{Tx} = \begin{bmatrix} 0 \\ 0 \\ w_{Tx} \end{bmatrix} . \tag{A.4}$$

$$\underline{Q}_{Tx} = \begin{bmatrix} 0 & 0 & 0 \\ 0 & 0 & 0 \\ 0 & 0 & q_{Tx} \end{bmatrix} \tag{A.5}$$

These equations indicate that acceleration, velocity, and position are related by integrations, and that acceleration is taken as a first-order Markov process. Analogous models are formulated for the random motion along the $y$ and $z$ coordinates.

The Singer model is a function of two parameters: $\alpha_{Tx}$ and $\sigma^2_{Tx}$. These parameters are set as follows ([Singer, 1969]). The parameter $\alpha$ is the reciprocal of the correlation time $\tau$,

$$\alpha = \frac{1}{\tau}. \tag{A.6}$$

The correlation time is initially set to

$$\tau = 5 \text{ sec.} \tag{A.7}$$

This value may be considered representative of turbulence and autopilot maneuvers.

The power parameter, $\sigma^2_{Tx}$, is set based on the anticipated magnitude of the maneuvers according to the formula

$$\sigma^2_{Tx} = \frac{A^2_{\max}}{3}[1 + 4P_{\max} - P_0]. \tag{A.8}$$

In this equation,

$P_0$ = Probability that the acceleration is zero

$A_{\max}$ = Maximum expected acceleration

$P_{\max}$ = Probability that the acceleration is $A_{\max}$.

Equation A.8 is derived in [Singer, 1969] by assuming a uniform probability density function for acceleration with spikes at zero and $\pm A_{max}$. The power parameter specifies the spectral density of the white noise $w_{Tx}$,

$$q_{Tx} = 2\alpha_{Tx}\sigma_{Tx}^2. \tag{A.9}$$

The covariance of the random component of T motion ("Singer covariance") is defined by

$$\underline{P}_{T,L}(t) = E\{\begin{bmatrix} \underline{x}_{Tx}(t) \\ \underline{x}_{Ty}(t) \\ \underline{x}_{Tz}(t) \end{bmatrix} \begin{bmatrix} \underline{x}_{Tx}(t) \\ \underline{x}_{Ty}(t) \\ \underline{x}_{Tz}(t) \end{bmatrix}^T\}. \tag{A.10}$$

The subscript $L$ in $\underline{P}_{T,L}(t)$ indicates that this covariance is a location covariance as opposed to an estimation covariance.

## A.2 M Random Motion Model

The random component of the M motion is also given by $x$-, $y$-, and $z$-Singer models, each model characterized by equations analogous to Equations A.2 to A.4. The parameters for the Singer models ($\alpha_{Tx}$ and $\sigma_{Tx}^2$) are set by the procedure described in Subsection A.1. The covariance of the random component of M motion ("Singer covariance") is similarly defined as

$$\underline{P}_{M,L}(t) = E\{\begin{bmatrix} \underline{x}_{Mx}(t) \\ \underline{x}_{My}(t) \\ \underline{x}_{Mz}(t) \end{bmatrix} \begin{bmatrix} \underline{x}_{Mx}(t) \\ \underline{x}_{My}(t) \\ \underline{x}_{Mz}(t) \end{bmatrix}^T\}. \tag{A.11}$$

The deterministic component of the M motion is given in Section A.9 which addresses the guidance model.

## A.3 LP Deterministic Trajectory Model

### A.3.1 Introduction

The notation used in describing the LP trajectory model is as follows:

- Superscripts indicate Cartesian reference frames. Five frames are of interest:
  - The *"inertial" frame* ($i$-frame), having its origin at the center of the Earth, $x$-axis pointing to the vernal equinox and the $z$-axis pointing to the North pole
  - The *Earth-centered Earth-fixed frame* ($e$-frame), having its origin at the center of the Earth, $x$-axis on the Equatorial plane and through the Greenwich meridian, and the $z$-axis pointing to the North pole
  - The *geographic frame* ($n$-frame), having its origin at the center of mass of the vehicle (LP), $x$-axis pointing North, $y$-axis East, and $z$-axis down

- The *tangential frame* ($t$-frame), a geographic frame with origin at a fixed location relative to the Earth. The location of the origin is determined by its latitude, longitude, and altitude, $(L_{O,TAN}, \ell_{O,TAN}, h_{O,TAN})$, which are simulation inputs. Values for these three coordinates should be chosen to specify a location near the launch point
- The *body frame* ($b$-frame), having its origin at the center of mass of the vehicle, $x$-frame along the roll axis, $y$-frame along the pitch axis, and $z$ along the yaw axis.

- $C_b^n$ is the direction cosine matrix (DCM) for transforming a vector in the $b$-frame to one in the $n$-frame ([Britting, 1971]). A similar notation is used for other DCM transformations with the exception of the roll, pitch, and azimuth (yaw) transformation matrices ([Etkin, 1972]):

$$L_r(\phi) = \begin{bmatrix} 1 & 0 & 0 \\ 0 & \cos\phi & \sin\phi \\ 0 & -\sin\phi & \cos\phi \end{bmatrix} \quad \text{(roll)} \tag{A.12}$$

$$L_p(\theta) = \begin{bmatrix} \cos\theta & 0 & -\sin\theta \\ 0 & 1 & 0 \\ \sin\theta & 0 & \cos\theta \end{bmatrix} \quad \text{(pitch)} \tag{A.13}$$

$$L_a(\psi) = \begin{bmatrix} \cos\psi & \sin\psi & 0 \\ -\sin\psi & \cos\psi & 0 \\ 0 & 0 & 1 \end{bmatrix} \quad \text{(azimuth)} \tag{A.14}$$

  where $\phi$, $\theta$, and $\psi$ are roll, pitch, and azimuth angles.

- Time ($t$) is GMT.

This section contains the algorithms for computing thirty-one deterministic (non-random) motion variables for each of six possible LP motion events. The thirty-one variables are listed in Table A.2 which also specifies the frame in which the variable is expressed and the corresponding symbol. These variables are necessary for specifying the propagation of INS errors as summarized in Table 3.3.

The six LP motion events are considered in the following subsections as follows:

- Level flight at constant velocity: Subsection A.3.3
- Right-turn / Left-turn to a given heading: Subsection A.3.4
- Climb / descent to a given altitude: Subsection A.3.5
- Change of speed at a constant altitude: Subsection A.3.6
- Azimuth change while on the ground: Subsection A.3.7.

In addition to these motion events, two additional events are considered:

Table A.2: LP TRAJECTORY MOTION VARIABLES AND SYMBOLS

| MOTION VARIABLE | RELATIVE TO | FRAME | SYMBOL |
|---|---|---|---|
| Position | Rotating Earth | Tangential | $p^t_{LP}$ |
| Velocity | // | // | $v^t_{LP}$ |
| Acceleration | // | // | $a^t_{LP}$ |
| Specific Force | Inertial space | Geographic, Body | $f^n$, $f^b$ |
| Latitude | The Equator | — | $L_{LP}$ |
| Celestial Longitude | Vernal Equinox | — | $\lambda_{LP}$ |
| Terrestrial Longitude | Greenwich | — | $\ell_{LP}$ |
| Altitude | Reference Ellipsoid | — | $h_{LP}$ |
| Rates | — | — | $\dot{L}_{LP}$, $\dot{\lambda}_{LP}$, $\dot{\ell}_{LP}$, $\dot{h}_{LP}$ |
| Accelerations | — | — | $\ddot{L}_{LP}$, $\ddot{\lambda}_{LP}$, $\ddot{\ell}_{LP}$ |
| Bank | (Euler angle) | — | $\phi$ |
| Elevation | // | — | $\theta$ |
| Azimuth | // | — | $\psi$ |
| Roll rate | Inertial space | Body | $p$ |
| Pitch rate | // | // | $q$ |
| Yaw rate | // | // | $r$ |

- A one-time initialization is performed at the beginning of the simulation, described in the following subsection (Subsection A.3.2)
- A trajectory with constant three-dimensional acceleration. This trajectory, necessary for the propagation of the M INS dynamics considered in Subsection A.9.9, is described in Subsection A.3.8.

## A.3.2 Initialization

Assumptions — The model for the initial condition of the LP is based on the following assumptions:

- At the initial time, $t_{\text{LP,INIT}}$:
  - the LP is stationary at a known (BASE) location and oriented at a known azimuth
  - Pitch and roll angles are zero
- After $t_{\text{LP,INIT}}$:
  - Ground align is performed
  - The LP takes off by executing, as required, a combination of: azimuth change while on the ground (Subsection A.3.7); change of speed (Subsection A.3.6); and climb (Subsection A.3.5).

Input Parameters — The initial conditions for the LP are determined by the following input parameters:

- Initial time, $t_{\text{LP,INIT}}$
- Initial LP location, $(L_{\text{BASE}}, \ell_{\text{BASE}}, h_{\text{BASE}})$
- Initial azimuth $\psi_{\text{LP,INIT}}$.

Computation Algorithm – The objective of the computation algorithm is to provide initial values for the variables listed in Table A.2. A four-step procedure is followed.

*1. Computation of point mass t-frame location ($p^t_{LP}$, $v^t_{LP}$, $a^t_{LP}$) at $t_{\text{LP,INIT}}$:*

1a. Velocity and Acceleration:

$$v^t_{LP}(t_{\text{LP,INIT}}) = a^t_{LP}(t_{\text{LP,INIT}}) = 0. \tag{A.15}$$

1b. Compute the location of the origin of the $t$-frame in $e$-frame coordinates:

$$r^e_{\text{O,TAN}} \equiv \begin{bmatrix} x^e_{\text{O,TAN}} \\ y^e_{\text{O,TAN}} \\ z^e_{\text{O,TAN}} \end{bmatrix}^e \tag{A.16}$$

$$= \begin{bmatrix} (R_\oplus + h_{\text{O,TAN}}) \cos L_{\text{O,TAN}} \cos \ell_{\text{O,TAN}} \\ (R_\oplus + h_{\text{O,TAN}}) \cos L_{\text{O,TAN}} \sin \ell_{\text{O,TAN}} \\ (R_\oplus + h_{\text{O,TAN}}) \sin L_{\text{O,TAN}} \end{bmatrix}^e, \tag{A.17}$$

where $R_\oplus$ is the radius of a spherical Earth (6378 km).

1c. Compute the location of the LP in $t$-frame coordinates:

$$r^e_{\text{BASE}} \equiv \begin{bmatrix} x^e_{\text{BASE}} \\ y^e_{\text{BASE}} \\ z^e_{\text{BASE}} \end{bmatrix}^e \tag{A.18}$$

$$= \begin{bmatrix} (R_\oplus + h_{\text{BASE}}) \cos L_{\text{BASE}} \cos \ell_{\text{BASE}} \\ (R_\oplus + h_{\text{BASE}}) \cos L_{\text{BASE}} \sin \ell_{\text{BASE}} \\ (R_\oplus + h_{\text{BASE}}) \sin L_{\text{BASE}} \end{bmatrix}^e. \tag{A.19}$$

1d. Compute the location of the LP in $e$-frame coordinates:

$$p^t_{LP}(t_{\text{LP,INIT}}) = C^t_e (r^e_{\text{BASE}} - r^e_{\text{O,TAN}}) \tag{A.20}$$

where the $e$-frame to $t$-frame DCM is given by

$$C^t_e = (C^e_t)^T \tag{A.21}$$

$$C^e_t = C^e_n C^n_t \tag{A.22}$$

$$C^n_t : \text{ Given by Equation A.94} \tag{A.23}$$

$$C^e_n = \begin{bmatrix} -\sin L_{\text{BASE}} \cos \ell_{\text{BASE}} & -\sin \ell_{\text{BASE}} & -\cos L_{\text{BASE}} \cos \ell_{\text{BASE}} \\ -\sin L_{\text{BASE}} \sin \ell_{\text{BASE}} & \cos \ell_{\text{BASE}} & -\cos L_{\text{BASE}} \sin \ell_{\text{BASE}} \\ \cos L_{\text{BASE}} & 0 & -\sin L_{\text{BASE}} \end{bmatrix} \tag{A.24}$$

where the superscript $T$ indicates matrix transposition.

*2. Computation of specific force,* $(f^n, f^b)$: Because the LP experiences zero acceleration, the specific force in the $n$-frame is given by

$$f^n \equiv \begin{bmatrix} f_N \\ f_E \\ f_D \end{bmatrix}^n = \begin{bmatrix} 0 \\ 0 \\ -g \end{bmatrix}^n, \tag{A.25}$$

and in the $b$-frame

$$f^b = C_n^b f^n \tag{A.26}$$

where the formula for $C_n^b$ is given below in Step 4 (Equation A.30).

*3. Computation of latitude, longitude, altitude, and rates,* ($L_{LP}$, $\lambda_{LP}$, $\ell_{LP}$, $h_{LP}$, and rates): These quantities are computed using the following equations:

$$\begin{aligned}
L_{LP} &= L_{\text{BASE}} \\
\ell_{LP} &= \ell_{\text{BASE}} \\
\lambda_{LP} &: \text{Equation A.112} \\
h_{LP} &= h_{\text{BASE}} \\
\dot{L}_{LP} &= 0 \\
\dot{\ell}_{LP} &= 0 \\
\dot{\lambda}_{LP} &: \text{Equation A.117} \\
\dot{h}_{LP} &= 0 \\
\ddot{L}_{LP} &= 0 \\
\ddot{\ell}_{LP} &= 0 \\
\ddot{\lambda}_{LP} &: \text{Equation A.121.}
\end{aligned}$$

*4. Computation of rotational parameters,* $(\phi, \theta, \psi, p, q, r)$:

4a. Compute Euler angles and DCM: During $[t_1, t_2]$, the Euler angles (roll, pitch, and yaw) are given by:

$$\phi(t) = 0 \tag{A.27}$$

$$\theta(t) = 0 \tag{A.28}$$

$$\psi(t) = \psi_{\text{LP,INIT}} \tag{A.29}$$

where $\psi_{\text{LP,INIT}}$ is the azimuth at time $t_{\text{LP,INIT}}$. The corresponding $n$-frame to $b$-frame DCM is:

$$C_n^b(t) = L_a(\psi_{\text{LP,INIT}}). \tag{A.30}$$

4b. Compute angular rates: The angular rates with respect to inertial space ($p$, $q$, and $r$) are computed from the angular rates with respect to the $n$-frame ($P$, $Q$, and $R$), which in turn are computed from the Euler angle rates ($\dot{\phi}$, $\dot{\theta}$, and $\dot{\psi}$):

$$\begin{bmatrix} \dot{\phi} \\ \dot{\theta} \\ \dot{\psi} \end{bmatrix} = \begin{bmatrix} 0 \\ 0 \\ 0 \end{bmatrix} \tag{A.31}$$

$$\begin{bmatrix} P \\ Q \\ R \end{bmatrix} = \begin{bmatrix} 0 \\ 0 \\ 0 \end{bmatrix} \tag{A.32}$$

$$\begin{bmatrix} p \\ q \\ r \end{bmatrix} = C_n^b(t) \begin{bmatrix} (\Omega_\oplus + \dot{\ell}) \cos L \\ -\dot{L} \\ -(\Omega_\oplus + \dot{\ell}) \sin L \end{bmatrix} \tag{A.33}$$

where $C_n^b(t)$ is given by Equation A.30.

### A.3.3 Level Flight at Constant Velocity

Assumptions — The model for level flight is based on the following assumptions:

- Level flight begins at time $t_1$ and ends at time $t_2$
- Within the $[t_1, t_2]$ time interval:
  - The pitch and roll angles are zero
  - All accelerations are zero
  - Vertical velocity is zero (altitude is constant)
- The variables listed in Table A.2 are known at $t_1$.

Input Parameters — A level flight segment is determined by one input parameter: the duration of the segment, $t_2 - t_1$.

Computation Algorithm — The objective of the computation algorithm is to compute the variables listed in Table A.2 within the $[t_1, t_2]$ interval. A four-step procedure is followed.

*1. Computation of point mass t-frame trajectory* ($p_{LP}^t$, $v_{LP}^t$, $a_{LP}^t$):

$$a_{LP}^t(t) = 0 \tag{A.34}$$

$$v_{LP}^t(t) = v_{LP}^t(t_1) \tag{A.35}$$

$$p_{LP}^t(t) = p_{LP}^t(t_1) + v_{LP}^t(t_1)(t - t_1). \tag{A.36}$$

*2. Computation of specific force*, ($f^n$, $f^b$): Because the LP experiences zero acceleration, the specific force in the $n$-frame is given by

$$f^n \equiv \begin{bmatrix} f_N \\ f_E \\ f_D \end{bmatrix}^n = \begin{bmatrix} 0 \\ 0 \\ -g \end{bmatrix}^n, \tag{A.37}$$

and in the $b$-frame

$$f^b = C_n^b f^n \tag{A.38}$$

where the formula for $C_n^b$ is given below in Step *4*.

*3. Computation of latitude, longitude, altitude, and rates,* ($L_{LP}$, $\lambda_{LP}$, $\ell_{LP}$, $h_{LP}$, and rates): These quantities are computed using the following equations:

$L_{LP}$ : Equation A.110
$\ell_{LP}$ : Equation A.111
$\lambda_{LP}$ : Equation A.112
$h_{LP}$ : Equation A.113
$\dot{L}_{LP}$ : Equation A.115
$\dot{\ell}_{LP}$ : Equation A.116
$\dot{\lambda}_{LP}$ : Equation A.117
$\dot{h}_{LP}$ : Equation A.118
$\ddot{L}_{LP}$ : Equation A.119
$\ddot{\ell}_{LP}$ : Equation A.120
$\ddot{\lambda}_{LP}$ : Equation A.121.

*4. Computation of rotational parameters,* ($\phi$, $\theta$, $\psi$, $p$, $q$, $r$):

4a. Compute Euler angles and DCM: During $[t_1, t_2]$, the Euler angles (roll, pitch, and yaw) are given by:

$$\phi(t) = 0 \tag{A.39}$$
$$\theta(t) = 0 \tag{A.40}$$
$$\psi(t) = \psi_1 \tag{A.41}$$

where $\psi_1$ is the azimuth at time $t_1$ and the small variation in azimuth because due to translational motion is neglected. The corresponding $n$-frame to $b$-frame DCM is:

$$C_n^b(t) = L_a(\psi_1). \tag{A.42}$$

4b. Compute angular rates: The angular rates with respect to inertial space ($p$, $q$, and $r$) are computed from the angular rates with respect to the $n$-frame ($P$, $Q$, and $R$), which in turn are computed from the Euler angle rates ($\dot{\phi}$, $\dot{\theta}$, and $\dot{\psi}$):

$$\begin{bmatrix} \dot{\phi} \\ \dot{\theta} \\ \dot{\psi} \end{bmatrix} = \begin{bmatrix} 0 \\ 0 \\ 0 \end{bmatrix} \tag{A.43}$$

$$\begin{bmatrix} P \\ Q \\ R \end{bmatrix} = \begin{bmatrix} 0 \\ 0 \\ 0 \end{bmatrix} \tag{A.44}$$

$$\begin{bmatrix} p \\ q \\ r \end{bmatrix} = C_n^b(t) \begin{bmatrix} (\Omega_\oplus + \dot{\ell}) \cos L \\ -\dot{L} \\ -(\Omega_\oplus + \dot{\ell}) \sin L \end{bmatrix} \tag{A.45}$$

where $C_n^b(t)$ is given by Equation A.42.

### A.3.4 Right-Turn / Left-Turn

Assumptions — The model for the turn is based on the following assumptions:

- The turn begins at time $t_1$ and ends at time $t_4$
- At time $t_1^-$ (immediately before the turn) and at time $t_4$ (at the end of the turn):
  - The pitch and roll angles are zero
  - All accelerations are zero
  - Vertical velocity is zero
- The variables listed in Table A.2 are known at $t_1^-$
- During the turn ($t_1 \leq t \leq t_4$) the LP flies at a constant altitude
- The turn is divided into three time intervals:

  $t_1 \leq t \leq t_2$: Roll from zero to the bank angle required by the turn[1]

  $t_2 \leq t \leq t_3$: Turn at a constant bank angle

  $t_3 \leq t \leq t_4$: Roll back to zero bank angle
- Within $[t_1, t_2]$ and $[t_3, t_4]$ the LP rolls at a constant roll rate. This roll rate is assumed to be $\dot{\phi}_T = \pm 90$ deg/sec, positive for right-turn (RT) and negative for left-turn (LT) ([McCormick, 1979]).

Input Parameters — A steady turn segment (also called a "truly banked" or "coordinated" turn, [Etkin, 1972], [Dole, 1981]) is determined by the following input parameters:

- Direction of the turn (right or left)
- Load factor (the number of $g$'s the aircraft "pulls"), $n_T$
- Final heading, $\psi_4$.

Computation Algorithm — The objective of the computation algorithm is to compute the variables listed in Table A.2 within each of the three intervals ($[t_1, t_2]$, $[t_2, t_3]$, and $[t_3, t_4]$). The development that follows is divided into three parts:

- Preliminary computations
- Computations for $[t_1, t_2]$
- Computations for $[t_2, t_3]$
- Computations for $[t_3, t_4]$.

[1] "Bank angle" is synonymous with "roll angle."

The development is based on [Etkin, 1972], [Dole, 1981], [Anderson, 1989], and [Britting, 1971].

Preliminary Computations:

*1. Computation of t-frame speed:*

$$V_T = \sqrt{(v^t_{LPx})^2 + (v^t_{LPy})^2}. \tag{A.46}$$

*2. Computation of turn radius:*

$$R_T = \frac{V_T^2}{g\sqrt{n_T^2 - 1}} \tag{A.47}$$

where $g = 9.8$ m/sec$^2$ is the acceleration of gravity.

*3. Computation of turn rate:*

$$\omega_T = \pm\frac{g\sqrt{n_T^2 - 1}}{V_T} \tag{A.48}$$

where the plus sign corresponds to RT and the negative sign to LT.

*4. Computation of turn interval duration:* To compute the turn rate, compute first the total turn angle, $\Delta\psi$,

$$\Delta\psi = [\psi_4 - \psi_1]_{360}. \tag{A.49}$$

In this equation, the subtraction is modulus 360 deg, $\psi_4$ is the final heading (an input parameter), and $\psi_1$ is the initial heading computed from

$$\psi_1 = \arctan\left(\frac{v^t_{LPx}}{v^t_{LPy}}\right). \tag{A.50}$$

The duration of the turn interval is given by

$$T_T = \frac{\Delta\psi}{\omega_T}. \tag{A.51}$$

*5. Computation of roll angle:*

$$\phi_T = \pm\arccos\left(\frac{1}{n_T}\right), \tag{A.52}$$

"+" for RT, "−" for LT.

*6. Computation of roll interval:* The duration of the roll interval is given by

$$T_r = \frac{\phi_T}{\dot{\phi}_T} \quad . \tag{A.53}$$

*7. Computation of times:*

$$t_2 = t_1 + T_r \tag{A.54}$$

$$t_3 = t_1 + T_r + T_T \tag{A.55}$$

$$t_4 = t_1 + 2T_r + T_T \tag{A.56}$$

*8. Computation of turn center:* The turn circle is located at $(x_{TC}, y_{TC}, z_{TC})$ in the $t$-frame. Because the turn occurs at a constant altitude,

$$z_{TC} = p^t_{LPz}(t_1) = p^t_{LPz}(t_2). \tag{A.57}$$

Let the vector from the location of LP at $t_2$ to the center of the turn circle be $\vec{R}_{NT}$ (the subscript indicates that this vector is the negative turn radius vector). Because of Equation A.57, the $z$-component of $\vec{R}_{NT}$ is zero. The $x$- and $y$-components are computed by noting that at time $t_2$ the turn circle is in a direction orthogonal to the velocity vector, to the right or the left of the pilot, depending on the direction of the turn, and at a distance $R_T$ from the LP. Two cases need to be considered as follows:

**If** $v_{LPx}(t_2) \neq 0$:

$$R_{NTx} = -\rho \frac{a R_T}{\sqrt{1+\rho^2}} \tag{A.58}$$

$$R_{NTy} = \frac{a R_T}{\sqrt{1+\rho^2}} \tag{A.59}$$

where

$$\rho = \frac{v_{LPy}(t_2)}{v_{LPx}(t_2)}. \tag{A.60}$$

The constant $a$ is set according to the following conditions:

$$\begin{aligned}
&\text{If LT and} \quad v_{LPx}(t_2) > 0 \quad \text{then } a = -1 \\
&\text{If LT and} \quad v_{LPx}(t_2) < 0 \quad \text{then } a = +1 \\
&\text{If RT and} \quad v_{LPx}(t_2) > 0 \quad \text{then } a = +1 \\
&\text{If RT and} \quad v_{LPx}(t_2) < 0 \quad \text{then } a = -1.
\end{aligned}$$

**If** $v_{LPx}(t_2) = 0$:

$$R_{NTx} = a R_T \tag{A.61}$$

$$R_{NTy} = 0. \tag{A.62}$$

For this case, the constant $a$ is set according to the following conditions:

$$\begin{aligned}
&\text{If LT and} \quad v_{LPy}(t_2) > 0 \quad \text{then } a = +1 \\
&\text{If LT and} \quad v_{LPy}(t_2) < 0 \quad \text{then } a = -1 \\
&\text{If RT and} \quad v_{LPy}(t_2) > 0 \quad \text{then } a = -1 \\
&\text{If RT and} \quad v_{LPy}(t_2) < 0 \quad \text{then } a = +1.
\end{aligned}$$

The center of the turn circle is then computed from the negative turn radius vector,

$$\begin{bmatrix} x_{TC} \\ y_{TC} \\ z_{TC} \end{bmatrix}^t = \begin{bmatrix} p^t_{LPx}(t_2) \\ p^t_{LPy}(t_2) \\ p^t_{LPz}(t_2) \end{bmatrix}^t + \begin{bmatrix} R_{NTx} \\ R_{NTy} \\ R_{NTz} \end{bmatrix}^t. \tag{A.63}$$

Computations for $[t_1, t_2]$: Within this interval a four-step procedure is followed.

*1. Computation of point mass t-frame trajectory* ($p^t_{LP}$, $v^t_{LP}$, $a^t_{LP}$):

$$a^t_{LP}(t) = 0 \tag{A.64}$$
$$v^t_{LP}(t) = v^t_{LP}(t_1) \tag{A.65}$$
$$p^t_{LP}(t) = p^t_{LP}(t_1) + v^t_{LP}(t_1)(t - t_1). \tag{A.66}$$

*2. Computation of specific force,* ($f^n$, $f^b$): Because the LP experiences zero acceleration (and the INS is assumed to be located at the center of mass), the specific force in the $n$-frame is given by

$$f^n \equiv \begin{bmatrix} f_N \\ f_E \\ f_D \end{bmatrix}^n = \begin{bmatrix} 0 \\ 0 \\ -g \end{bmatrix}^n, \tag{A.67}$$

and in the $b$-frame

$$f^b = C^b_n f^n \tag{A.68}$$

where the formula for $C^b_n$ is given below in Step *4*.

*3. Computation of latitude, longitude, altitude, and rates,* ($L_{LP}$, $\lambda_{LP}$, $\ell_{LP}$, $h_{LP}$, and rates): These quantities are computed using the following equations:

$L_{LP}$ : Equation A.110
$\ell_{LP}$ : Equation A.111
$\lambda_{LP}$ : Equation A.112
$h_{LP}$ : Equation A.113
$\dot{L}_{LP}$ : Equation A.115
$\dot{\ell}_{LP}$ : Equation A.116
$\dot{\lambda}_{LP}$ : Equation A.117
$\dot{h}_{LP}$ : Equation A.118
$\ddot{L}_{LP}$ : Equation A.119
$\ddot{\ell}_{LP}$ : Equation A.120
$\ddot{\lambda}_{LP}$ : Equation A.121.

*4. Computation of rotational parameters,* ($\phi$, $\theta$, $\psi$, $p$, $q$, $r$):

4a. Compute Euler angles and DCM: During $[t_1, t_2]$, the Euler angles (roll, pitch, and yaw) are given by:

$$\phi(t) = \dot{\phi}_T(t - t_1) \tag{A.69}$$
$$\theta(t) = 0 \tag{A.70}$$
$$\psi(t) = \psi_1 \tag{A.71}$$

where $\psi_1$ is the azimuth at time $t_1$. The corresponding $n$-frame to $b$-frame DCM is:

$$C^b_n(t) = L_r(\phi(t))L_a(\psi_1). \tag{A.72}$$

4b. Compute angular rates: The angular rates with respect to inertial space ($p$, $q$, and $r$) are computed from the angular rates with respect to the $n$-frame ($P$, $Q$, and $R$), which in turn are computed from the Euler angle rates ($\dot{\phi}$, $\dot{\theta}$, and $\dot{\psi}$):

$$\begin{bmatrix} \dot{\phi} \\ \dot{\theta} \\ \dot{\psi} \end{bmatrix} = \begin{bmatrix} \dot{\phi}_T \\ 0 \\ 0 \end{bmatrix} \tag{A.73}$$

$$\begin{bmatrix} P \\ Q \\ R \end{bmatrix} = L_r(\phi(t)) \begin{bmatrix} \dot{\phi} \\ \dot{\theta} \\ \dot{\psi} \end{bmatrix} \tag{A.74}$$

$$\begin{bmatrix} p \\ q \\ r \end{bmatrix} = \begin{bmatrix} P \\ Q \\ R \end{bmatrix} + C_n^b(t) \begin{bmatrix} (\Omega_\oplus + \dot{\ell}) \cos L \\ -\dot{L} \\ -(\Omega_\oplus + \dot{\ell}) \sin L \end{bmatrix} \tag{A.75}$$

where $C_n^b(t)$ is given by Equation A.72.

Computations for $[t_2, t_3]$: Within this interval a four-step procedure is followed.

*1. Computation of point mass t-frame trajectory* ($p_{LP}^t$, $v_{LP}^t$, $a_{LP}^t$): Consider first the position, $p_{LP}^t(t)$, $t\epsilon[t_2, t_3]$. In the $b(t_2)$-frame (body frame at time $t_2$) the trajectory during the turn is simply a circle specified by

$$p_{LP}(t)_{\mathrm{RT}}^{b(t_1)} = \begin{bmatrix} c(t) \sin \alpha(t) \\ c(t) \cos \alpha(t) \\ 0 \end{bmatrix}^{b(t_1)} \tag{A.76}$$

$$p_{LP}(t)_{\mathrm{LT}}^{b(t_1)} = \begin{bmatrix} c(t) \sin \alpha(t) \\ -c(t) \cos \alpha(t) \\ 0 \end{bmatrix}^{b(t_1)} \tag{A.77}$$

where the first/second equation apply to RT/LT, and:

$$c(t) = \frac{\sin \gamma(t)}{\sin \alpha(t)} R_T \tag{A.78}$$

$$\gamma(t) = \omega_T (t - t_2) \tag{A.79}$$

$$\alpha(t) = \frac{\pi - \gamma(t)}{2} \quad \text{(rad)}. \tag{A.80}$$

The trajectory in the $b(t_1)$-frame is transformed to the $t$-frame by means of:

$$p_{LP}(t)^t = p_{LP}(t_2)^t + C_{n(t_2)}^t C_{b(t_2)}^{n(t_2)} p_{LP}(t)^{b(t_2)}. \tag{A.81}$$

This equation states that the LP position in the $t$-frame is the sum of two vectors expressed in the $t$-frame: the position of the origin of the $b(t_2)$-frame plus the location of the LP in the $b(t_2)$-frame. To express the second vector in the $t$-frame, the vector is transformed, using DCMs, from the $b(t_2)$ to the $n(t_2)$ to the $t$ frames. The DCM for the first transformation is given by:

$$C_{b(t_2)}^{n(t_2)} = \begin{bmatrix} \cos \psi_1 & -\sin \psi_1 & 0 \\ \sin \psi_1 & \cos \psi_1 & 0 \\ 0 & 0 & 1 \end{bmatrix} \tag{A.82}$$

where $\psi_1$ is the heading at the beginning of the turn maneuver. And the DCMs for the second transformation is given by:

$$C^t_{n(t_2)} = \left[\begin{array}{c|c|c} 1 - \frac{\Delta L_1^2}{2} - \frac{\Delta \ell_1^2}{2}\sin^2 L_o & \Delta\ell_1 \sin L_o & -\Delta L_1 - \frac{\Delta \ell_1^2}{4}\sin 2L_o \\ -\Delta\ell_1(\sin L_o + \Delta L_1 \cos L_o) & 1 - \frac{\Delta \ell_1^2}{2} & -\Delta\ell_1(\cos L_o - \Delta L_1 \sin L_o) \\ \Delta L_1 - \frac{\Delta \ell_1^2}{4}\sin 2L_o & \Delta\ell_1 \cos L_o & 1 - \frac{\Delta L_1^2}{2} - \frac{\Delta \ell_1^2}{2}\cos^2 L_o \end{array}\right] \tag{A.83}$$

where

$$\begin{aligned} \Delta L_1 &= L_1 - L_{\text{O,TAN}} \\ \Delta \ell_1 &= \ell_1 - \ell_{\text{O,TAN}} \\ L_1, \ell_1 &= \text{Latitude and terrestrial longitude of the origin of the } n(t_1)\text{-frame} \\ L_{\text{O,TAN}}, \ell_{\text{O,TAN}} &= \text{Latitude and terrestrial longitude of the origin of the } t\text{-frame.} \end{aligned}$$

The velocity and acceleration in the $t$-frame ($v^t_{LP}$ and $a^t_{LP}$) are obtained by differentiating Equation A.81 to obtain:

$$v_{LP}(t)^t = C^t_{n(t_2)} C^{n(t_2)}_{b(t_2)} \frac{d}{dt} p_{LP}(t)^{b(t_2)} \tag{A.84}$$

$$a_{LP}(t)^t = C^t_{n(t_2)} C^{n(t_2)}_{b(t_2)} \frac{d^2}{dt^2} p_{LP}(t)^{b(t_2)}. \tag{A.85}$$

The derivatives on the right-hand side for right-turns are:

$$\left[\frac{d}{dt} p_{LP}(t)^{b(t_2)}\right]_{\text{RT}} = \left[\begin{array}{c} \omega_T R_T \cos\gamma(t) \\ f_1(t) \\ 0 \end{array}\right]^{b(t_2)} \tag{A.86}$$

$$\left[\frac{d^2}{dt^2} p_{LP}(t)^{b(t_2)}\right]_{\text{RT}} = \left[\begin{array}{c} -\omega_T^2 R_T \sin\gamma(t) \\ f_2(t) \\ 0 \end{array}\right]^{b(t_2)} \tag{A.87}$$

where the functions $f_1$ and $f_2$ are given by:

$$f_1(t) = \omega_T R_T \frac{\cos\gamma(t)}{\tan\alpha(t)} + \frac{\omega_T R_T}{2} \frac{\sin\gamma(t)}{\sin^2\alpha(t)} \tag{A.88}$$

$$f_2(t) = -\omega_T^2 R_T \frac{\sin\gamma(t)}{\tan\alpha(t)} + \omega_T^2 R_T \frac{\cos\gamma(t)}{\sin^2\alpha(t)} + \frac{\omega_T^2 R_T}{2} \sin\gamma(t) \frac{\cos\alpha(t)}{\sin^3\alpha(t)}. \tag{A.89}$$

And for left-turns:

$$\left[\frac{d}{dt} p_{LP}(t)^{b(t_2)}\right]_{\text{LT}} = \left[\begin{array}{c} \omega_T R_T \cos\gamma(t) \\ -f_1(t) \\ 0 \end{array}\right]^{b(t_2)} \tag{A.90}$$

$$\left[\frac{d^2}{dt^2} p_{LP}(t)^{b(t_2)}\right]_{\text{LT}} = \left[\begin{array}{c} -\omega_T^2 R_T \sin\gamma(t) \\ -f_2(t) \\ 0 \end{array}\right]^{b(t_2)}. \tag{A.91}$$

*2. Computation of specific force,* $(f^n,\ f^b)$: The computation of specific forces is a five-step process.

2a. Compute the LP current latitude, terrestrial longitude, and rates as follows:[2]

- $L$ and $\ell$ from $p_{LP}(t)^t$ (which is available from Equation A.81)
- $\dot{L}$ and $\dot{\ell}$ from $v_{LP}(t)^t$ (which is available from Equation A.84)
- $\ddot{L}$ and $\ddot{\ell}$ from $a_{LP}(t)^t$ (which is available from Equation A.85).

The equations for these computations are given in paragraph *3*, below.

2b. Transform $v_{LP}(t)^t$ (given by Equation A.84) from the $t$-frame to the current $n$-frame:

$$v_{LP}(t)^n \equiv \begin{bmatrix} v^n_{LP,N} \\ v^n_{LP,E} \\ v^n_{LP,D} \end{bmatrix}^n \tag{A.92}$$

$$= C^n_t v_{LP}(t)^t \tag{A.93}$$

where

$$C^n_t = \left[\begin{array}{c|c|c} 1 - \frac{\Delta L^2}{2} - \frac{\Delta \ell^2}{2}\sin^2 L_o & -\Delta\ell(\sin L_o + \Delta L \cos L_o) & \Delta L - \frac{\Delta \ell^2}{4}\sin 2L_o \\ \Delta\ell \sin L_o & 1 - \frac{\Delta\ell^2}{2} & \Delta\ell \cos L_o \\ -\Delta L - \frac{\Delta\ell^2}{4}\sin 2L_o & -\Delta\ell(\cos L_o - \Delta L \sin L_o) & 1 - \frac{\Delta L^2}{2} - \frac{\Delta\ell^2}{2}\cos^2 L_o \end{array}\right] \tag{A.94}$$

and, as in Equation A.83,

$$\Delta L = L - L_{\mathrm{O,TAN}} \tag{A.95}$$

$$\Delta \ell = \ell - \ell_{\mathrm{O,TAN}}. \tag{A.96}$$

2c. Transform $a_{LP}(t)^t$ (given by Equation A.85) from the $t$-frame to the current $n$-frame using the theorem of Coriolis ([Britting, 1971]):

$$a_{LP}(t)^n \equiv \begin{bmatrix} a^n_{LP,N} \\ a^n_{LP,E} \\ a^n_{LP,D} \end{bmatrix}^n \tag{A.97}$$

$$= C^n_t a_{LP}(t)^t + \Omega^n_{nt} C^n_t v_{LP}(t)^t \tag{A.98}$$

where $C^n_t$ is given by Equation A.94 and $\Omega^n_{nt}$ is the skew-symmetric matrix ([Britting, 1971]) corresponding to the angular velocity of the $t$-frame relative to the $n$-frame:

$$\Omega^n_{nt} = \begin{bmatrix} 0 & -\dot{\ell}\sin L & \dot{L} \\ \dot{\ell}\sin L & 0 & \dot{\ell}\cos L \\ -\dot{L} & -\dot{\ell}\cos L & 0 \end{bmatrix}. \tag{A.99}$$

[2]Shorthand notation: $L \equiv L_{LP}$, $\ell \equiv \ell_{LP}$, $\lambda \equiv \lambda_{LP}$, $h \equiv h_{LP}$.

2d. Compute the specific force in the $n$-frame:

$$f^n \equiv \begin{bmatrix} f_N \\ f_E \\ f_D \end{bmatrix}^n \tag{A.100}$$

$$= \begin{bmatrix} a^n_{LP,N} + v^n_{LP,E}(\dot{\ell} + 2\Omega_\oplus)\sin L - \dot{L}v^n_{LP,D} \\ a^n_{LP,E} - v^n_{LP,N}(\dot{\ell} + 2\Omega_\oplus)\sin L - v^n_{LP,D}(\dot{\ell} + 2\Omega_\oplus)\cos L \\ a^n_{LP,D} + v^n_{LP,E}(\dot{\ell} + 2\Omega_\oplus)\cos L + \dot{L}v^n_{LP,N} - g \end{bmatrix}^n \tag{A.101}$$

where the subscripts $N$, $E$, and $D$ identify the North, East, and Down components.

2e. Compute the specific force in the $b$-frame:

$$f^b = C^b_n f^n \tag{A.102}$$

where $C^b_n$ is computed in Step *4*.

*3. Computation of latitude, longitude, altitude, and rates,* ($L_{LP}$, $\lambda_{LP}$, $\ell_{LP}$, $h_{LP}$, and rates): The computation of these quantities is a 5-step process.[3]

3a. Compute the location of the origin of the $t$-frame in $e$-frame coordinates:

$$r^e_{\mathrm{O,TAN}} \equiv \begin{bmatrix} x^e_{\mathrm{O,TAN}} \\ y^e_{\mathrm{O,TAN}} \\ z^e_{\mathrm{O,TAN}} \end{bmatrix}^e \tag{A.103}$$

$$= \begin{bmatrix} (R_\oplus + h_{\mathrm{O,TAN}})\cos L_{\mathrm{O,TAN}}\cos \ell_{\mathrm{O,TAN}} \\ (R_\oplus + h_{\mathrm{O,TAN}})\cos L_{\mathrm{O,TAN}}\sin \ell_{\mathrm{O,TAN}} \\ (R_\oplus + h_{\mathrm{O,TAN}})\sin L_{\mathrm{O,TAN}} \end{bmatrix}^e, \tag{A.104}$$

where $R_\oplus$ is the radius of a spherical Earth (6378 km).

3b. Compute the location of the LP in $e$-frame coordinates:

$$r^e_{LP} \equiv \begin{bmatrix} x^e_{LP} \\ y^e_{LP} \\ z^e_{LP} \end{bmatrix}^e \tag{A.105}$$

$$= r^e_{\mathrm{O,TAN}} + C^e_t p^t_{LP} \tag{A.106}$$

where the $t$-frame to $e$-frame DCM is given by

$$C^e_t = C^e_n C^n_t \tag{A.107}$$

$$C^n_t : \text{Given by Equation A.94} \tag{A.108}$$

$$C^e_n = \begin{bmatrix} -\sin L\cos \ell & -\sin \ell & -\cos L\cos \ell \\ -\sin L\sin \ell & \cos \ell & -\cos L\sin \ell \\ \cos L & 0 & -\sin L \end{bmatrix}. \tag{A.109}$$

[3]Shorthand notation: $L \equiv L_{LP}$, $\ell \equiv \ell_{LP}$, $\lambda \equiv \lambda_{LP}$, $h \equiv h_{LP}$.

3c. Compute the latitude, longitudes, and altitude of the LP:

$$L = \arcsin\left(\frac{z^e_{LP}}{\|r^e_{LP}\|}\right) \quad \text{(A.110)}$$

$$\ell = \arctan\left(\frac{y^e_{LP}}{x^e_{LP}}\right) \quad \text{(A.111)}$$

$$\lambda = \ell + \Omega_\oplus t \quad \text{(A.112)}$$

$$h = h_{\mathrm{O,TAN}} - p^t_{LPz} + \Delta L\, p^t_{LPx} + \Delta\ell \cos L_{\mathrm{O,TAN}}\, p^t_{LPy} \quad \text{(A.113)}$$

where time ($t$) is GMT and

$$\|r^e_{LP}\| = \sqrt{(x^e_{LP})^2 + (y^e_{LP})^2 + (z^e_{LP})^2}. \quad \text{(A.114)}$$

3d. Compute first derivatives:

$$\dot{L} = \frac{v^n_{LP,N}}{R_\oplus + h} \quad \text{(A.115)}$$

$$\dot{\ell} = \frac{v^n_{LP,E}}{(R_\oplus + h)\cos L} \quad \text{(A.116)}$$

$$\dot{\lambda} = \dot{\ell} + \Omega_\oplus \quad \text{(A.117)}$$

$$\dot{h} = -v^t_{LPz} + \dot{L} p^t_{LPx} + \Delta L\, v^t_{LPx} + \dot{\ell} \cos L_{\mathrm{O,TAN}}\, p^t_{LPy} + \Delta\ell \cos L_{\mathrm{O,TAN}}\, v^t_{LPy} \quad \text{(A.118)}$$

3e. Compute second derivatives:

$$\ddot{L} = \frac{a^n_{LP,N} - \dot{h}\dot{L}}{R_\oplus + h} \quad \text{(A.119)}$$

$$\ddot{\ell} = \frac{a^n_{LP,E} - \dot{h}\dot{\ell}\cos L + (R_\oplus + h)\dot{\ell}\dot{L}\sin L}{(R_\oplus + h)\cos L} \quad \text{(A.120)}$$

$$\ddot{\lambda} = \ddot{\ell}. \quad \text{(A.121)}$$

*4. Computation of rotational parameters, ($\phi$, $\theta$, $\psi$, $p$, $q$, $r$):*

4a. Compute Euler angles and DCM: During $[t_2, t_3]$, the Euler angles are given by:

$$\phi(t) = \phi_T \quad \text{(A.122)}$$

$$\theta(t) = 0 \quad \text{(A.123)}$$

$$\psi(t) = \psi_1 + \omega_T(t - t_2). \quad \text{(A.124)}$$

The corresponding $n$-frame to $b$-frame DCM is:

$$C^b_n(t) = L_r(\phi_T) L_a(\psi(t)). \quad \text{(A.125)}$$

4b. Compute angular rates: Following a procedure similar to that for the $[t_1, t_2]$ interval, the following calculations provide the angular rates with respect to inertial space

($p$, $q$, and $r$):

$$\begin{bmatrix} \dot{\phi} \\ \dot{\theta} \\ \dot{\psi} \end{bmatrix} = \begin{bmatrix} 0 \\ 0 \\ \omega_T \end{bmatrix} \tag{A.126}$$

$$\begin{bmatrix} P \\ Q \\ R \end{bmatrix} = L_r(\phi_T) \begin{bmatrix} \dot{\phi} \\ \dot{\theta} \\ \dot{\psi} \end{bmatrix} \tag{A.127}$$

$$\begin{bmatrix} p \\ q \\ r \end{bmatrix} = \begin{bmatrix} P \\ Q \\ R \end{bmatrix} + C_n^b(t) \begin{bmatrix} (\Omega_\oplus + \dot{\ell}) \cos L \\ -\dot{L} \\ -(\Omega_\oplus + \dot{\ell}) \sin L \end{bmatrix} \tag{A.128}$$

where $C_n^b(t)$ is given by Equation A.125.

Computations for $[t_3, t_4]$: Within this interval a four-step procedure is followed.

*1. Computation of point mass t-frame trajectory* ($p_{LP}^t$, $v_{LP}^t$, $a_{LP}^t$):

$$a_{LP}^t(t) = 0 \tag{A.129}$$

$$v_{LP}^t(t) = v_{LP}^t(t_3) \tag{A.130}$$

$$p_{LP}^t(t) = p_{LP}^t(t_3) + v_{LP}^t(t_3)(t - t_3). \tag{A.131}$$

*2. Computation of specific force,* ($f^n$, $f^b$): Because the LP experiences zero acceleration the specific force in the $n$-frame is given by

$$f^n \equiv \begin{bmatrix} f_N \\ f_E \\ f_D \end{bmatrix}^n = \begin{bmatrix} 0 \\ 0 \\ -g \end{bmatrix}^n, \tag{A.132}$$

and in the $b$-frame

$$f^b = C_n^b f^n \tag{A.133}$$

where the formula for $C_n^b$ is given below in Step *4*.

*3. Computation of latitude, longitude, altitude, and rates.* ($L_{LP}$, $\lambda_{LP}$, $\ell_{LP}$, $h_{LP}$, and rates): These quantities are computed using the following equations:

$L_{LP}$ : Equation A.110
$\ell_{LP}$ : Equation A.111
$\lambda_{LP}$ : Equation A.112
$h_{LP}$ : Equation A.113
$\dot{L}_{LP}$ : Equation A.115
$\dot{\ell}_{LP}$ : Equation A.116
$\dot{\lambda}_{LP}$ : Equation A.117
$\dot{h}_{LP}$ : Equation A.118
$\ddot{L}_{LP}$ : Equation A.119
$\ddot{\ell}_{LP}$ : Equation A.120
$\ddot{\lambda}_{LP}$ : Equation A.121.

*4. Computation of rotational parameters,* ($\phi$, $\theta$, $\psi$, $p$, $q$, $r$):

4a. Compute Euler angles and DCM: During $[t_3, t_4]$, the Euler angles are given by:

$$\phi(t) = \phi_T - \dot{\phi}_T(t - t_3) \quad \text{(A.134)}$$

$$\theta(t) = 0 \quad \text{(A.135)}$$

$$\psi(t) = \psi_3. \quad \text{(A.136)}$$

The corresponding $n$-frame to $b$-frame DCM is:

$$C_n^b(t) = L_r(\phi(t))L_a(\psi_3). \quad \text{(A.137)}$$

4b. Compute angular rates: Following a procedure similar to that for the $[t_1, t_2]$ interval, the following calculations provide the angular rates with respect to inertial space ($p$, $q$, and $r$):

$$\begin{bmatrix} \dot{\phi} \\ \dot{\theta} \\ \dot{\psi} \end{bmatrix} = \begin{bmatrix} -\dot{\phi}_T \\ 0 \\ 0 \end{bmatrix} \quad \text{(A.138)}$$

$$\begin{bmatrix} P \\ Q \\ R \end{bmatrix} = L_r(\phi(t)) \begin{bmatrix} \dot{\phi} \\ \dot{\theta} \\ \dot{\psi} \end{bmatrix} \quad \text{(A.139)}$$

$$\begin{bmatrix} p \\ q \\ r \end{bmatrix} = \begin{bmatrix} P \\ Q \\ R \end{bmatrix} + C_n^b(t) \begin{bmatrix} (\Omega_\oplus + \dot{\ell}) \cos L \\ -\dot{L} \\ -(\Omega_\oplus + \dot{\ell}) \sin L \end{bmatrix} \quad \text{(A.140)}$$

where $C_n^b(t)$ is given by Equation A.137.

### A.3.5 Climb and Descent

Assumptions — The model for climb and descent segments is based on the following assumptions:

- The segment begins at time $t_1$ and ends at time $t_3$
- The $[t_1, t_3]$ interval is divided into two subintervals during which a bang-bang acceleration control is applied:
  - During $[t_1, t_2]$, the LP experiences a total (inclusive of gravity) *upward* vertical acceleration $+n_{CD}\,g$. (If $n_{CD}$ is negative then the acceleration is downward)
  - During $[t_2, t_3]$, the LP experiences a total upward vertical acceleration $-n_{CD}g$
- At times $t_1$ and $t_3$, vertical velocity and acceleration are zero
- At all times, the horizontal acceleration and the roll angle are zero
- At all times, the velocity vector points along the centerline of the LP

- At all times, the pitch rate equals the flight-path angle rate[4]
- The variables listed in Table A.2 are known at $t_1$.

Input Parameters — A climb/descend flight segment is determined by two parameters:

- Final altitude at time $t_3$, $h_3$
- Magnitude of the vertical acceleration of the LP in $g$'s, $|n_{CD}|$.

Computation Algorithm — The objective of the computation algorithm is to compute the variables listed in Table A.2 within the $[t_1, t_3]$ interval. A five-step procedure is followed.

*1. Preliminary Computations.*

1a. Compute times ($t_2$ and $t_3$):

$$t_2 = t_1 + \Delta \tag{A.141}$$
$$t_3 = t_2 + \Delta \tag{A.142}$$
$$\Delta = \sqrt{\frac{h_3 - h_1}{n_{CD}\, g}} \tag{A.143}$$

1b. Compute $n_{CD}$:

$$\text{If} \quad h_3 > h_1 \quad \text{then} \quad n_{CD} = +|n_{CD}| \tag{A.144}$$
$$\text{If} \quad h_3 < h_1 \quad \text{then} \quad n_{CD} = -|n_{CD}|. \tag{A.145}$$

*2. Computation of point mass t-frame trajectory ($p^t_{LP}$, $v^t_{LP}$, $a^t_{LP}$):*

Horizontal motion, $t_1 \le t \le t_3$:

$$a^t_{LPx}(t) = 0 \tag{A.146}$$
$$a^t_{LPy}(t) = 0 \tag{A.147}$$
$$v^t_{LPx}(t) = v^t_{LPx}(t_1) \tag{A.148}$$
$$v^t_{LPy}(t) = v^t_{LPy}(t_1) \tag{A.149}$$
$$p^t_{LPx}(t) = p^t_{LPx}(t_1) + v^t_{LPx}(t_1)(t - t_1) \tag{A.150}$$
$$p^t_{LPy}(t) = p^t_{LPy}(t_1) + v^t_{LPy}(t_1)(t - t_1). \tag{A.151}$$

Vertical motion, $t_1 \le t \le t_2$:

$$a^t_{LPz}(t) = -n_{CD}\, g \tag{A.152}$$
$$v^t_{LPz}(t) = -n_{CD}\, g\,(t - t_1) \tag{A.153}$$
$$p^t_{LPz}(t) = h_{\text{O.TAN}} - h_1 - \frac{n_{CD}\, g}{2}(t - t_1)^2. \tag{A.154}$$

[4]The flight-path angle is the angle between the velocity vector and the horizontal plane (e.g., [Farrell, 1976]).

Vertical motion, $t_2 \leq t \leq t_3$:

$$a^t_{LPz}(t) = +n_{CD}\, g \tag{A.155}$$
$$v^t_{LPz}(t) = -\dot{h}_2 + n_{CD}\, g\,(t - t_2) \tag{A.156}$$
$$p^t_{LPz}(t) = h_{\text{O.TAN}} - h_2 - \dot{h}_2(t - t_2) + \frac{n_{CD}\, g}{2}(t - t_2)^2 \tag{A.157}$$

where

$$h_2 = \frac{h_1 + h_3}{2} \tag{A.158}$$
$$\dot{h}_2 = n_{CD}\, g\,(t_2 - t_1). \tag{A.159}$$

*3. Computation of specific force,* ($f^n$, $f^b$): The acceleration experienced by the LP in the $t$-frame is given by

$$a^t_{LP} = \begin{bmatrix} 0 \\ 0 \\ a^t_{LPz} \end{bmatrix}^t. \tag{A.160}$$

Consequently the specific force experienced by the LP in the $n$-frame is given by

$$f^n \equiv \begin{bmatrix} f_N \\ f_E \\ f_D \end{bmatrix}^n = C^n_t a^t_{LP} - \begin{bmatrix} 0 \\ 0 \\ g \end{bmatrix}^n, \tag{A.161}$$

where $C^n_t$ is given by Equation A.94. In the $b$-frame

$$f^b = C^b_n f^n \tag{A.162}$$

where the formula for $C^b_n$ is given below in Step *5*.

*4. Computation of latitude, longitude, altitude, and rates,* ($L_{LP}$, $\lambda_{LP}$, $\ell_{LP}$, $h_{LP}$, and rates): These quantities are computed using the following equations:

$L_{LP}$ : Equation A.110
$\ell_{LP}$ : Equation A.111
$\lambda_{LP}$ : Equation A.112
$h_{LP}$ : Equation A.113
$\dot{L}_{LP}$ : Equation A.115
$\dot{\ell}_{LP}$ : Equation A.116
$\dot{\lambda}_{LP}$ : Equation A.117
$\dot{h}_{LP}$ : Equation A.118
$\ddot{L}_{LP}$ : Equation A.119
$\ddot{\ell}_{LP}$ : Equation A.120
$\ddot{\lambda}_{LP}$ : Equation A.121.

*5. Computation of rotational parameters,* ($\phi$, $\theta$, $\psi$, $p$, $q$, $r$):

5a. Compute Euler angles and DCM: During $[t_1, t_3]$, the Euler angles (roll, pitch, and yaw) are given by:

$$\phi(t) = 0 \tag{A.163}$$

$$\theta(t) = \arctan\left(\frac{-v^t_{LPz}}{v_l}\right) \tag{A.164}$$

$$\psi(t) = \psi_1 \tag{A.165}$$

where $\psi_1$ is the azimuth at time $t_1$ and

$$v_l = \text{Velocity in the level (horizontal) plane} \tag{A.166}$$

$$= \sqrt{(v^t_{LPx})^2 + (v^t_{LPy})^2}. \tag{A.167}$$

The corresponding $n$-frame to $b$-frame DCM is:

$$C^b_n(t) = L_p(\theta) L_a(\psi_1). \tag{A.168}$$

5b. Compute angular rates: The angular rates with respect to inertial space ($p$, $q$, and $r$) are computed from the angular rates with respect to the $n$-frame ($P$, $Q$, and $R$), which in turn are computed from the Euler angle rates ($\dot{\phi}$, $\dot{\theta}$, and $\dot{\psi}$):

$$\begin{bmatrix} \dot{\phi} \\ \dot{\theta} \\ \dot{\psi} \end{bmatrix} = \begin{bmatrix} 0 \\ \frac{-v_l}{(v_l)^2 + (v^t_{LPz})^2} a^t_{LPz} \\ 0 \end{bmatrix} \tag{A.169}$$

$$\begin{bmatrix} P \\ Q \\ R \end{bmatrix} = \begin{bmatrix} 1 & 0 & -\sin\theta \\ 0 & 1 & 0 \\ 0 & 0 & \cos\theta \end{bmatrix} \begin{bmatrix} \dot{\phi} \\ \dot{\theta} \\ \dot{\psi} \end{bmatrix} \tag{A.170}$$

$$\begin{bmatrix} p \\ q \\ r \end{bmatrix} = \begin{bmatrix} P \\ Q \\ R \end{bmatrix} + C^b_n(t) \begin{bmatrix} (\Omega_\oplus + \dot{\ell}) \cos L \\ -\dot{L} \\ -(\Omega_\oplus + \dot{\ell}) \sin L \end{bmatrix} \tag{A.171}$$

where $C^b_n(t)$ is given by Equation A.168.

### A.3.6 Level Change of Speed

Assumptions — The model for a level change-of-speed is based on the following assumptions:

- Flight begins at time $t_1$ and ends at time $t_2$
- Within the $[t_1, t_2]$ time interval:
  - The heading angle remains constant
  - The pitch and roll angles are zero
  - Vertical acceleration and velocity are zero (altitude is constant)

- The magnitude of the level acceleration is constant (and representative of the maximum acceleration that the LP can develop)

- The variables listed in Table A.2 are known at $t_1$.

Input Parameters — A change-of-speed flight segment is determined by two input parameters:

- Final horizontal (level) velocity, $v_{l2}$
- Magnitude of level acceleration in $g$'s, $|n_l|$ .

Computation Algorithm — The objective of the computation algorithm is to compute the variables listed in Table A.2 within the $[t_1, t_2]$ interval. A four-step procedure is followed.

*1. Preliminary Computations.*

1a. Compute the initial speed, $v_{l1}$:

$$v_{l1} = \sqrt{v^t_{LPx}(t_1)^2 + v^t_{LPy}(t_1)^2}. \tag{A.172}$$

1b. Compute the final time, $t_2$:

$$t_2 = t_1 + \frac{|v_{l2} - v_{l1}|}{|n_l|\, g}. \tag{A.173}$$

1c. Compute the final/initial speed ratio, $\rho_l$, if $v_{l1} > 0$:

$$\rho_l = \frac{v_{l2}}{v_{l1}}. \tag{A.174}$$

1d. Compute $n_l$:

$$\text{If} \quad v_{l1} = 0 \text{ or } \rho_l > 1 \quad \text{then } n_l = +|n_l| \qquad \text{(speed-up)} \tag{A.175}$$

$$\text{If} \quad \rho_l < 1 \quad \text{then } n_l = -|n_l| \qquad \text{(slow-down).} \tag{A.176}$$

*2. Computation of point mass t-frame trajectory ($p^t_{LP}$, $v^t_{LP}$, $a^t_{LP}$):*

2a. Compute acceleration in the $t$-frame, $a_{LP}$, $t_1 \le t \le t_2$:

**If** $v_{l1} = 0$ (start-up on the ground):

$$a^t_{LPx} = |n_l|\, g \cos\psi_1 \tag{A.177}$$

$$a^t_{LPy} = |n_l|\, g \sin\psi_1 \tag{A.178}$$

$$a^t_{LPz} = 0 \tag{A.179}$$

where $\psi_1$ is the heading at $t_1$.

**If** $v_{l1} \neq 0$ (speed-up or slow-down):

$$a^t_{LPx} = \frac{v^t_{LPx}(t_1)}{v_{l1}} n_l\, g \tag{A.180}$$

$$a^t_{LPy} = \frac{v^t_{LPy}(t_1)}{v_{l1}} n_l\, g \tag{A.181}$$

$$a^t_{LPz} = 0. \tag{A.182}$$

2b. Compute position and velocity, $t_1 \leq t \leq t_2$:

$$v^t_{LP}(t) = v^t_{LP}(t_1) + a^t_{LP}(t - t_1) \quad \text{(A.183)}$$

$$p^t_{LP}(t) = p^t_{LP}(t_1) + v^t_{LP}(t_1)(t - t_1) + \frac{1}{2}a^t_{LP}(t - t_1)^2. \quad \text{(A.184)}$$

*3. Computation of specific force,* ($f^n$, $f^b$):

$$f^n \equiv \begin{bmatrix} f_N \\ f_E \\ f_D \end{bmatrix}^n = C^n_t a^t_{LP} - \begin{bmatrix} 0 \\ 0 \\ g \end{bmatrix}^n, \quad \text{(A.185)}$$

where $C^n_t$ is given by Equation A.94. In the $b$-frame

$$f^b = C^b_n f^n \quad \text{(A.186)}$$

where the formula for $C^b_n$ is given below in Step *5* (Equation A.190).

*4. Computation of latitude, longitude, altitude, and rates,* ($L_{LP}$, $\lambda_{LP}$, $\ell_{LP}$, $h_{LP}$, and rates): These quantities are computed using the following equations:

$L_{LP}$ : Equation A.110
$\ell_{LP}$ : Equation A.111
$\lambda_{LP}$ : Equation A.112
$h_{LP}$ : Equation A.113
$\dot{L}_{LP}$ : Equation A.115
$\dot{\ell}_{LP}$ : Equation A.116
$\dot{\lambda}_{LP}$ : Equation A.117
$\dot{h}_{LP}$ : Equation A.118
$\ddot{L}_{LP}$ : Equation A.119
$\ddot{\ell}_{LP}$ : Equation A.120
$\ddot{\lambda}_{LP}$ : Equation A.121.

*5. Computation of rotational parameters,* ($\phi$, $\theta$, $\psi$, $p$, $q$, $r$):

5a. Compute Euler angles and DCM: During $[t_1, t_2]$, the Euler angles (roll, pitch, and yaw) are given by:

$$\phi(t) = 0 \quad \text{(A.187)}$$

$$\theta(t) = 0 \quad \text{(A.188)}$$

$$\psi(t) = \psi_1 \quad \text{(A.189)}$$

where $\psi_1$ is the azimuth at time $t_1$ and the small variation in azimuth because due to translational motion is neglected. The corresponding $n$-frame to $b$-frame DCM is:

$$C^b_n(t) = L_a(\psi_1). \quad \text{(A.190)}$$

5b. Compute angular rates: The angular rates with respect to inertial space ($p$, $q$, and $r$) are computed from the angular rates with respect to the $n$-frame ($P$, $Q$, and $R$), which in turn are computed from the Euler angle rates ($\dot{\phi}$, $\dot{\theta}$, and $\dot{\psi}$):

$$\begin{bmatrix} \dot{\phi} \\ \dot{\theta} \\ \dot{\psi} \end{bmatrix} = \begin{bmatrix} 0 \\ 0 \\ 0 \end{bmatrix} \tag{A.191}$$

$$\begin{bmatrix} P \\ Q \\ R \end{bmatrix} = \begin{bmatrix} 0 \\ 0 \\ 0 \end{bmatrix} \tag{A.192}$$

$$\begin{bmatrix} p \\ q \\ r \end{bmatrix} = C_n^b(t) \begin{bmatrix} (\Omega_\oplus + \dot{\ell}) \cos L \\ -\dot{L} \\ -(\Omega_\oplus + \dot{\ell}) \sin L \end{bmatrix} \tag{A.193}$$

where $C_n^b(t)$ is given by Equation A.190.

### A.3.7 Ground Azimuth Change

An azimuth change while on the ground is executed by rotating the aircraft about the *D*own axis of the $n$-frame.

Assumptions — The model for an azimuth change is based on the following assumptions:

- Azimuth change begins at time $t_1$ and ends at time $t_2$
- Within the $[t_1, t_2]$ time interval:
  - The heading angle varies linearly with time
  - The pitch and roll angles are zero
  - Horizontal and vertical accelerations and velocities are zero
- The magnitude of the azimuth rate is $|\omega_a| = 20$ deg/sec
- The variables listed in Table A.2 are known at $t_1$.

Input Parameters — A change of azimuth is determined by two input parameters:

- Final heading, $\psi_2$
- Clockwise (CW) or Counter-Clockwise (CCW) turn.

Computation Algorithm — The objective of the computation algorithm is to compute the variables listed in Table A.2 within the $[t_1, t_2]$ interval. A five-step procedure is followed.

*1. Preliminary Computations.*

1a. Compute $\omega_a$:

$$\omega_a = \begin{cases} +20 \text{ deg/sec} & \text{if CW} \\ -20 \text{ deg/sec} & \text{if CCW} \end{cases} \tag{A.194}$$

1b. Compute the final time, $t_2$:

$$t_2 = \frac{[\psi_2 - \psi_1]_{\text{modulo}}}{\omega_a} \tag{A.195}$$

where $\psi_1$ and $\psi_2$ are the initial and final azimuths and the qualifier "modulo" indicates that the difference should be taken modulo 360 deg and taking into account the direction of turn.

*2. Computation of point mass t-frame trajectory* ($p^t_{LP}$, $v^t_{LP}$, $a^t_{LP}$):

2a. Velocity and Acceleration: For $t_1 \leq t \leq t_2$,

$$v^t_{LP}(t) = a^t_{LP}(t) = 0. \tag{A.196}$$

2b. Position: For $t_1 \leq t \leq t_2$,

$$p^t_{LP}(t) = p^t_{LP}(t_1). \tag{A.197}$$

*3. Computation of specific force,* ($f^n$, $f^b$): Because the center of mass of the LP experiences zero acceleration, the specific force in the $n$-frame is given by

$$f^n \equiv \begin{bmatrix} f_N \\ f_E \\ f_D \end{bmatrix}^n = \begin{bmatrix} 0 \\ 0 \\ -g \end{bmatrix}^n, \tag{A.198}$$

and in the $b$-frame

$$f^b = C^b_n f^n \tag{A.199}$$

where the formula for $C^b_n$ is given below in Step *5* (Equation A.203).

*4. Computation of latitude, longitude, altitude, and rates,* ($L_{LP}$, $\lambda_{LP}$, $\ell_{LP}$, $h_{LP}$, and rates): During the $[t_1, t_2]$ interval these quantities are given by:

$$\begin{aligned}
L_{LP} &= L_{t_1} \\
\ell_{LP} &= \ell_{t_1} \\
\lambda_{LP} &: \text{ Equation A.112} \\
h_{LP} &= h_{t_1} \\
\dot{L}_{LP} &= 0 \\
\dot{\ell}_{LP} &= 0 \\
\dot{\lambda}_{LP} &: \text{ Equation A.117} \\
\dot{h}_{LP} &= 0 \\
\ddot{L}_{LP} &= 0 \\
\ddot{\ell}_{LP} &= 0 \\
\ddot{\lambda}_{LP} &: \text{ Equation A.121.}
\end{aligned}$$

*5. Computation of rotational parameters, ($\phi$, $\theta$, $\psi$, $p$, $q$, $r$):*

5a. Compute Euler angles and DCM: During $[t_1, t_2]$, the Euler angles (roll, pitch, and yaw) are given by:

$$\phi(t) = 0 \tag{A.200}$$
$$\theta(t) = 0 \tag{A.201}$$
$$\psi(t) = \psi_1 + \omega_a (t_2 - t_1). \tag{A.202}$$

The corresponding $n$-frame to $b$-frame DCM is:

$$C_n^b(t) = L_a(\psi(t)). \tag{A.203}$$

5b. Compute angular rates: The angular rates with respect to inertial space ($p$, $q$, and $r$) are computed from the angular rates with respect to the $n$-frame ($P$, $Q$, and $R$), which coincide with the Euler angle rates ($\dot{\phi}$, $\dot{\theta}$, and $\dot{\psi}$):

$$\begin{bmatrix} \dot{\phi} \\ \dot{\theta} \\ \dot{\psi} \end{bmatrix} = \begin{bmatrix} 0 \\ 0 \\ \omega_a \end{bmatrix} \tag{A.204}$$

$$\begin{bmatrix} P \\ Q \\ R \end{bmatrix} = \begin{bmatrix} \dot{\phi} \\ \dot{\theta} \\ \dot{\psi} \end{bmatrix} = \begin{bmatrix} 0 \\ 0 \\ \omega_a \end{bmatrix} \tag{A.205}$$

$$\begin{bmatrix} p \\ q \\ r \end{bmatrix} = \begin{bmatrix} P \\ Q \\ R \end{bmatrix} + C_n^b(t) \begin{bmatrix} (\Omega_\oplus + \dot{\ell}) \cos L \\ -\dot{L} \\ -(\Omega_\oplus + \dot{\ell}) \sin L \end{bmatrix} \tag{A.206}$$

where $C_n^b(t)$ is given by Equation A.203.

## A.3.8 Constant Acceleration

A constant acceleration trajectory is needed for the propagation of the M INS dynamics during flyout as described in Subsection A.9.9. Motion variables for such a trajectory are defined in the following paragraphs.[5]

Assumptions — The model for a constant acceleration segment is based on the following assumptions:

- The segment begins at time $t_1$
- After $t_1$ all accelerations are constant
- At all times, the roll angle is zero

[5]Notation: Even though the constant acceleration event is necessary only to analyze M motion after launch, "LP" is used to label variables in this subsection to maintain consistency with the development of previous subsections.

- At all times, the velocity vector points along the centerline of the LP (pitch rate equals the flight-path angle rate)
- The variables listed in Table A.2 are known at $t_1$.

Input Parameters — A constant acceleration segment is determined by three parameters:

- $a_{l,x}$ = level acceleration in the North direction
- $a_{l,y}$ = level acceleration in the East direction
- $a_z$ = vertical acceleration (Down direction).

Computation Algorithm — The objective of the computation algorithm is to compute the variables listed in Table A.2 for times after $t_1$. A five-step procedure is followed.

*1. Preliminary Computations.*

*2. Computation of point mass t-frame trajectory* ($p^t_{LP}$, $v^t_{LP}$, $a^t_{LP}$):

Acceleration:

$$a^t_{LP} = \begin{bmatrix} a_{l,x} \\ a_{l,y} \\ a_z \end{bmatrix}^t . \tag{A.207}$$

Velocity:

$$v^t_{LP}(t) = v^t_{LP}(t_1) + (t - t_1)a^t_{LP}. \tag{A.208}$$

Position:

$$p^t_{LP}(t) = p^t_{LP}(t_1) + (t - t_1)v^t_{LP}(t_1) + \frac{1}{2}(t - t_1)^2 a^t_{LP}. \tag{A.209}$$

*3. Computation of specific force,* ($f^n$, $f^b$): The acceleration experienced by the LP in the $i$-frame is given in Equation A.207. Consequently the specific force experienced by the LP in the $n$-frame is given by

$$f^n \equiv \begin{bmatrix} f_N \\ f_E \\ f_D \end{bmatrix}^n = C^n_t a^t_{LP} - \begin{bmatrix} 0 \\ 0 \\ g \end{bmatrix}^n , \tag{A.210}$$

where $C^n_t$ is given by Equation A.94. In the $b$-frame

$$f^b = C^b_n f^n \tag{A.211}$$

where the formula for $C^b_n$ is given below in Step 5.

*4. Computation of latitude, longitude, altitude, and rates,* ($L_{LP}$, $\lambda_{LP}$, $\ell_{LP}$, $h_{LP}$, and rates): These quantities are computed using the following equations:

$$\begin{aligned}
L_{LP} &: \text{Equation A.110} \\
\ell_{LP} &: \text{Equation A.111} \\
\lambda_{LP} &: \text{Equation A.112} \\
h_{LP} &: \text{Equation A.113} \\
\dot{L}_{LP} &: \text{Equation A.115} \\
\dot{\ell}_{LP} &: \text{Equation A.116} \\
\dot{\lambda}_{LP} &: \text{Equation A.117} \\
\dot{h}_{LP} &: \text{Equation A.118} \\
\ddot{L}_{LP} &: \text{Equation A.119} \\
\ddot{\ell}_{LP} &: \text{Equation A.120} \\
\ddot{\lambda}_{LP} &: \text{Equation A.121.}
\end{aligned}$$

*5. Computation of rotational parameters,* ($\phi$, $\theta$, $\psi$, $p$, $q$, $r$):

5a. Compute Euler angles and DCM: After $t_1$, the Euler angles (roll, pitch, and yaw) are given by:

$$\phi(t) = 0 \tag{A.212}$$

$$\theta(t) = \arctan\left(\frac{-v^t_{LPz}}{v_l}\right) \tag{A.213}$$

$$\psi(t) = \arctan\left(\frac{v_{LPy}}{v_{LPx}}\right) \tag{A.214}$$

where

$$v_l = \text{Velocity in the level (horizontal) plane} \tag{A.215}$$

$$= \sqrt{(v^t_{LPx})^2 + (v^t_{LPy})^2}. \tag{A.216}$$

The corresponding $n$-frame to $b$-frame DCM is:

$$C^b_n(t) = L_p(\theta)L_a(\psi). \tag{A.217}$$

5b. Compute angular rates: The angular rates with respect to inertial space ($p$, $q$, and $r$) are computed from the angular rates with respect to the $n$-frame ($P$, $Q$, and $R$), which in turn are computed from the Euler angle rates ($\dot{\phi}$, $\dot{\theta}$, and $\dot{\psi}$):

$$\begin{bmatrix} \dot{\phi} \\ \dot{\theta} \\ \dot{\psi} \end{bmatrix} = \begin{bmatrix} 0 \\ \frac{-v_l}{(v_l)^2+(v^t_{LPx})^2} a^t_{LPz} \\ \frac{v^t_{LPx}a_{l,y} - v^t_{LPy}a_{l,x}}{(v^t_{LPx})^2+(v^t_{LPy})^2} \end{bmatrix} \tag{A.218}$$

$$\begin{bmatrix} P \\ Q \\ R \end{bmatrix} = \begin{bmatrix} 1 & 0 & -\sin\theta \\ 0 & 1 & 0 \\ 0 & 0 & \cos\theta \end{bmatrix} \begin{bmatrix} \dot{\phi} \\ \dot{\theta} \\ \dot{\psi} \end{bmatrix} \tag{A.219}$$

$$\begin{bmatrix} p \\ q \\ r \end{bmatrix} = \begin{bmatrix} P \\ Q \\ R \end{bmatrix} + C_n^b(t) \begin{bmatrix} (\Omega_\oplus + \dot{\ell}) \cos L \\ -\dot{L} \\ -(\Omega_\oplus + \dot{\ell}) \sin L \end{bmatrix} \tag{A.220}$$

where $C_n^b(t)$ is given by Equation A.217.

## A.4 M INS Model

The model for the M strapdown INS is given by Equation B.1 of Appendix B with the following modifications:

- Because the M INS is a strapdown system, the direction cosine matrix (DCM) $\underline{C}_p^n$ in Equation B.5 is replaced by the DCM $\underline{C}_b^n$ specifying the transformation from the body to the navigation frame in Equations B.5 and B.8. This DCM is a function of the trajectory followed by the M as specified in Section A.9.
- The altimeter gains $K_1$ and $K_2$ which appear in Figure B.1 and Equation B.11 are set to the values given in Table B.3 for the M.
- The sensor error models, characterizing the vectors $\underline{\varepsilon}$ $\underline{\alpha}$ and $\delta h_A$, are as given in Table A.3.
- The white noise vector $\underline{w}_n$ is non-zero as described in Subsection B.8.

Table A.3: M INS SENSOR ERROR MODELS[6]

| INSTRUMENT | ERROR SOURCE | MODEL | MODEL PARAMETERS[7] |
|---|---|---|---|
| Laser Gyro | Turn-on Repeatability Bias | Bias | $\sigma$ = 1.0 deg/hr |
| | Bias Drift Rate | Markov | $\sigma$ =0.1 deg/hr, $\tau$ = 1 hr |
| | Random Drift Rate[8] | White Noise | $Q = (0.030 \text{ deg}/\sqrt{\text{hr}})^2$ |
| | Scale Factor | Bias | $\sigma$ = 100 ppm |
| | Misalignment | Bias | $\sigma$ = 6 $\widehat{\text{sec}}$ |
| Accelerometer | Turn-on Repeatability Bias | Bias | $\sigma$ = 1500 $\mu$g |
| | Bias #1 | Markov | $\sigma$ = 240 $\mu$g, $\tau$ = 60 min |
| | Bias #2 | Markov | $\sigma$ = 120 $\mu$g, $\tau$ = 15 min |
| | Scale Factor | Bias | $\sigma$ =500 ppm |
| | Misalignment | Bias | $\sigma$ = 20 $\widehat{\text{sec}}$ |
| Altimeter | Bias | Markov | $\sigma$ = 150 m, $\tau = 463000/v$ sec |
| | Scale Factor | Bias | $\sigma$ = 0.03 |

[6]Source: [Levinson et al., 1977] and [Maybeck, 1977]. Error characteristics comparable to Sperry SLIC-15 INS with Hamilton Standard accelerometer model ([Maybeck, 1976] and [Maybeck, 1977]) scaled to SLIC-15 (Q-Flex accelerometer) bias error level.

[7]Notation: $\sigma$ is the standard deviation of bias and Markov error sources; $\tau$ is the correlation time of Markov error sources; $Q$ is the $Q$-matrix (spectral level, [Gelb, 1974]) of the white noise; $v$ is the M velocity in m/sec.

[8]The white noise random drift rate is modeled as a first-order Markov with $\tau = \Delta/2$ and $\sigma^2 = Q/\Delta$ where $\Delta$ is the sampling interval between propagations or updates.

## A.5 LP INS Model

The model for the LP strapdown INS is given by Equation B.1 of Appendix B with the following modifications:

- Because the M INS is a strapdown system, the direction cosine matrix (DCM) $\underline{C}_p^n$ in Equation B.5 is replaced by the DCM $\underline{C}_b^n$ specifying the transformation from the body to the navigation frame in Equations B.5 and B.8. This DCM is a function of the trajectory followed by the LP as specified in Subsection A.3 (Equations A.3, A.30, A.42, A.72, A.125, A.137, A.168, A.190, A.203).
- The altimeter gains $K_1$ and $K_2$ which appear in Figure B.1 and Equation B.11 are set to the values given in Table B.3 for the LP.
- The sensor error models, characterizing the vectors $\underline{\varepsilon}$ $\underline{\alpha}$ and $\delta h_A$, are as given in Table A.4.
- The white noise vector $\underline{w}_n$ is non-zero as described in Subsection B.8.

Table A.4: LP INS SENSOR ERROR MODELS[9]

| INSTRUMENT | ERROR SOURCE | MODEL | MODEL PARAMETERS[10] |
|---|---|---|---|
| Laser Gyro | Turn-on Repeatability Bias | Bias | $\sigma = 0.004$ deg/hr |
| | Random Drift Rate[11] | White Noise | $Q = (0.004 \text{ deg}/\sqrt{\text{hr}})^2$ |
| | Scale Factor | Bias | 10 ppm |
| | Misalignment | Bias | $\sigma = 6$ sec |
| Accelerometer | Turn-on Repeatability Bias | Bias | $\sigma = 100$ $\mu$g |
| | Bias #1 | Markov | $\sigma = 16$ $\mu$g, $\tau = 60$ min |
| | Bias #2 | Markov | $\sigma = 8$ $\mu$g, $\tau = 15$ min |
| | Scale Factor | Bias | $\sigma$ =200 ppm |
| | Misalignment | Bias | $\sigma = 4$ sec |
| Altimeter | Bias | Markov | $\sigma = 150$ m, $\tau = 463000/v$ sec |
| | Scale Factor | Bias | $\sigma = 0.03$ |

## A.6 SP INS Model

The model for the SP strapdown INS is given by Equation B.1 of Appendix B with the following modifications:

[9]Source: [Levinson, 1978] and [Maybeck, 1977]. Error characteristics comparable to Honeywell LINS-0 INS with Hamilton Standard accelerometer model ([Maybeck, 1976] and [Maybeck, 1977]) scaled to LINS-0 bias error level.

[10]Notation: $\sigma$ is the standard deviation of bias and Markov error sources; $\tau$ is the correlation time of Markov error sources; $Q$ is the $Q$-matrix of the white noise; $v$ is the LP velocity in m/sec.

[11]The white noise random drift rate is modeled as a first-order Markov with $\tau = \Delta/2$ and $\sigma^2 = Q/\Delta$ where $\Delta$ is the sampling interval between propagations or updates.

- Because the SP INS is a level-platform system, the direction cosine matrix (DCM) $\underline{C}_p^n$ in Equation B.5 is replaced by the identity matrix in Equations B.5 and B.8.
- The altimeter gains $K_1$ and $K_2$ which appear in Figure B.1 and Equation B.11 are set to the values given in Table B.3 for the SP.
- The sensor error models, characterizing the vectors $\underline{\varepsilon}$, $\underline{\alpha}$, and $\delta h_A$, are as given in Table A.5
- The white noise vector $\underline{w}_n$ is zero as described in Subsection B.8.

Table A.5: SP INS SENSOR ERROR MODELS[12]

| INSTRUMENT | ERROR SOURCE | MODEL | MODEL PARAMETERS[13] |
|---|---|---|---|
| SDOF Gyro | G-Insensitive Bias | Bias | $\sigma = 0.005$ deg/hr |
| | G-, $G^2$-Sensitive Bias | — | Neglected[14] |
| | Bias #1 | Markov | $\sigma = 0.002$ deg/hr, $\tau = 60$ min |
| | Bias #2 | Markov | $\sigma = 0.001$ deg/hr, $\tau = 15$ min |
| | Scale Factor | Markov | $\sigma = 0.0025$ deg/hr $\tau = 60$ min |
| | Misalignment | Bias | $\sigma = 0.2$ $\widehat{\text{sec}}$ |
| Accelerometer | Turn-on Repeatability Bias | Bias | $\sigma = 10$ $\mu$g |
| | Bias #1 | Markov | $\sigma = 3$ $\mu$g, $\tau = 60$ min |
| | Bias #2 | Markov | $\sigma = 2$ $\mu$g, $\tau = 15$ min |
| | Scale Factor | — | Neglected[14] |
| | Misalignment | Bias | $\sigma = 2$ $\widehat{\text{sec}}$ |
| Altimeter | Bias | Markov | $\sigma = 6$ m, $\tau = 30$ sec |

Table A.6

Table A.6: GRAVITY ERROR MODEL FOR SP INS[15]

| ERROR SOURCE | SYMBOL | MODEL | MODEL PARAMETERS[16] |
|---|---|---|---|
| Meridian Deflection (about East) | $\xi$ | Markov | $\sigma = 26.0 \times 10^{-6}$ rad, $\tau = 1.852 \times 10^4/v$ sec |
| Prime Deflection (about North) | $\eta$ | Markov | $\sigma = 17.0 \times 10^{-6}$ rad, $\tau = 1.852 \times 10^4/v$ sec |
| Gravity Anomaly | $\Delta G$ | Markov | $\sigma = 343.0 \times 10^{-6}$ m/sec$^2$, $\tau = 1.111 \times 10^5/v$ sec |

[12]Source: Error characteristics comparable to high-accuracy (conventional gyro) model in [Mueller et al., 1977] with: gyro Markov biases and misalignments from Hamilton Standard model ([Maybeck, 1976] and [Maybeck, 1977]) scaled to the gyro bias error level; and Hamilton Standard accelerometer model scaled to the accelerometer bias error level.

[13]Notation: $\sigma$ is the standard deviation of bias and Markov error sources; $\tau$ is the correlation time of Markov error sources.

[14]SP acceleration is neglected.

[15]Source: [Maybeck, 1977].

[16]Notation: $\sigma$ is the standard deviation and $\tau$ is the correlation time of Markov error sources; $v$ is the magnitude of SP velocity.

[17]Source: [Perlmutter et al., 1977].

[18]Uncorrelated measurement sequence.

Table A.7: GPS ERROR MODEL PARAMETERS[17]

| PARAMETER | PARAMETER VALUE |
|---|---|
| Position Measurement Std. Dev.[18] | 15 m |
| Position Velocity Std. Dev.[18] | 0.1 m/sec |
| Update Interval | 10 sec |

## A.7 M, LP, and SP Ground Align Model

The simulation of ground alignment has three steps:

1. Covariance initialization
2. State augmentation
3. Riccatti equation propagation.

These three steps are described in the following three paragraphs.

*Covariance Initialization.* The INS covariance ($P_{\text{M INS}}$, $P_{\text{M INS}}$, or $P_{\text{M INS}}$, depending on the INS under consideration) is initialized to a diagonal matrix indicative of the errors in the approximate initialization entered by ground personnel. Table A.8 gives the RMS levels of the first nine diagonal entries in the initial covariance matrix for all three vehicles (M, LP, and SP). The RMS levels of the other diagonal entries (gyro, accelerometer, and altimeter error sources) are set to the RMS levels listed in Tables A.3, A.4, and A.5.

Table A.8: RMS LEVELS OF INITIAL INS STATES[19]

| SYMBOL[20] | DEFINITION | RMS LEVEL |
|---|---|---|
| $\delta\theta_{*N}$ | Attitude Error About N Axis | 60 min |
| $\delta\theta_{*E}$ | Attitude Error About E Axis | 60 min |
| $\delta\theta_{*D}$ | Attitude Error About D Axis | 300 min |
| $\delta\dot{L}_*$ | Latitude Rate Error | 0.016 sec /sec |
| $\delta\dot{\ell}_*$ | Longitude Rate Error | 0.022 sec /sec |
| $\delta\dot{h}_*$ | Altitude Rate Error | 0.5 m/sec |
| $\delta L_*$ | Latitude Error | 5 m |
| $\delta\ell*$ | Longitude Error | 5 min |
| $\delta h_*$ | Altitude Error | 170 m |

*State Augmentation.* Ground align is modeled by simulating seven noisy measurements of the INS state: a magnetic heading as measured with a flux valve, three positions (the

[19]Source: [San Giovanni, 1977]. Assumed ground alignment location (near Norfolk Va.): Latitude North = 37 deg; longitude West = 76 deg; altitude = 3 m.

[20]Notation: "*" indicates M, L (for LP), or S (for SP).

approximately known position of the aircraft at home-base), and three velocities (indicative of wind buffeting of a stationary aircraft). The error models for these measurements are given in Table A.9.

Table A.9: GROUND ALIGN MEASUREMENT ACCURACIES[21]

| MEASUREMENT | MEASUREMENT MODEL | MODEL PARAMETER[22] |
|---|---|---|
| Heading | Bias + White Noise | $\sigma_{\text{bias}} = 2$ deg<br>$\sigma_{\text{white noise}} = 15$ min |
| North Position | White Noise | $\sigma = 3$ m |
| East Position | " | " |
| Down Position | " | " |
| North Velocity | White Noise | $\sigma = 0.005$ m/sec |
| East Velocity | " | " |
| Down Velocity | " | " |

The magnetic heading error model includes two components: a bias due to uncompensated error in magnetic variation; and a white noise component due to flux valve error. To simulate the bias component, the covariance matrix of the INS needs to be augmented with an additional bias state having the RMS accuracy shown in Table A.9. This state is removed after completion of the ground align simulation.

*Riccatti Equation Propagation.* The Riccatti equation is propagated for a 10 min interval with measurements every 30 sec using the following state-space matrices:

- $\underline{F}$ and $\underline{Q}$ matrices from the INS error models for the M, LP, and SP described in Subsections A.4, A.5, and A.6, each with an additional zero-row and zero-column to model the bias magnetic heading error described in the previous paragraph. These matrices specify the state-space equations
- Initial covariance matrix as described in the *Covariance Initialization* paragraph
- Measurement equation of the form

$$\underline{z}_{\mathbf{ga}} = \underline{H}_{\mathbf{ga}}\underline{\ } + \underline{v}_{\mathbf{ga}} \tag{A.221}$$

  where the entries in the vector $\underline{z}_{\mathbf{ga}}$ correspond to the seven measurements listed in Table A.9

- $\underline{H}$-Matrix given by

$$\underline{H}_{\mathbf{ga}} = \left[\ \underline{H}_{\mathbf{ga1}} \mid \underline{H}_{\mathbf{ga2}} \mid \underline{H}_{\mathbf{ga3}}\ \right] \tag{A.222}$$

[21] Source: [San Giovanni, 1977].

[22] Notation: $\sigma$ is the standard deviation of the bias or discrete-time white noise.

where:

$$\underline{H}_{\text{ga1}} = \left[\begin{array}{ccc|ccc|ccc} 0 & 0 & 1 & 0 & 0 & 0 & 0 & 0 & 0 \\ \hline 0 & 0 & 0 & 1 & 0 & 0 & 0 & 0 & 0 \\ 0 & 0 & 0 & 0 & 1 & 0 & 0 & 0 & 0 \\ 0 & 0 & 0 & 0 & 0 & 1 & 0 & 0 & 0 \\ \hline 0 & 0 & 0 & 0 & 0 & 0 & 1 & 0 & 0 \\ 0 & 0 & 0 & 0 & 0 & 0 & 0 & 1 & 0 \\ 0 & 0 & 0 & 0 & 0 & 0 & 0 & 0 & 1 \end{array}\right] \tag{A.223}$$

$$\underline{H}_{\text{ga2}} = \underline{0}_{7\times(\dim\{\underline{\varepsilon}\}+\dim\{\underline{\alpha}\}+1)} \tag{A.224}$$

$$\underline{H}_{\text{ga3}} = \left[\begin{array}{c} 1 \\ \hline 0 \\ 0 \\ 0 \\ \hline 0 \\ 0 \\ 0 \end{array}\right] \tag{A.225}$$

The blocks within $\underline{H}_{\text{ga}}$ are as follows. The first row of $\underline{H}_{\text{ga1}}$ and the first row of $\underline{H}_{\text{ga3}}$ model the heading measurement as a linear combination of the heading error state (e.g., $\delta\theta_{\text{MD}}$) and the heading instrument bias (to which white noise is added via the first entry in $\underline{v}_{\text{ga}}$). The other non-zero entries in $\underline{H}_{\text{ga1}}$ model the measurement of position and velocity. The $\underline{H}_{\text{ga2}}$ is zero because the gyro, accelerometer, and altimeter error states are not directly measured.

- The $\underline{R}$-Matrix is specified by the white noise entries listed in Table A.9.

# A.8 M Transfer Align Model

The transfer-align model is composed of two parts:

- A state-space model (dynamics and measurement equations) which specifies the transfer-align Kalman filter
- An LP maneuver model (deterministic) which specifies the trajectory followed by the LP during transfer-alignment.

These two models are described in Subsections A.8.1 and A.8.2.

## A.8.1 State-Space Transfer-Align Model

Background -- The objective of the development that follows is to obtain a state-space model for the transfer-alignment measurements, $\underline{Z}_{TA}$:

$$\begin{aligned} \dot{\underline{X}}_{TA} &= \underline{F}_{TA}\,\underline{X}_{TA} + \underline{W}_{TA} \\ \underline{Z}_{TA} &= \underline{H}_{TA}\,\underline{X}_{TA} + \underline{V}_{TA}\,. \end{aligned} \tag{A.226}$$

The variables in these equations can be divided into four groups as follows. State equation variables:

$$\underline{X}_{TA} = \begin{bmatrix} \underline{x}_{LP} \\ \underline{x}_{M} \end{bmatrix} \tag{A.227}$$

$\underline{x}_{LP}$ = LP INS error state vector specified in Table 3.4

$\underline{x}_{M}$ = M INS error state vector specified in Table 3.8

$\underline{F}_{TA}$ = $F$-matrix

$$= \begin{bmatrix} \underline{F}_{LP} & \underline{0} \\ \underline{0} & \underline{F}_{M} \end{bmatrix} \tag{A.228}$$

$\underline{W}_{TA}$ = White-noise vector

$$= \begin{bmatrix} \underline{w}_{LP} \\ \underline{w}_{M} \end{bmatrix}. \tag{A.229}$$

where $\underline{F}_{LP}$ and $\underline{F}_{M}$ are the $F$-matrices of the LP and M INS appearing in Equation B.1, and $\underline{w}_{LP}$ and $\underline{w}_{M}$ are the corresponding white-noise vectors. Measurements:

$$\underline{Z}_{TA} = \begin{bmatrix} \underline{Z}_{TA,p} \\ \underline{Z}_{TA,v} \end{bmatrix} \tag{A.230}$$

$\underline{Z}_{TA,p}$ = Position difference measurement

$$= \hat{p}^n_M - \hat{p}^n_{LP}|_M \tag{A.231}$$

$\underline{Z}_{TA,v}$ = Velocity difference measurement

$$= \hat{v}^n_M - \hat{v}^n_{LP}|_M \tag{A.232}$$

$\hat{p}^n_M$ = Position read-out of M INS in the $n$-frame

$\hat{p}^n_{LP}|_M$ = Position of M based on read-out of LP INS in the $n$-frame

$\hat{v}^n_M$ = Velocity read-out of M INS in the $n$-frame

$\hat{v}^n_{LP}|_M$ = Velocity of M based on read-out of LP INS in the $n$-frame.

$H$-matrix:

$$\underline{H}_{TA} = \begin{bmatrix} \underline{H}_{TA,p} \\ \underline{H}_{TA,v} \end{bmatrix} \tag{A.233}$$

$\underline{H}_{TA,p}$ = $3 \times [\dim\{\underline{x}_{LP}\} + \dim\{\underline{x}_{M}\}]$ matrix specifying the position measurement

$\underline{H}_{TA,v}$ = $3 \times [\dim\{\underline{x}_{LP}\} + \dim\{\underline{x}_{M}\}]$ matrix specifying the velocity measurement.

Measurement noise:

$$\underline{V}_{TA} = \begin{bmatrix} \underline{V}_{TA,p} \\ \underline{V}_{TA,v} \end{bmatrix} \tag{A.234}$$

$\underline{V}_{TA,p}$ = $3 \times 1$ position measurement noise vector

$\underline{V}_{TA,v}$ = $3 \times 1$ velocity measurement noise vector.

The position and velocity measurement noise is specified by the covariance matrix

$$\underline{R}_{TA} = E\{\underline{V}_{TA}\,\underline{V}^T_{TA}\}. \tag{A.235}$$

The equations listed above specify a Kalman filter which estimates the state of the M INS based on measurements generated by subtracting (appropriately) the difference in the position and velocity read-outs of the M and LP INSs.[23] The accuracy of the estimates provided by the Kalman filter is specified by the error covariance matrix of the state $\underline{X}_{TA}$,

$$\underline{P}_{TA} = E\{(\underline{X}_{TA} - \hat{\underline{X}}_{TA})(\underline{X}_{TA} - \hat{\underline{X}}_{TA})^T\} \tag{A.236}$$

($\hat{\underline{X}}_{TA}$ is the Kalman estimate). This matrix is obtained by propagating the associated Riccatti equation ([Gelb, 1974]). From $\underline{P}_{TA}$, the error covariance matrix for the M at the end of the transfer alignment is obtained by a $CPC^T$ transformation:

$$\underline{P}_M(t_{\text{END TA}}) = \underline{C}\,\underline{P}_{TA}\,\underline{C}^T \tag{A.237}$$

where

$$\underline{C} = \left[\ \underline{0}_{\dim\{\underline{x}_{LP}\}} \quad \underline{I}_{\dim\{\underline{x}_M\}}\ \right]. \tag{A.238}$$

The computation of the covariance defined in Equation A.237 is the objective of the transfer-align simulation.

Input Parameters — The following parameters are set before the computation algorithm is begun:

- The time at which transfer-alignment begins, $t_{\text{BEGIN TA}}$. (Note: the time at which transfer-alignment ends, $t_{\text{END TA}}$ is the time at which the maneuver described in Subsection A.8.2 ends and consequently is not an input parameter.)

- The vector from the LP INS to the M INS, called lever-arm, when the LP is stationary (i.e., when the wings are not "flapping" or the body of the LP is not being deformed in any way) expressed in the $b_{LP}$-frame:

$$p^b_{LA} = \begin{bmatrix} -2\text{ m} \\ \pm 4\text{ m} \\ 0.5\text{ m} \end{bmatrix}. \tag{A.239}$$

  The sign selection in $\pm 4$ depends on whether the M is under the right wing (+) or the left wing (−).

- The covariance of the uncertainty, $\delta p^b_{LA}$, in $p^b_{LA}$ produced by aircraft deformation during flight:

$$\underline{P}_{LA,p} = \begin{bmatrix} (0.2\text{ m})^2 & 0 & 0 \\ 0 & (0.2\text{ m})^2 & 0 \\ 0 & 0 & (0.6\text{ m})^2 \end{bmatrix}. \tag{A.240}$$

  The covariance values indicate that the greatest uncertainty is in the "vertical" motion of the wings.

[23] The state of the LP INS is also estimated but is not expected to be significantly affected because of the better accuracy of the LP INS relative to the M INS.

- The covariance of the uncertainty, $\delta v^b_{LA}$, of the velocity of M relative to the origin of the $b_{LP}$-frame in $b_{LP}$-frame coordinates. This velocity is produced by aircraft deformations while in-flight and is taken to be

$$\underline{P}_{LA,p} = \frac{\underline{P}_{LA,v}}{0.5 \text{ sec}} \tag{A.241}$$

to reflect the time taken by a one-sigma position excursion.

Assumptions — The following simplifying assumptions provide an approximate model for the deformation motion of the aircraft:

- The vectors $\delta p^b_{LA}$ and $\delta v^b_{LA}$ are white noise processes and component-wise uncorrelated when sampled at 5 sec intervals
- The vectors $\delta p^b_{LA}$ and $\delta v^b_{LA}$ are uncorrelated when sampled at 5 sec intervals. (Basis: for any value of a component of $\delta p^b_{LA}$, the sign of the corresponding $\delta v^b_{LA}$ is equally likely to be + or −.)

Computation Algorithm — The objective of the computation algorithm is to compute $\underline{P}_M(t_{\text{END TA}})$. A seven-step procedure is followed based on the approximate analysis suggested in [Farrell, 1976] (also [Perlmutter et al., 1977]). A more exact (and more complicated) development is given in [Baziw and Leondes, 1972a] and [Baziw and Leondes, 1972b]).

*1. Increment time:* $t = t + 5$ sec while $t_{\text{BEGIN TA}} \leq t \leq t_{\text{END TA}}$

*2. Compute the state-space model variables,* $\underline{F}_{TA}$ *and the covariance of* $\underline{W}_{TA}$*:* The matrix $\underline{F}_{TA}$ is computed using Equation A.228 where $\underline{F}_{LP}$ and $\underline{F}_M$ are the $F$-matrices of the LP and M INS appearing in Equation B.1. The $Q$-matrix of $\underline{W}_{TA}$ is similarly computed from the $Q$-matrices of $\underline{w}_{LP}$ and $\underline{w}_M$. Both of these quantities depend on the trajectory being followed by the LP at time $t$.

*3. Compute the position-difference measurement matrix,* $\underline{H}_{TA,p}$*:* To form the difference-position measurement, the position read-out of the LP INS is subtracted from that of the M INS. This subtraction is accomplished by the matrix $\underline{H}_{TA,p}$ which multiplies the composite state vector $X_T$:

$$\underline{H}_{TA,p} = \left[ \; -(\underline{H}_{TA,p,LP1} + \underline{H}_{TA,p,LP2}) \;\middle|\; \underline{H}_{TA,p,M} \; \right] \tag{A.242}$$

If the LP and M INSs were colocated, the subtraction is accomplished by multiplying the state vectors of the M and LP by the matrices $\underline{H}_{TA,p,M}$ and $\underline{H}_{TA,p,LP1}$ respectively, and subtracting. These matrices, which convert latitude/longitude to NED position by taking into account the spherical shape of the Earth, are shown in Figures A.1 and A.2 (the matrices are almost identical). Because the INSs are not colocated, the effect of the lever-arm needs to be taken into account by the product $\underline{H}_{TA,p,LP2}x_{LP}$ with the matrix $\underline{H}_{TA,p,LP2}$ as defined in Figure A.3. The dummy variables $d_1$, $d_2$, and $d_3$ used in Figure A.3 are defined by

$$\begin{bmatrix} d_1 \\ d_2 \\ d_3 \end{bmatrix} = -C^n_b p^b_{LA} \tag{A.243}$$

$$\left[\begin{array}{c|c|ccc|c} & & R_{\oplus} & 0 & L & \\ \underline{0}_{3\times 3} & \underline{0}_{3\times 3} & -R_{\oplus}\ell\sin L & R_{\oplus}\cos L & \ell\cos L & \underline{0}_{3\times(\dim\{\underline{x}_{LP}\}-9)} \\ & & 0 & 0 & -1 & \end{array}\right]$$

Figure A.1: Matrix $\underline{H}_{TA,p,LP1}$

$$\left[\begin{array}{c|c|ccc|c} & & R_{\oplus} & 0 & L & \\ \underline{0}_{3\times 3} & \underline{0}_{3\times 3} & -R_{\oplus}\ell\sin L & R_{\oplus}\cos L & \ell\cos L & \underline{0}_{3\times(\dim\{\underline{x}_{M}\}-9)} \\ & & 0 & 0 & -1 & \end{array}\right]$$

Figure A.2: Matrix $\underline{H}_{TA,p,M}$

$$\left[\begin{array}{ccc|c} 0 & d_3 & -d_2 & \\ -d_3 & 0 & d_1 & \underline{0}_{3\times(\dim\{\underline{x}_{LP}\}-3)} \\ d_2 & -d_1 & 0 & \end{array}\right]$$

Figure A.3: Matrix $\underline{H}_{TA,p,LP2}$

where $p^b_{LA}$ is the lever-arm vector (Equation A.239) and $b$ is the LP $b$-frame.

*4. Compute the velocity-difference measurement matrix, $\underline{H}_{TA,v}$:* The velocity measurement matrix, $\underline{H}_{TA,v}$, is the sum of three terms:

$$\underline{H}_{TA,v} = \underline{H}_{TA,v1} + \underline{H}_{TA,v2} + \underline{H}_{TA,v3}. \tag{A.244}$$

These three terms are as follows.

The first term, $\underline{H}_{TA,v1}$, forms the difference between the velocity read-out of the M and LP INSs. If the M and the LP INSs were colocated, this term would be the only one required in Equation A.244. To form this difference, the longitude-, latitude-, and altitude-rate entries in the M and LP INS states have to be multiplied by factors containing the radius of the Earth and then subtracted. These operations are implemented by

$$\underline{H}_{TA,v1} = \left[ \begin{array}{c|c} \underline{H}_{TA,v1,LP} & \underline{H}_{TA,v1,M} \end{array} \right] \tag{A.245}$$

where the left/right partitions (which multiply the LP/M states) are given in Figures A.4 and A.5. In the figures, $v_N$, $v_E$, and $L$ are the North-velocity, East-Velocity, and latitude of the LP as given, for example, by Equations A.92 to A.94 for the Right-Turn/Left-Turn LP motion event (Subsection A.3.4) and similarly for other events.

$$\left[ \begin{array}{c|ccc|ccc|c} & -R_\oplus & 0 & 0 & 0 & 0 & -\frac{v_N}{R_\oplus} & \\ \underline{0}_{3\times 3} & 0 & -R_\oplus \cos L & 0 & v_E \tan L & 0 & -\frac{v_E}{R_\oplus} & \underline{0}_{3\times(\dim\{\underline{x}_{LP}\}-9)} \\ & 0 & 0 & 1 & 0 & 0 & 0 & \end{array} \right]$$

Figure A.4: Matrix $\underline{H}_{TA,v1,LP}$

$$\left[ \begin{array}{c|ccc|ccc|c} & R_\oplus & 0 & 0 & 0 & 0 & \frac{v_N}{R_\oplus} & \\ \underline{0}_{3\times 3} & 0 & R_\oplus \cos L & 0 & -v_E \tan L & 0 & \frac{v_E}{R_\oplus} & \underline{0}_{3\times(\dim\{\underline{x}_M\}-9)} \\ & 0 & 0 & -1 & 0 & 0 & 0 & \end{array} \right]$$

Figure A.5: Matrix $\underline{H}_{TA,v1,M}$

The second term, $\underline{H}_{TA,v2}$, takes into account the error in estimating the angular velocity of the lever-arm based on the attitude read-out of the LP INS. (The angular velocity of the lever-arm contributes to the velocity of the point where the M INS is located.) This error is computed by "multiplying" (appropriately) the attitude error rates of the LP ($\delta\dot{\theta}_{\mathrm{LN}}$, $\delta\dot{\theta}_{\mathrm{LE}}$, and $\delta\dot{\theta}_{\mathrm{LD}}$, Table 3.8) by the entries in the lever arm vector, $p^b_{LA}$ (Equation A.239):

$$\underline{H}_{TA,v2} = \left[ \begin{array}{cccc|c} \underline{D}\,\underline{F}_n & \underline{D}\,\underline{F}_{ne} & \underline{D}\,\underline{F}_{n\alpha} & \underline{D}\,\underline{F}_{nh} & \underline{0}_{3\times\dim\{\underline{x}_M\}} \end{array} \right] \tag{A.246}$$

where the $F$-matrix blocks are used to form the attitude error rates as in Equation B.1. The dummy matrix $\underline{D}$ selects the attitude error rates from $\underline{n}$ (Equation B.1) and multiplies by the lever-arm vector:

$$\underline{D} = C_b^n \underline{P} C_n^b \underline{I}_{3\times 9} \tag{A.247}$$

$$C_b^n \text{ and } C_n^b \ : \text{ As in Section A.3} \tag{A.248}$$

$$\underline{I}_{3\times 9} = \left[ \begin{array}{ccc} \underline{I}_{3\times 3} & \underline{0}_{3\times 3} & \underline{0}_{3\times 3} \end{array} \right] \tag{A.249}$$

$$\underline{P} = \left[ \begin{array}{ccc} 0 & p_3 & -p_2 \\ -p_3 & 0 & p_1 \\ p_2 & -p_1 & 0 \end{array} \right] \tag{A.250}$$

$$\left[ \begin{array}{c} p_1 \\ p_2 \\ p_3 \end{array} \right] \equiv p_{LA}^b. \tag{A.251}$$

The third term, $\underline{H}_{TA,v3}$, takes into account the effect of attitude errors of the LP in determining the orientation of the angular velocity vector of the LP. This matrix acts on the attitude errors of the LP according to

$$\underline{H}_{TA,v3} = \left[ \begin{array}{ccc|c|c} 0 & d_3 & -d_2 & & \\ -d_3 & 0 & d_1 & \underline{0}_{3\times(\dim\{\underline{x}_{LP}\}-3)} & \underline{0}_{3\times\dim\{\underline{x}_M\}} \\ d_2 & -d_1 & 0 & & \end{array} \right] \tag{A.252}$$

where the dummy variables $d_1$, $d_2$, and $d_3$ are defined by

$$\left[ \begin{array}{c} d_1 \\ d_2 \\ d_3 \end{array} \right] = C_b^n W_{nb}^b p_{LA}^b. \tag{A.253}$$

In this equation, $W_{nb}^b$ is the matrix of angular rates with respect to the $n$-frame,

$$W_{nb}^b = \left[ \begin{array}{ccc} 0 & -R & Q \\ R & 0 & -P \\ -Q & P & 0 \end{array} \right] \tag{A.254}$$

where $P$, $Q$, and $R$ are as defined in Section A.3.

*5. Compute the position and velocity measurement noise covariance, $\underline{R}_{TA}$* The measurement noise originates from the uncertainties in measuring the position and velocity of the lever-arm, $\delta p_{LA}^b$ and $\delta v_{LA}^b$. These uncertainties, with covariance given by Equations A.240 and A.241, affects the position and velocity difference measurements according to

$$\underline{V}_{TA} \equiv \left[ \begin{array}{c} \underline{V}_{TA,p} \\ \underline{V}_{TA,v} \end{array} \right] \tag{A.255}$$

$$= -\underline{D} \left[ \begin{array}{c} \delta p_{LA}^b \\ \delta v_{LA}^b \end{array} \right] \tag{A.256}$$

where the matrix $\underline{D}$,

$$\underline{D} = \begin{bmatrix} C_b^n & \underline{0}_{3\times3} \\ C_b^n W_{nb}^b & C_b^n \end{bmatrix} \tag{A.257}$$

accounts for two effects: (1) the transformation from the $b$-frame to the $n$-frame; and (2) the effect of the position uncertainty on velocity error because of the angular rate of the LP, $W_{nb}^b$.

Equations A.256 and A.257 indicate that the covariance matrix of the position and velocity difference measurement noise is given by (Equation A.235)

$$\underline{R}_{TA} = \underline{D} \begin{bmatrix} \underline{P}_{LA,p} & \underline{0}_{3\times3} \\ \underline{0}_{3\times3} & \underline{P}_{LA,v} \end{bmatrix} \underline{D}^T \tag{A.258}$$

where the diagonal entries are given in Equations A.240 and A.241.

*6. Propagate the Riccatti equation:* A continuous-discrete propagate/update is performed as described in [Gelb, 1974].

*7. End iteration:* If done ($t = t_{\text{END TA}}$), compute $\underline{P}_M(t_{\text{END TA}})$ from Equation A.237; else goto Step 1.

## A.8.2 Transfer-Align LP Trajectory Model

Background — The transfer-align maneuver has three segments ([Perlmutter et al., 1977], [Schmidt, 1978]):

1. An initial constant-velocity segment for the calibration of level attitude and level gyro bias
2. An S-maneuver which produces lateral acceleration and azimuth changes for the calibration of azimuth and accelerometer bias
3. A final constant-velocity segment for the calibration of level attitude errors which may be excited by the S-maneuver.

These segments are specified in the following paragraphs in terms of the LP "motion events" described in Section A.3.

Initial Constant-Velocity Segment — The LP executes a "Level Flight at Constant Velocity" trajectory (Subsection A.3.3) for 90 sec.

S-Maneuver Segment — The LP executes a sequence of four "Right-Turn / Left-Turn" trajectories (Subsection A.3.4) as follows ($\psi_{\text{BEGIN TA}}$ is the initial LP heading):

- Right-turn at 0.65 $g$ to a heading $\psi_{\text{BEGIN TA}} + 30$ deg
- Left-turn at 0.65 $g$ to a heading $\psi_{\text{BEGIN TA}} - 30$ deg
- Right-turn at 0.65 $g$ to a heading $\psi_{\text{BEGIN TA}} + 30$ deg
- Left-turn at 0.65 $g$ to a heading $\psi_{\text{BEGIN TA}}$ .

Final Constant-Velocity Segment — The LP executes a "Level Flight at Constant Velocity" trajectory (Subsection A.3.3) for 30 sec.

During all three of these segments, the calculations described in Subsection A.8.1 are executed.

# A.9 M Mid-Course Guidance Model

## A.9.1 Introduction

The guidance model has two objectives:

- To compute the mean and covariance of the M position and velocity at handover
- To compute the mean and covariance of the T position and velocity at handover.

These quantities determine the outcome of the endgame.

The algorithms to compute these quantities are developed in the following subsections as follows:

- Subsection A.9.2 lists the inputs to the guidance algorithm
- Subsection A.9.3 lists the outputs of the guidance algorithm
- Subsection A.9.4 provides an overview of the algorithm used to compute the outputs from the inputs
- Subsections A.9.5 to A.9.11 describe the details of the algorithm.

## A.9.2 Guidance Inputs

The inputs to the guidance algorithm and their source are as follows.

*M true position and velocity at launch* ($p^t_M(t_{\text{LAUNCH}})$, $v^t_M(t_{\text{LAUNCH}})$): These quantities are computed from the true LP position and velocity according to:

$$p^t_M(t_{\text{LAUNCH}}) = p^t_{LP}(t_{\text{LAUNCH}}) + C^n_b p^b_{LA} \quad \text{(A.259)}$$

$$v^t_M(t_{\text{LAUNCH}}) = v^t_{LP}(t_{\text{LAUNCH}}) \quad \text{(A.260)}$$

where $p^b_{LA}$ is the lever arm vector (Equation A.239). The LP position and velocity ($p_{LP}$ and $v_{LP}$) and the transformation $C^n_b$ are specified by the LP trajectory events prior to launch as described in Section A.3. The addition of $n$-frame and $t$-frame quantities in Equation A.259 is justified because the origin of the $t$-frame is assumed to be near the launch point.

*M INS error covariance matrix at launch* ($\underline{P}_M(t_{\text{LAUNCH}})$): This matrix, defined by

$$\underline{P}_M(t_{\text{LAUNCH}}) = E\{\underline{x}_M(t_{\text{LAUNCH}})\underline{x}_M(t_{\text{LAUNCH}})^T\} \quad \text{(A.261)}$$

$$\underline{x}_M = \text{M INS state vector (Table 3.4)},$$

is available from the propagation of the M INS covariance from the end of the transfer alignment procedure (Section A.8) to the time of launch.

*T mean position and velocity at launch* ($p^t_T(t_{\text{LAUNCH}})$, $v^t_T(t_{\text{LAUNCH}})$): The mean T position and velocity is the deterministic component of T motion as described in Subsection A.1.2. This component is specified by the input parameters listed in Table A.1.

*T position and velocity estimation error covariance from SP tracking filter at* $t_0$ ($\underline{P}_{TR,pv}(t_0)$): This matrix, defined by Equation A.366, is computed according to Equation A.375. (The time $t_0$ is defined on page 66.)

*Miscellaneous inputs:* The following parameters are inputs to the simulation:

$$\begin{aligned} R_M &= \text{Range of M (indicative of M fuel/aerodynamic characteristics)} \\ &= 50 \text{ km} \qquad \text{(A.262)} \\ R_{\text{SEEKER ACQ}} &= \text{Seeker acquisition range}^{24} \\ &= 8 \text{ km} \qquad \text{(A.263)} \\ V_M &= \text{M cruising speed} \\ &= 5 \text{ M} \qquad \text{(A.264)} \\ a_{\text{LAUNCH}} &= \text{M acceleration at launch} \\ &= 15 \text{ g} \qquad \text{(A.265)} \\ a_{l,\max} &= \text{M maximum available level (North/East) acceleration} \\ &= 10 \text{ g} \qquad \text{(A.266)} \\ a_{z,\max} &= \text{M maximum available vertical acceleration} \\ &= 10 \text{ g} \qquad \text{(A.267)} \\ m_{\max} &= \text{Measure of available M maneuverability} \\ &= 600 \text{ g} \cdot \text{sec.} \qquad \text{(A.268)} \end{aligned}$$

The last parameter in the above list, maneuverability, is a measure of the capability of the M to execute corrective maneuvers according to the formula

$$m = |a_l|\tau_l + |a_z|\tau_z, \qquad \text{(A.269)}$$

where

$$\begin{aligned} a_l &= \text{Constant acceleration applied in the level direction} \\ a_z &= \text{Constant acceleration applied in the vertical direction} \\ \tau_l &= \text{Time interval during which } a_l \text{ is applied} \\ \tau_z &= \text{Time interval during which } a_z \text{ is applied.} \end{aligned}$$

Maneuvers during flyout are required to obey the feasibility constraint $M \leq m_{\max}$. Large accelerations sustained for a long time interval would tend to exceed the maximum maneuver capability $m_{\max}$.

## A.9.3 Guidance Outputs

The outputs produced by the guidance model are as follows.

*Zero-error handover time* ($\bar{t}_{HO}$): This quantity is the time at which handover occurs in the absence of errors.[25]

[25] In the presence of errors, the handover time is a random variable as described below.

*Means:*

$$\begin{aligned} p_T^t(\bar{t}_{HO}) &= \text{Mean T position at } \bar{t}_{HO} \\ v_T^t(\bar{t}_{HO}) &= \text{Mean T velocity at } \bar{t}_{HO} \\ p_M^t(\bar{t}_{HO}) &= \text{Mean M position at } \bar{t}_{HO} \\ v_M^t(\bar{t}_{HO}) &= \text{Mean M velocity at } \bar{t}_{HO}. \end{aligned}$$

*Covariances:* Output covariances are identified by the subscript "$L$" to indicate a measure of the variability of the physical *location* (actually, position and velocity) of the M or T. These covariances are different from *estimation* covariances which measure the variability of numbers stored in a computer.

Two output location covariances are computed:

$$\begin{aligned} P_{L,T,pv}(\bar{t}_{HO}) &= \text{T position and velocity covariance at } \bar{t}_{HO} \\ P_{L,M,pv}(\bar{t}_{HO}) &= \text{M position and velocity covariance at } \bar{t}_{HO}. \end{aligned}$$

The first of these matrices, $P_{L,T,pv}(\bar{t}_{HO})$, is obtained from a $CPC^T$ transformation of the covariance of the T random motion (Singer) model (described in Subsection A.1.2). The second matrix, $P_{L,M,pv}(\bar{t}_{HO})$, is the sum of two terms: one term is caused by guidance uncertainty (as described below); the other term represents uncertainty in M motion (Singer model described in Section A.2).

### A.9.4 Guidance Algorithm Overview

The procedure for computing the output quantities from the input quantities is divided into seven steps as follows:

1. *Propagation from $t_{\text{LAUNCH}}$ to $t_0$:* The input quantities in Equations A.259, A.260, and A.261 are propagated from the time of launch to the time $t_0$ at which the M achieves its cruise speed. All guidance computations are assumed to begin at $t_0$. This step is described in Subsection A.9.5.

2. *Computation of mean trajectories:* The trajectories of the M and T from launch to handover are computed in the absence of any random effects (which in actuality are produced by instrument errors and trajectory fluctuations). This step is described in Subsection A.9.6.

3. *Feasibility test:* The mean trajectories are tested to determine if an intercept can occur in the absence of errors and other random fluctuations. If an intercept is feasible in this ideal case, then the linearized error analysis described in Steps 2 to 6 is executed. Otherwise, one of the following actions is executed:

   - The simulation terminates, indicating that a change in the input parameters is necessary to insure a geometry that makes intercepts possible

- One of the guidance model input parameters listed in Subsection A.9.2 is modified and Steps 1 and 2 are executed again.[26]

This step is described in Subsection A.9.7.

4. *Initialization of the flyout guidance state vector covariance:* The flyout guidance state vector, $\underline{x}_G$, contains all the relevant random quantities from which the M output covariance is computed. The covariance of this vector is initialized at a time $t_0$ (defined below) based on the navigation and tracking errors. This step is described in Section A.9.8.

5. *Propagation of flyout guidance covariance:* The covariance of $\underline{x}_G$ is propagated from $t_0$ to the mean handover time $\bar{t}_{HO}$. This step is described in Subsection A.9.9.

6. *Computation of M Location Covariance:* The matrix $P_{L,T,pv}(\bar{t}_{HO})$ is computed from the covariance of $\underline{x}_G$ and the M Singer motion model. This step is described in Subsection A.9.10.

7. *Computation of T Location Covariance:* The matrix of $P_{L,M,pv}(\bar{t}_{HO})$ is computed from the T Singer motion model. This step is described in Subsection A.9.11.

The M trajectory is computed based on the following assumptions:

- A *constant* three-dimensional acceleration is applied to M starting at time $t_0$ (a deterministic quantity) and ending at the handover time $\hat{t}_{HO}$ (a random variable, defined below)

- The acceleration levels are computed so that an intercept occurs at time $\hat{t}_{HO} + t_e$ where $t_e$ (a deterministic quantity) is an estimate of the duration of the endgame

- The applied acceleration has two components: level and vertical. Both components are assumed to be orthogonal to the estimated velocity of the M at $t_0$.

The "guidance law" defined by these assumptions produces an intercept in the absence of errors and T maneuvers without any further M maneuvering during the endgame. In the presence of errors, the endgame maneuvering counteracts the flyout (launch to handover) guidance errors.

### A.9.5 Propagate from $t_{\text{LAUNCH}}$ to $t_0$

The first step in the guidance algorithm propagates the input variables listed in Subsection A.9.2 from the time of launch ($t_{\text{LAUNCH}}$) to the time ($t_0$) when the M achieves its cruising speed ($V_M$). Time $t_0$ is assumed to be the starting point for all guidance computations: lateral and vertical accelerations to achieve an intercept are applied only after the M has achieved its cruising speed. Input quantities are propagated to $t_0$ as follows.

[26] For example, suppose the mean trajectory is unfeasible because of insufficient maneuvering time during flyout. By reducing the acquisition range $R_{\text{SEEKER ACQ}}$ additional flyout time is provided at the expense of less time during endgame.

*M true position and velocity at launch* ($p_M^t(t_{\text{LAUNCH}})$, $v_M^t(t_{\text{LAUNCH}})$): These variables, computed according to Equations A.259 and A.260, are propagated to $t_0$ via a "Change of Speed" trajectory event as described in Subsection A.3.6. The input parameters to this event are the final velocity and the magnitude of the level acceleration. Values for these parameters are given in Equations A.264 and A.265.

*M INS state vector covariance* $\underline{P}_M(t_{\text{LAUNCH}})$: The covariance of the M INS state vector (Equation A.261) are propagated from $t_{\text{LAUNCH}}$) to $t_0$ according to the M INS dynamics (Section A.4).

*T mean position and velocity at launch* ($p_T^t(t_{\text{LAUNCH}})$, $v_T^t(t_{\text{LAUNCH}})$): The mean T position and velocity is the deterministic component of T motion as described in Subsection A.1.2. This component is specified by the input parameters listed in Table A.1.

*Tracking position and velocity error covariance* ($\underline{P}_{TR,pv}(t_0)$): This matrix is already available at $t_0$, making propagation unnecessary.

## A.9.6 Compute Mean Trajectories

The second step in the guidance algorithm computes the mean trajectories followed by the M and the T. The mean M trajectory is the trajectory followed by the M in the absence of any errors. The mean (predicted) T trajectory is the trajectory followed by the T in the absence of maneuvers after $t_0$. To compute these trajectories, eight steps are followed.

*1. Compute the closing velocity ($V_C$):* The closing velocity at $t_0$ is the magnitude of the difference between the velocities of the T and the M:

$$V_C \triangleq \|v_T^t(t_0) - v_M^t(t_0)\|. \tag{A.270}$$

*2. Compute the duration of the endgame ($t_e$):* The duration of the endgame is defined to be

$$t_e \triangleq \frac{R_{\text{SEEKER ACQ}}}{V_C}. \tag{A.271}$$

This definition implies that the endgame begins as soon as the seeker is able to acquire the target.

*3. Compute the mean acceleration interval ($\bar{\tau}_a$):* The mean acceleration is interval is computed to achieve an intercept in the absence of errors:

$$\bar{\tau}_a = \frac{(\Delta x_0 - r\,\Delta y_0) + t_e(\Delta v_{x0} - r\,\Delta v_{y0})}{r\,\Delta v_{y0} - \Delta v_{x0}} \quad \text{if } v_{Mx0} \neq 0 \tag{A.272}$$

$$\bar{\tau}_a = \frac{\Delta y_0 + t_e\,\Delta v_{y0}}{-\Delta v_{y0}} \quad \text{if } v_{Mx0} = 0. \tag{A.273}$$

where

$$r = \frac{-v_{My0}}{v_{Mx0}} \tag{A.274}$$

$$\Delta x_0 = x_{M0} - x_{T0} \tag{A.275}$$

$$\Delta y_0 = y_{M0} - y_{T0} \tag{A.276}$$

$$\Delta z_0 = z_{M0} - z_{T0} \tag{A.277}$$

$$\Delta v_{x0} = v_{Mx0} - v_{Tx0} \quad \text{(A.278)}$$

$$\Delta v_{y0} = v_{My0} - v_{Ty0} \quad \text{(A.279)}$$

$$\Delta v_{z0} = v_{Mz0} - v_{Tz0} \quad \text{(A.280)}$$

$$p_M^t(t_0) = [x_{M0} \quad y_{M0} \quad z_{M0}]^T \quad \text{(A.281)}$$

$$p_T^t(t_0) = [x_{T0} \quad y_{T0} \quad z_{T0}]^T \quad \text{(A.282)}$$

$$v_M^t(t_0) = [v_{Mx0} \quad v_{My0} \quad v_{Mz0}]^T \quad \text{(A.283)}$$

$$v_T^t(t_0) = [v_{Tx0} \quad v_{Ty0} \quad v_{Tz0}]^T. \quad \text{(A.284)}$$

*4. Compute the mean handover time ($t_{HO}$):* This time is the handover time in the absence of errors:

$$t_{HO} = t_0 + \tau_a. \quad \text{(A.285)}$$

*5. Compute the mean level acceleration ($a_l$):* The level (North/East) acceleration that results produces an intercept in the absence of errors is given by

$$\vec{a}_l = \frac{a_l}{V_M} \begin{bmatrix} -v_{My0} \\ v_{Mx0} \end{bmatrix}^{\text{North,East}} \quad \text{(A.286)}$$

where:

$$V_M = \|v_M^t(t_0)\| \quad \text{(A.287)}$$

$$a_l = \frac{\Delta x_0 + (t_c + \tau_a)\Delta v_{x0}}{\frac{v_{My0}}{V_M}(t_c\tau_a + \frac{1}{2}\tau_a^2)} \quad \text{if } v_{My0} \neq 0 \quad \text{(A.288)}$$

$$a_l = \frac{\Delta y_0 + (t_c + \tau_a)\Delta v_{y0}}{-\frac{v_{Mx0}}{V_M}(t_c\tau_a + \frac{1}{2}\tau_a^2)} \quad \text{if } v_{Mx0} \neq 0. \quad \text{(A.289)}$$

*6. Compute the mean vertical acceleration ($\vec{a}_z$):* The vertical acceleration that will produce an intercept in the absence of errors is given by

$$a_z = -\frac{\Delta z_0 + (t_c + \tau_a)\Delta v_{z0}}{-(t_c\tau_a + \frac{1}{2}\tau_a^2)}. \quad \text{(A.290)}$$

*7. Compute the mean position and velocity of M:*

**Before handover:** For $t_0 \leq t \leq t_{HO}$:

$$p_M^t(t) = p_M^t(t_0) + v_M^t(t_0)(t - t_0) + \frac{1}{2}a_c(t - t_0)^2 \quad \text{(A.291)}$$

$$v_M^t(t) = v_M^t(t_0) + a_c(t - t_0) \quad \text{(A.292)}$$

where the vector $a_c$ is the *computed* acceleration

$$a_c = \begin{bmatrix} \vec{a}_l \\ a_z \end{bmatrix}. \quad \text{(A.293)}$$

The computed acceleration $a_c$ is a number that exists in the M computer. In the presence of errors, this acceleration is different from the *resulting* acceleration, $a_r$ which is the acceleration actually experienced by the M. In the error free case, however, $a_c = a_r$.

**After handover:** For $\bar{t}_{HO} \leq t \leq \bar{t}_I$, where $\bar{t}_I$ is the mean intercept time, $\bar{t}_I = \bar{t}_{HO} + t_e$:

$$p_M^t(t) = p_M^t(\bar{t}_{HO}) + v_M^t(\bar{t}_{HO})(t - \bar{t}_{HO}). \tag{A.294}$$

*8. Compute the mean predicted position of T:* The position of T if the M does not maneuver after time $t_0$ is given by:

$$p_{T,\text{predicted}}^t(t) = p_T^t(t_0) + v_M^t(t_0)(t - t_0), \tag{A.295}$$

for $t_0 \leq t \leq \bar{t}_I$.

### A.9.7 Test Feasibility of Intercept

The third step in the guidance algorithm is to test the feasibility of an intercept in the absence of any errors. An intercept is considered *feasible* if the mean trajectories are such that the following conditions hold:

1. The length of the acceleration interval is realizable:

$$\bar{\tau}_a > 0. \tag{A.296}$$

2. The maximum accelerations are not exceeded:

$$\|\vec{\bar{a}}_l\| \leq a_{l,\max} \tag{A.297}$$

$$|\bar{a}_z| \leq a_{z,\max}. \tag{A.298}$$

3. The maximum maneuverability is not exceeded:

$$(\|\vec{\bar{a}}_l\| + |\bar{a}_z|)\bar{\tau}_a, \leq m_{\max}. \tag{A.299}$$

4. An intercept is achieved in the mean:

$$p_M^t(t_I) = p_{T,\text{predicted}}^t(\bar{t}_I). \tag{A.300}$$

(Note: this equation needs to hold only within numerical round-off error; e.g., to within four significant digits.)

If an intercept is unfeasible in the mean, then the deterministic LP and T trajectories are not likely to result in a significant probability of intercept.[27] For these cases, an analysis of the flyout guidance error lacks practical significance. Consequently, if the intercept is unfeasible, the simulation should take one of the two following courses of action:

- Exit (after printing a suitable message)
- Change one of the guidance model input parameters, re-compute the mean trajectories, and re-try the feasibility test.

[27] Even if the intercept is feasible, however, some of the sample paths may result in unfeasible intercepts because the tails of the Gaussian distribution extend to infinity.

## A.9.8 Compute Initial Mid-Course Guidance Covariance, $\underline{P_G}(t_0)$

Background — The fourth step in the guidance algorithm begins the evaluation of the random perturbations on the mean M and T locations at handover. These perturbations are caused by random errors; consequently, variables that include random components need to be defined as follows:

$$\hat{p}_M^t(t) = p_M^t(t) + \delta p_M^t(t) \quad \text{(A.301)}$$
$$= \text{Position read-out of the M INS}$$
$$\hat{v}_M^t(t) = v_M^t(t) + \delta v_M^t(t) \quad \text{(A.302)}$$
$$= \text{Velocity read-out of the M INS}$$
$$\hat{p}_T^t(t_0) = p_T^t(t_0) + \delta p_T^t(t_0) \quad \text{(A.303)}$$
$$= \text{Estimate of T position obtained from the SP tracking filter}$$
$$\hat{v}_T^t(t_0) = v_T^t(t_0) + \delta v_T^t(t_0) \quad \text{(A.304)}$$
$$= \text{Estimate of T velocity obtained from the SP tracking filter}$$
$$\hat{\tau}_{a,c} = \bar{\tau}_{a,c} + \delta\tau_{a,c} \quad \text{(A.305)}$$
$$= \text{Computed duration of applied acceleration}$$
$$\vec{\hat{a}}_{l,c} = \vec{\bar{a}}_{l,c} + \delta\vec{a}_{l,c} \quad \text{(A.306)}$$
$$= \text{Computed level (North/East) acceleration (2-dimensional vector)}$$
$$\hat{a}_{z,c} = \bar{a}_{z,c} + \delta a_{z,c} \quad \text{(A.307)}$$
$$= \text{Computed vertical (down) acceleration.}$$

The notation used in these equations is as follows:

- Quantities which include errors are identified by a "hat" (e.g., $\hat{p}_M^t$)[28]
- Errors are identified by the prefix "$\delta$"
- Mean error-free quantities are identified by an over-bar or by the absence of a "hat" or $\delta$
- The subscript "$c$" identifies *computed* quantities:
  - The computed accelerations ($\vec{\hat{a}}_{l,c}$ and $\hat{a}_{z,c}$) differ from the *resulting* acceleration by the misalignment of the M INS. Other differences between computed and resulting accelerations (such as autopilot inaccuracies and delays) are neglected
  - The computed duration of the acceleration interval ($\hat{\tau}_{a,c}$) differs from the resulting duration because of clock and autopilot inaccuracies. These differences are neglected.

[28]This notation, often found in the navigation literature (e.g., [Britting, 1971]), differs from the notation used in the estimation literature (e.g., [Gelb, 1974]) where "hats" identify estimates.

The errors quantities defined in Equations A.301 to A.307 are included in the flyout guidance state vector, $\underline{x}_G$, which has entries as defined in Table 3.5 of Section 3.7. In the following paragraphs equations are given for the "initial" covariance of $\underline{x}_G$:

$$\underline{P}_G(t_0) = E\{\underline{x}_G(t_0)\underline{x}_G(t_0)^T\}. \tag{A.308}$$

To obtain this covariance, the vector $\underline{x}_G$ is partitioned into five vectors corresponding to the partitions shown in Table 3.5 using the following notation:

$$\underline{x}_{M,pv} \triangleq \begin{bmatrix} \delta p_M^t \\ \delta v_M^t \end{bmatrix} \tag{A.309}$$

$$\underline{x}_{TR,pv} \triangleq \begin{bmatrix} \delta p_T^t \\ \delta v_T^t \end{bmatrix} \tag{A.310}$$

$$\underline{x}_g \triangleq \begin{bmatrix} \delta\tau_{a,c} \\ \delta\vec{a}_{l,c} \\ \delta a_{z,c} \end{bmatrix}. \tag{A.311}$$

With this notation, an expression is obtained for $\underline{x}_G$ *at* $t_0$:

$$\underline{x}_G(t_0) = \begin{bmatrix} \underline{x}_M(t_0) \\ \underline{x}_{M,pv}(t_0) \\ \underline{x}_{TR,pv}(t_0) \\ \underline{x}_g(t_0) \\ \underline{x}_d(t_0) \end{bmatrix} \tag{A.312}$$

$$= \begin{bmatrix} \underline{I}_{\dim\{\underline{x}_M\}\times\dim\{\underline{x}_M\}} & \underline{0}_{\dim\{\underline{x}_M\}\times 6} \\ \underline{C}_{M,pv} & \underline{0}_{6\times 6} \\ \underline{0}_{6\times\dim\{\underline{x}_M\}} & \underline{I}_{6\times 6} \\ \underline{C}_{g1}\underline{C}_{M,pv} & \underline{C}_{g2} \\ \underline{0}_{6\times\dim\{\underline{x}_M\}} & \underline{0}_{6\times 6} \end{bmatrix} \begin{bmatrix} \underline{x}_M(t_0) \\ \underline{x}_{TR,pv}(t_0) \end{bmatrix} \tag{A.313}$$

$$\equiv \underline{C}_g \begin{bmatrix} \underline{x}_M(t_0) \\ \underline{x}_{TR,pv}(t_0) \end{bmatrix}. \tag{A.314}$$

These equations contains four transformation matrices:

- $\underline{C}_{M,pv}$ transforms the M INS error vector ($\underline{x}_M$) into the errors in M INS indicated position and velocity
- $\underline{C}_{g1}$ transforms the errors in M INS indicated position and velocity into the contribution of these errors to the guidance errors ($\underline{x}_g$)
- $\underline{C}_{g2}$ transforms the tracking errors ($\underline{x}_{TR,pv}$) into the contribution of these errors to the guidance errors ($\underline{x}_g$)

- $\underline{C}_g$ in Equation A.314 is defined to be equal to the partitioned matrix in Equation A.313 (as evident from Equations A.313 and A.314).

Equations A.313 and A.314 show that the initial covariance of the guidance state vector $\underline{x}_G$ is given by

$$\underline{P}_G(t_0) = \underline{C}_g \begin{bmatrix} \underline{P}_M(t_0) & \underline{0}_{\dim\{\underline{x}_M\}\times 6} \\ \underline{0}_{6\times\dim\{\underline{x}_M\}} & \underline{P}_{TR,pv}(t_0) \end{bmatrix} \underline{C}_g^T \tag{A.315}$$

where $\underline{P}_M(t_0)$ is the covariance of the M INS state vector and $\underline{P}_{TR,pv}(t_0)$ is the covariance of the tracking filter position and velocity errors given by Equation A.375. A procedure for computing $\underline{P}_G(t_0)$ is given below.

Procedure for computing $\underline{P}_G(t_0)$ — The top-level procedure for computing $\underline{P}_G(t_0)$ has five steps as follows:

1. Compute $\underline{C}_{M,pv}$
2. Compute $\underline{C}_{g1}$
3. Compute $\underline{C}_{g2}$
4. Compute $\underline{C}_g$
5. Compute $\underline{P}_G(t_0)$ .

Details of these steps are given in the following paragraphs.

Computation of $\underline{C}_{M,pv}$ — The $6 \times dim\{\underline{x}_M\}$ matrix $\underline{C}_{M,pv}$ is given in Figure A.6.

$$\left[\begin{array}{ccc|ccc|ccc|c} 0 & 0 & 0 & 0 & 0 & 0 & R_\oplus & 0 & L & \\ 0 & 0 & 0 & 0 & 0 & 0 & -R_\oplus \ell \sin L & R_\oplus \cos L & \ell \cos L & \underline{0}_{3\times(\dim\{\underline{x}_M\}-9)} \\ 0 & 0 & 0 & 0 & 0 & 0 & 0 & 0 & -1 & \\ \hline 0 & 0 & 0 & R_\oplus & 0 & 0 & 0 & 0 & \frac{v_N}{R_\oplus} & \\ 0 & 0 & 0 & 0 & R_\oplus \cos L & 0 & -v_E \tan L & 0 & \frac{v_E}{R_\oplus} & \underline{0}_{3\times(\dim\{\underline{x}_M\}-9)} \\ 0 & 0 & 0 & 0 & 0 & -1 & 0 & 0 & 0 & \end{array}\right]$$

Figure A.6: Matrix $\underline{C}_{M,pv}$

Computation of $\underline{C}_{g1}$ — The $4 \times 6$ matrix $\underline{C}_{g1}$ can be partitioned into four $1 \times 6$ row matrices,

$$\underline{C}_{g1} = \begin{bmatrix} \underline{C}_{11} \\ \underline{C}_{12} \\ \underline{C}_{13} \\ \underline{C}_{14} \end{bmatrix}, \tag{A.316}$$

where:

$$\underline{C}_{11} = \frac{\partial \delta \tau_{a,c}}{\partial \underline{x}_{M,pv}} \tag{A.317}$$

$$\underline{C}_{12} = \frac{\partial \delta a_{l,x,c}}{\partial \underline{x}_{M,pv}} \tag{A.318}$$

$$\underline{C}_{13} = \frac{\partial \delta a_{l,y,c}}{\partial \underline{x}_{M,pv}} \tag{A.319}$$

$$\underline{C}_{14} = \frac{\partial \delta a_{z,c}}{\partial \underline{x}_{M,pv}} \tag{A.320}$$

and

$$\begin{bmatrix} \delta a_{l,x,c} \\ \delta a_{l,y,c} \end{bmatrix}^{North\ East} = \delta \vec{a}_{l,c}. \tag{A.321}$$

Expressions for the row matrices $\underline{C}_{1i}$, $i = 1, \ldots, 4$, are given in Figures A.7 to A.10. Expressions for the partials appearing in these figures are given in Tables A.11 to A.15. The notation used in all these figures and tables is summarized in Table A.10.

$$\left[ \begin{array}{ccc|ccc} \frac{\partial \tau_{a,c}}{\partial x_{M0}} & \frac{\partial \tau_{a,c}}{\partial y_{M0}} & \frac{\partial \tau_{a,c}}{\partial z_{M0}} & \frac{\partial \tau_{a,c}}{\partial v_{Mx0}} & \frac{\partial \tau_{a,c}}{\partial v_{My0}} & \frac{\partial \tau_{a,c}}{\partial v_{Mz0}} \end{array} \right]$$

Figure A.7: Row Matrix $\underline{C}_{11}$

$$\left[ \begin{array}{ccc|ccc} a_1 \frac{\partial \bar{a}_{l,c}}{\partial x_{M0}} & a_1 \frac{\partial \bar{a}_{l,c}}{\partial y_{M0}} & a_1 \frac{\partial \bar{a}_{l,c}}{\partial z_{M0}} & a_1 \frac{\partial \bar{a}_{l,c}}{\partial v_{Mx0}} & \left( a_1 \frac{\partial \bar{a}_{l,c}}{\partial v_{My0}} - \frac{\bar{a}_{l,c}}{V_M} \right) & a_1 \frac{\partial \bar{a}_{l,c}}{\partial v_{Mz0}} \end{array} \right]$$

Figure A.8: Row Matrix $\underline{C}_{12}$

$$\left[ \begin{array}{ccc|ccc} a_2 \frac{\partial \bar{a}_{l,c}}{\partial x_{M0}} & a_2 \frac{\partial \bar{a}_{l,c}}{\partial y_{M0}} & a_2 \frac{\partial \bar{a}_{l,c}}{\partial z_{M0}} & \left( a_2 \frac{\partial \bar{a}_{l,c}}{\partial v_{Mx0}} + \frac{\bar{a}_{l,c}}{V_M} \right) & a_2 \frac{\partial \bar{a}_{l,c}}{\partial v_{My0}} & a_2 \frac{\partial \bar{a}_{l,c}}{\partial v_{Mz0}} \end{array} \right]$$

Figure A.9: Row Matrix $\underline{C}_{13}$

Computation of $\underline{C}_{g2}$ — The $4 \times 6$ matrix $\underline{C}_{g2}$ can be partitioned into four $1 \times 6$ row matrices,

$$\underline{C}_{g2} = \begin{bmatrix} \underline{C}_{21} \\ \underline{C}_{22} \\ \underline{C}_{23} \\ \underline{C}_{24} \end{bmatrix}, \tag{A.322}$$

$$\left[\begin{array}{ccc|ccc} \frac{\partial a_{z,c}}{\partial x_{M0}} & \frac{\partial a_{z,c}}{\partial y_{M0}} & \frac{\partial a_{z,c}}{\partial z_{M0}} & \frac{\partial a_{z,c}}{\partial v_{Mx0}} & \frac{\partial a_{z,c}}{\partial v_{My0}} & \frac{\partial a_{z,c}}{\partial v_{Mz0}} \end{array}\right]$$

Figure A.10: Row Matrix $\underline{C}_{14}$

Table A.10: NOTATION FOR GUIDANCE PARTIAL DERIVATIVES

| |
|---|
| $[x_{M0} \quad y_{M0} \quad z_{M0}]^T = p_M^t(t_0)$<br>$[x_{T0} \quad y_{T0} \quad z_{T0}]^T = p_T^t(t_0)$ |
| $[v_{Mx0} \quad v_{My0} \quad v_{Mz0}]^T = v_M^t(t_0)$<br>$[v_{Tx0} \quad v_{Ty0} \quad v_{Tz0}]^T = v_T^t(t_0)$ |
| $\Delta x_0 = x_{M0} - x_{T0}$<br>$\Delta y_0 = y_{M0} - y_{T0}$<br>$\Delta z_0 = z_{M0} - z_{T0}$<br>$\Delta v_{x0} = v_{Mx0} - v_{Tx0}$<br>$\Delta v_{y0} = v_{My0} - v_{Ty0}$<br>$\Delta v_{z0} = v_{Mz0} - v_{Tz0}$ |
| $a_1 = -\frac{v_{My0}}{V_M}$<br>$a_2 = \frac{v_{Mx0}}{V_M}$ |
| $\bar{a}_l$ : Given in Equations A.288 and A.289<br>$V_M$ : Given in Equation A.287 |

Table A.11: PARTIAL DERIVATIVES OF $\tau_{a,c}$ FOR $v_{Mx0} \neq 0$

For $\gamma = x_{M0},\ y_{M0},\ z_{M0},\ v_{Mx0},\ v_{My0},\ v_{Mz0},\ x_{T0},\ y_{T0},\ z_{T0},\ v_{Tx0},\ v_{Ty0},\ v_{Tz0}$:

$$\frac{\partial \tau_{a,c}}{\partial \gamma} = -\frac{N_\tau}{D_\tau^2}\frac{\partial D_\tau}{\partial \gamma} + \frac{1}{D_\tau}\frac{\partial N_\tau}{\partial \gamma}$$

| $N_\tau = \Delta x_0 + \frac{v_{My0}}{v_{Mx0}}\Delta y_0 + t_e\left[\Delta v_{x0} + \frac{v_{My0}}{v_{Mx0}}\Delta v_{y0}\right]$ | $D_\tau = -\frac{v_{My0}}{v_{Mx0}}\Delta v_{y0} - \Delta v_{x0}$ |
|---|---|
| $\frac{\partial N_\tau}{\partial x_{M0}} = 1$ | $\frac{\partial D_\tau}{\partial x_{M0}} = 0$ |
| $\frac{\partial N_\tau}{\partial y_{M0}} = \frac{v_{My0}}{v_{Mx0}}$ | $\frac{\partial D_\tau}{\partial y_{M0}} = 0$ |
| $\frac{\partial N_\tau}{\partial z_{M0}} = 0$ | $\frac{\partial D_\tau}{\partial z_{M0}} = 0$ |
| $\frac{\partial N_\tau}{\partial v_{Mx0}} = -\frac{v_{My0}}{v_{Mx0}^2}\Delta y_0 + t_e\left[1 - \frac{v_{My0}}{v_{Mx0}^2}\Delta v_{y0}\right]$ | $\frac{\partial D_\tau}{\partial v_{Mx0}} = \frac{v_{My0}}{v_{Mx0}^2}\Delta v_{y0} - 1$ |
| $\frac{\partial N_\tau}{\partial v_{My0}} = \frac{1}{v_{Mx0}}\Delta y_0 + t_e\left[\frac{2v_{My0} - v_{Ty0}}{v_{Mx0}}\right]$ | $\frac{\partial D_\tau}{\partial v_{My0}} = -\frac{1}{v_{Mx0}}(2v_{My0} - v_{Ty0})$ |
| $\frac{\partial N_\tau}{\partial v_{Mz0}} = 0$ | $\frac{\partial D_\tau}{\partial v_{Mz0}} = 0$ |
| $\frac{\partial N_\tau}{\partial x_{T0}} = -1$ | $\frac{\partial D_\tau}{\partial x_{T0}} = 0$ |
| $\frac{\partial N_\tau}{\partial y_{T0}} = -\frac{v_{My0}}{v_{Mx0}}$ | $\frac{\partial D_\tau}{\partial y_{T0}} = 0$ |
| $\frac{\partial N_\tau}{\partial z_{T0}} = 0$ | $\frac{\partial D_\tau}{\partial z_{T0}} = 0$ |
| $\frac{\partial N_\tau}{\partial v_{Tx0}} = -t_e$ | $\frac{\partial D_\tau}{\partial v_{Tx0}} = 1$ |
| $\frac{\partial N_\tau}{\partial v_{Ty0}} = -t_e\frac{v_{My0}}{v_{Mx0}}$ | $\frac{\partial D_\tau}{\partial v_{Ty0}} = \frac{v_{My0}}{v_{Mx0}}$ |
| $\frac{\partial N_\tau}{\partial v_{Tz0}} = 0$ | $\frac{\partial D_\tau}{\partial v_{Tz0}} = 0$ |

Table A.12: PARTIAL DERIVATIVES OF $\tau_{a,c}$ FOR $v_{Mx0} = 0$

For $\gamma = x_{M0}, y_{M0}, z_{M0}, v_{Mx0}, v_{My0}, v_{Mz0}, x_{T0}, y_{T0}, z_{T0}, v_{Tx0}, v_{Ty0}, v_{Tz0}$:

$$\frac{\partial \tau_{a,c}}{\partial \gamma} = -\frac{N_\tau}{D_\tau^2}\frac{\partial D_\tau}{\partial \gamma} + \frac{1}{D_\tau}\frac{\partial N_\tau}{\partial \gamma}$$

| $N_\tau = \Delta y_0 + t_e \Delta v_{y0}$ | $D_\tau = -\Delta v_{y0}$ |
|---|---|
| $\frac{\partial N_\tau}{\partial x_{M0}} = 0$ | $\frac{\partial D_\tau}{\partial x_{M0}} = 0$ |
| $\frac{\partial N_\tau}{\partial y_{M0}} = 1$ | $\frac{\partial D_\tau}{\partial y_{M0}} = 0$ |
| $\frac{\partial N_\tau}{\partial z_{M0}} = 0$ | $\frac{\partial D_\tau}{\partial z_{M0}} = 0$ |
| $\frac{\partial N_\tau}{\partial v_{Mx0}} = 0$ | $\frac{\partial D_\tau}{\partial v_{Mx0}} = 0$ |
| $\frac{\partial N_\tau}{\partial v_{My0}} = t_e$ | $\frac{\partial D_\tau}{\partial v_{My0}} = -1$ |
| $\frac{\partial N_\tau}{\partial v_{Mz0}} = 0$ | $\frac{\partial D_\tau}{\partial v_{Mz0}} = 0$ |
| $\frac{\partial N_\tau}{\partial x_{T0}} = 0$ | $\frac{\partial D_\tau}{\partial x_{T0}} = 0$ |
| $\frac{\partial N_\tau}{\partial y_{T0}} = -1$ | $\frac{\partial D_\tau}{\partial y_{T0}} = 0$ |
| $\frac{\partial N_\tau}{\partial z_{T0}} = 0$ | $\frac{\partial D_\tau}{\partial z_{T0}} = 0$ |
| $\frac{\partial N_\tau}{\partial v_{Tx0}} = 0$ | $\frac{\partial D_\tau}{\partial v_{Tx0}} = 0$ |
| $\frac{\partial N_\tau}{\partial v_{Ty0}} = -t_e$ | $\frac{\partial D_\tau}{\partial v_{Ty0}} = 1$ |
| $\frac{\partial N_\tau}{\partial v_{Tz0}} = 0$ | $\frac{\partial D_\tau}{\partial v_{Tz0}} = 0$ |

Table A.13: PARTIAL DERIVATIVES OF $\bar{a}_{l,c}$ FOR $v_{My0} \neq 0$

For $\gamma = x_{M0}, y_{M0}, z_{M0}, v_{Mx0}, v_{My0}, v_{Mz0}, x_{T0}, y_{T0}, z_{T0}, v_{Tx0}, v_{Ty0}, v_{Tz0}$:

$$\frac{\partial \bar{a}_{l,c}}{\partial \gamma} = -\frac{N_{a,l}}{D_{a,l}^2}\frac{\partial D_{a,l}}{\partial \gamma} + \frac{1}{D_{a,l}}\frac{\partial N_{a,l}}{\partial \gamma}$$

| $N_{a,l} = \Delta x_0 + (t_e + \tau_{a,c})\Delta v_{x0}$ | $D_{a,l} = -a_1(t_e\tau_{a,c} + \frac{1}{2}\tau_{a,c}^2)$ |
|---|---|
| $\frac{\partial N_{a,l}}{\partial x_{M0}} = 1 + \Delta v_{x0}\frac{\partial \tau_{a,c}}{\partial x_{M0}}$ | $\frac{\partial D_{a,l}}{\partial x_{M0}} = -a_1(t_e + \tau_{a,c})\frac{\partial \tau_{a,c}}{\partial x_{M0}}$ |
| $\frac{\partial N_{a,l}}{\partial y_{M0}} = \Delta v_{x0}\frac{\partial \tau_{a,c}}{\partial y_{M0}}$ | $\frac{\partial D_{a,l}}{\partial y_{M0}} = -a_1(t_e + \tau_{a,c})\frac{\partial \tau_{a,c}}{\partial y_{M0}}$ |
| $\frac{\partial N_{a,l}}{\partial z_{M0}} = 0$ | $\frac{\partial D_{a,l}}{\partial z_{M0}} = 0$ |
| $\frac{\partial N_{a,l}}{\partial v_{Mx0}} = (t_e + \tau_{a,c}) + \Delta v_{x0}\frac{\partial \tau_{a,c}}{\partial v_{Mx0}}$ | $\frac{\partial D_{a,l}}{\partial v_{Mx0}} = -a_1(t_e + \tau_{a,c})\frac{\partial \tau_{a,c}}{\partial v_{Mx0}}$ |
| $\frac{\partial N_{a,l}}{\partial v_{My0}} = \Delta v_{x0}\frac{\partial \tau_{a,c}}{\partial v_{My0}}$ | $\frac{\partial D_{a,l}}{\partial v_{My0}} = -a_1(t_e + \tau_{a,c})\frac{\partial \tau_{a,c}}{\partial v_{My0}} + \frac{t_e\tau_{a,c} + \frac{1}{2}\tau_{a,c}^2}{V_M}$ |
| $\frac{\partial N_{a,l}}{\partial v_{Mz0}} = 0$ | $\frac{\partial D_{a,l}}{\partial v_{Mz0}} = 0$ |
| $\frac{\partial N_{a,l}}{\partial x_{T0}} = -1 + \Delta v_{x0}\frac{\partial \tau_{a,c}}{\partial x_{T0}}$ | $\frac{\partial D_{a,l}}{\partial x_{T0}} = -a_1(t_e + \tau_{a,c})\frac{\partial \tau_{a,c}}{\partial x_{T0}}$ |
| $\frac{\partial N_{a,l}}{\partial y_{T0}} = \Delta v_{x0}\frac{\partial \tau_{a,c}}{\partial y_{T0}}$ | $\frac{\partial D_{a,l}}{\partial y_{T0}} = -a_1(t_e + \tau_{a,c})\frac{\partial \tau_{a,c}}{\partial y_{T0}}$ |
| $\frac{\partial N_{a,l}}{\partial z_{T0}} = 0$ | $\frac{\partial D_{a,l}}{\partial z_{T0}} = 0$ |
| $\frac{\partial N_{a,l}}{\partial v_{Tx0}} = -(t_e + \tau_{a,c}) + \Delta v_{x0}\frac{\partial \tau_{a,c}}{\partial v_{Tx0}}$ | $\frac{\partial D_{a,l}}{\partial v_{Tx0}} = -a_1(t_e + \tau_{a,c})\frac{\partial \tau_{a,c}}{\partial v_{Tx0}}$ |
| $\frac{\partial N_{a,l}}{\partial v_{Ty0}} = \Delta v_{x0}\frac{\partial \tau_{a,c}}{\partial v_{Ty0}}$ | $\frac{\partial D_{a,l}}{\partial v_{Ty0}} = -a_1(t_e + \tau_{a,c})\frac{\partial \tau_{a,c}}{\partial v_{Ty0}}$ |
| $\frac{\partial N_{a,l}}{\partial v_{Tz0}} = 0$ | $\frac{\partial D_{a,l}}{\partial v_{Tz0}} = 0$ |

Table A.14: PARTIAL DERIVATIVES OF $\bar{a}_{l,c}$ FOR $v_{My0} = 0$

For $\gamma = x_{M0},\ y_{M0},\ z_{M0},\ v_{Mx0},\ v_{My0},\ v_{Mz0},\ x_{T0},\ y_{T0},\ z_{T0},\ v_{Tx0},\ v_{Ty0},\ v_{Tz0}$:

$$\frac{\partial \bar{a}_{l,c}}{\partial \gamma} = -\frac{N_{a,l}}{D_{a,l}^2}\frac{\partial D_{a,l}}{\partial \gamma} + \frac{1}{D_{a,l}}\frac{\partial N_{a,l}}{\partial \gamma}$$

| $N_{a,l} = \Delta y_0 + (t_e + \tau_{a,c})\Delta v_{y0}$ | $D_{a,l} = -a_2(t_e\tau_{a,c} + \frac{1}{2}\tau_{a,c}^2)$ |
|---|---|
| $\frac{\partial N_{a,l}}{\partial x_{M0}} = \Delta v_{y0}\frac{\partial \tau_{a,c}}{\partial x_{M0}}$ | $\frac{\partial D_{a,l}}{\partial x_{M0}} = -a_2(t_e + \tau_{a,c})\frac{\partial \tau_{a,c}}{\partial x_{M0}}$ |
| $\frac{\partial N_{a,l}}{\partial y_{M0}} = 1 + \Delta v_{y0}\frac{\partial \tau_{a,c}}{\partial y_{M0}}$ | $\frac{\partial D_{a,l}}{\partial y_{M0}} = -a_2(t_e + \tau_{a,c})\frac{\partial \tau_{a,c}}{\partial y_{M0}}$ |
| $\frac{\partial N_{a,l}}{\partial z_{M0}} = 0$ | $\frac{\partial D_{a,l}}{\partial z_{M0}} = 0$ |
| $\frac{\partial N_{a,l}}{\partial v_{Mx0}} = \Delta v_{y0}\frac{\partial \tau_{a,c}}{\partial v_{Mx0}}$ | $\frac{\partial D_{a,l}}{\partial v_{Mx0}} = -a_2(t_e + \tau_{a,c})\frac{\partial \tau_{a,c}}{\partial v_{Mx0}} - \frac{t_e\tau_{a,c} + \frac{1}{2}\tau_{a,c}^2}{V_M}$ |
| $\frac{\partial N_{a,l}}{\partial v_{My0}} = (t_e + \tau_{a,c}) + \Delta v_{y0}\frac{\partial \tau_{a,c}}{\partial v_{My0}}$ | $\frac{\partial D_{a,l}}{\partial v_{My0}} = -a_2(t_e + \tau_{a,c})\frac{\partial \tau_{a,c}}{\partial v_{My0}}$ |
| $\frac{\partial N_{a,l}}{\partial v_{Mz0}} = 0$ | $\frac{\partial D_{a,l}}{\partial v_{Mz0}} = 0$ |
| $\frac{\partial N_{a,l}}{\partial x_{T0}} = \Delta v_{y0}\frac{\partial \tau_{a,c}}{\partial x_{T0}}$ | $\frac{\partial D_{a,l}}{\partial x_{T0}} = -a_2(t_e + \tau_{a,c})\frac{\partial \tau_{a,c}}{\partial x_{T0}}$ |
| $\frac{\partial N_{a,l}}{\partial y_{T0}} = -1 + \Delta v_{y0}\frac{\partial \tau_{a,c}}{\partial y_{T0}}$ | $\frac{\partial D_{a,l}}{\partial y_{T0}} = -a_2(t_e + \tau_{a,c})\frac{\partial \tau_{a,c}}{\partial y_{T0}}$ |
| $\frac{\partial N_{a,l}}{\partial z_{T0}} = 0$ | $\frac{\partial D_{a,l}}{\partial z_{T0}} = 0$ |
| $\frac{\partial N_{a,l}}{\partial v_{Tx0}} = \Delta v_{y0}\frac{\partial \tau_{a,c}}{\partial v_{Tx0}}$ | $\frac{\partial D_{a,l}}{\partial v_{Tx0}} = -a_2(t_e + \tau_{a,c})\frac{\partial \tau_{a,c}}{\partial v_{Tx0}}$ |
| $\frac{\partial N_{a,l}}{\partial v_{Ty0}} = -(t_e + \tau_{a,c}) + \Delta v_{y0}\frac{\partial \tau_{a,c}}{\partial v_{Ty0}}$ | $\frac{\partial D_{a,l}}{\partial v_{Ty0}} = -a_2(t_e + \tau_{a,c})\frac{\partial \tau_{a,c}}{\partial v_{Ty0}}$ |
| $\frac{\partial N_{a,l}}{\partial v_{Tz0}} = 0$ | $\frac{\partial D_{a,l}}{\partial v_{Tz0}} = 0$ |

Table A.15: PARTIAL DERIVATIVES OF $\bar{a}_z$

For $\gamma = x_{M0}, y_{M0}, z_{M0}, v_{Mx0}, v_{My0}, v_{Mz0}, x_{T0}, y_{T0}, z_{T0}, v_{Tx0}, v_{Ty0}, v_{Tz0}$:

$$\frac{\partial \bar{a}_z}{\partial \gamma} = -\frac{N_z}{D_z^2}\frac{\partial D_z}{\partial \gamma} + \frac{1}{D_z}\frac{\partial N_z}{\partial \gamma}$$

| $N_z = \Delta z_0 + (t_e + \tau_{a,c})\Delta v_{z0}$ | $D_z = -(t_e \tau_{a,c} + \frac{1}{2}\tau_{a,c}^2)$ |
|---|---|
| $\frac{\partial N_z}{\partial x_{M0}} = \Delta v_{z0}\frac{\partial \tau_{a,c}}{\partial x_{M0}}$ | $\frac{\partial D_z}{\partial x_{M0}} = -(t_e + \tau_{a,c})\frac{\partial \tau_{a,c}}{\partial x_{M0}}$ |
| $\frac{\partial N_z}{\partial y_{M0}} = \Delta v_{z0}\frac{\partial \tau_{a,c}}{\partial y_{M0}}$ | $\frac{\partial D_z}{\partial y_{M0}} = -(t_e + \tau_{a,c})\frac{\partial \tau_{a,c}}{\partial y_{M0}}$ |
| $\frac{\partial N_z}{\partial z_{M0}} = 1$ | $\frac{\partial D_z}{\partial z_{M0}} = 0$ |
| $\frac{\partial N_z}{\partial v_{Mx0}} = \Delta v_{z0}\frac{\partial \tau_{a,c}}{\partial v_{Mx0}}$ | $\frac{\partial D_z}{\partial v_{Mx0}} = -(t_e + \tau_{a,c})\frac{\partial \tau_{a,c}}{\partial v_{Mx0}}$ |
| $\frac{\partial N_z}{\partial v_{My0}} = \Delta v_{z0}\frac{\partial \tau_{a,c}}{\partial v_{My0}}$ | $\frac{\partial D_z}{\partial v_{My0}} = -(t_e + \tau_{a,c})\frac{\partial \tau_{a,c}}{\partial v_{My0}}$ |
| $\frac{\partial N_z}{\partial v_{Mz0}} = t_e + \tau_{a,c}$ | $\frac{\partial D_z}{\partial v_{Mz0}} = 0$ |
| $\frac{\partial N_z}{\partial x_{T0}} = \Delta v_{z0}\frac{\partial \tau_{a,c}}{\partial x_{T0}}$ | $\frac{\partial D_z}{\partial x_{T0}} = -(t_e + \tau_{a,c})\frac{\partial \tau_{a,c}}{\partial x_{T0}}$ |
| $\frac{\partial N_z}{\partial y_{T0}} = \Delta v_{z0}\frac{\partial \tau_{a,c}}{\partial y_{T0}}$ | $\frac{\partial D_z}{\partial y_{T0}} = -(t_e + \tau_{a,c})\frac{\partial \tau_{a,c}}{\partial y_{T0}}$ |
| $\frac{\partial N_z}{\partial z_{T0}} = -1$ | $\frac{\partial D_z}{\partial z_{T0}} = 0$ |
| $\frac{\partial N_z}{\partial v_{Tx0}} = \Delta v_{z0}\frac{\partial \tau_{a,c}}{\partial v_{Tx0}}$ | $\frac{\partial D_z}{\partial v_{Tx0}} = -(t_e + \tau_{a,c})\frac{\partial \tau_{a,c}}{\partial v_{Tx0}}$ |
| $\frac{\partial N_z}{\partial v_{Ty0}} = \Delta v_{z0}\frac{\partial \tau_{a,c}}{\partial v_{Ty0}}$ | $\frac{\partial D_z}{\partial v_{Ty0}} = -(t_e + \tau_{a,c})\frac{\partial \tau_{a,c}}{\partial v_{Ty0}}$ |
| $\frac{\partial N_z}{\partial v_{Tz0}} = -(t_e + \tau_{a,c})$ | $\frac{\partial D_z}{\partial v_{Tz0}} = 0$ |

where:

$$\underline{C}_{21} = \frac{\partial \delta \tau_{a,c}}{\partial \underline{x}_{TR,pv}} \tag{A.323}$$

$$\underline{C}_{22} = \frac{\partial \delta a_{l,x,c}}{\partial \underline{x}_{TR,pv}} \tag{A.324}$$

$$\underline{C}_{23} = \frac{\partial \delta a_{l,y,c}}{\partial \underline{x}_{TR,pv}} \tag{A.325}$$

$$\underline{C}_{24} = \frac{\partial \delta a_{z,c}}{\partial \underline{x}_{TR,pv}} \tag{A.326}$$

Expressions for the row matrices $\underline{C}_{2i}$, $i = 1, \ldots, 4$, are given in Figures A.11 to A.14. Expressions for the partials appearing in these figures are given in Tables A.11 to A.15. The notation used in all these figures and tables is summarized in Table A.10.

$$\left[ \begin{array}{ccc|ccc} \frac{\partial \tau_{a,c}}{\partial x_{T0}} & \frac{\partial \tau_{a,c}}{\partial y_{T0}} & \frac{\partial \tau_{a,c}}{\partial z_{T0}} & \frac{\partial \tau_{a,c}}{\partial v_{Tx0}} & \frac{\partial \tau_{a,c}}{\partial v_{Ty0}} & \frac{\partial \tau_{a,c}}{\partial v_{Tz0}} \end{array} \right]$$

Figure A.11: Row Matrix $\underline{C}_{21}$

$$\left[ \begin{array}{ccc|ccc} a_1 \frac{\partial \bar{a}_{l,c}}{\partial x_{T0}} & a_1 \frac{\partial \bar{a}_{l,c}}{\partial y_{T0}} & a_1 \frac{\partial \bar{a}_{l,c}}{\partial z_{T0}} & a_1 \frac{\partial \bar{a}_{l,c}}{\partial v_{Tx0}} & a_1 \frac{\partial \bar{a}_{l,c}}{\partial v_{Ty0}} & a_1 \frac{\partial \bar{a}_{l,c}}{\partial v_{Tz0}} \end{array} \right]$$

Figure A.12: Row Matrix $\underline{C}_{22}$

$$\left[ \begin{array}{ccc|ccc} a_2 \frac{\partial \bar{a}_{l,c}}{\partial x_{T0}} & a_2 \frac{\partial \bar{a}_{l,c}}{\partial y_{T0}} & a_2 \frac{\partial \bar{a}_{l,c}}{\partial z_{T0}} & a_2 \frac{\partial \bar{a}_{l,c}}{\partial v_{Tx0}} & a_2 \frac{\partial \bar{a}_{l,c}}{\partial v_{Ty0}} & a_2 \frac{\partial \bar{a}_{l,c}}{\partial v_{Tz0}} \end{array} \right]$$

Figure A.13: Row Matrix $\underline{C}_{23}$

Computation of $\underline{C}_g$ — The matrix $\underline{C}_g$ is computed from its definition in Equations A.313 and A.314.

Computation of $\underline{P}_G(t_0)$ — The matrix $\underline{P}_G(t_0)$ is computed from Equation A.315.

### A.9.9 Propagate $\underline{P}_G$

Background — The fifth step in the guidance algorithm is the propagation from $t_0$ to $\bar{t}_{HO}$ of the covariance ($\underline{P}_G$) of the guidance state vector. This propagation is specified by the initial covariance matrix $\underline{P}_G(t_0)$ (defined in the previous subsection) and by the matrices $\underline{F}_G$ and $\underline{Q}_G$ associated with the state equation

$$\dot{\underline{x}}_G = \underline{F}_G \underline{x}_G + \underline{w}_G \ . \tag{A.327}$$

$$\left[\begin{array}{ccc|ccc} \frac{\partial a_{x,c}}{\partial x_{T0}} & \frac{\partial a_{x,c}}{\partial y_{T0}} & \frac{\partial a_{x,c}}{\partial z_{T0}} & \frac{\partial a_{x,c}}{\partial v_{Tx0}} & \frac{\partial a_{x,c}}{\partial v_{Ty0}} & \frac{\partial a_{x,c}}{\partial v_{Tz0}} \end{array}\right]$$

Figure A.14: Row Matrix $\underline{C}_{24}$

Equations for $\underline{F}_G$ and $\underline{Q}_G$ follow.

Computation of $\underline{F}_G$: The matrix $\underline{F}_G$ is defined in Figure A.15. The figure shows that the partitions of the guidance state vector $\underline{x}_G$ (given in Equation A.312) propagate as follows:

$$\left[\begin{array}{ccccc} \underline{F}_M & \underline{0}_{\dim\{\underline{x}_M\}\times 6} & \underline{0}_{\dim\{\underline{x}_M\}\times 6} & \underline{0}_{\dim\{\underline{x}_M\}\times 4} & \underline{0}_{\dim\{\underline{x}_M\}\times 6} \\ \hline \multicolumn{5}{c}{\underline{0}_{16\times(\dim\{\underline{x}_M\}+22)}} \\ \hline \underline{F}_{dM} & \underline{0}_{6\times 6} & \underline{0}_{6\times 6} & \underline{0}_{6\times 4} & \underline{F}_d \end{array}\right]$$

Figure A.15: Matrix $\underline{F}_G$

- $\underline{x}_M(t)$ propagates according to the dynamics of the M INS state equation as described in Section A.4

- $\underline{x}_{M,pv}(t)$ propagates according to the state equation

$$\dot{\underline{x}}_{M,pv} = \underline{0}_6 \tag{A.328}$$

because $\underline{x}_{M,pv}(t)$ contains the M INS position and velocity read-out errors *at* $t_0$ which remain invariant with time

- Similarly, $\underline{x}_{TR,pv}(t)$ propagates according to

$$\dot{\underline{x}}_{TR,pv} = \underline{0}_6 \tag{A.329}$$

because the tracking errors at $t_0$ are also time-invariant

- Also time-invariant are the errors in the computed acceleration and acceleration interval:

$$\dot{\underline{x}}_g = \underline{0}_4. \tag{A.330}$$

- The errors $\underline{x}_d$ in "pointing" the computed acceleration (resulting from the erroneous attitude read-out of the M INS) propagate according to the state equation

$$\dot{\underline{x}}_d = \underline{F}_d\,\underline{x}_d + \underline{F}_{dM}\,\underline{x}_M. \tag{A.331}$$

In this equation:

$$\underline{x}_d = \begin{bmatrix} \delta p_{M,L,d} \\ \delta v_{M,L,d} \end{bmatrix} \tag{A.332}$$

$\delta p_{M,L,d}$ = Perturbation in the M location (NED position) due to M INS attitude errors

$\delta v_{M,L,d}$ = Perturbation in the M velocity (NED) due to M INS attitude errors

$$\underline{F}_d = \begin{bmatrix} \underline{0}_{3\times3} & \underline{I}_{3\times3} \\ \underline{0}_{3\times3} & \underline{0}_{3\times3} \end{bmatrix} \quad \text{(position is the integral of velocity)} \tag{A.333}$$

$$\underline{F}_{dM} = \left[\begin{array}{ccc|c} & \underline{0}_{3\times\dim\{\underline{x}_M\}} & & \\ \hline 0 & \bar{a}_{z,c} & -\bar{a}_{l,y,c} & \\ -\bar{a}_{z,c} & 0 & \bar{a}_{l,x,c} & \underline{0}_{3\times(\dim\{\underline{x}_M\}-3)} \\ \bar{a}_{l,y,c} & -\bar{a}_{l,x,c} & 0 & \end{array}\right] \tag{A.334}$$

(attitude error times acceleration drives velocity rates).

Computation of $\underline{Q}_G$: The only entries of $\underline{x}_G$ driven by white noise are some of the states corresponding to the M INS error vector. Consequently,

$$\underline{Q}_G = \begin{bmatrix} \underline{Q}_M & \underline{0}_{\dim\{\underline{x}_M\}\times22} \\ \underline{0}_{22\times\dim\{\underline{x}_M\}} & \underline{0}_{22\times22} \end{bmatrix}. \tag{A.335}$$

where $\underline{Q}_M$ is as described in Section A.4.

## A.9.10 Compute M Location Covariance

The sixth step in the guidance algorithm is the computation of the M position and velocity covariance at handover,

$$\underline{P}_{M,L,pv}(\bar{t}_{HO}) \triangleq E\{\begin{bmatrix} \delta p_{M,L}(\hat{t}_{HO}) \\ \delta v_{M,L}(\hat{t}_{HO}) \end{bmatrix} \begin{bmatrix} \delta p_{M,L}(\hat{t}_{HO}) \\ \delta v_{M,L}(\hat{t}_{HO}) \end{bmatrix}^T\}. \tag{A.336}$$

This covariance is one of the four main results computed in the simulation: it characterizes the M position ($\delta p_{M,L}$) and velocity ($\delta v_{M,L}$) deviations from the mean at handover.[29]

The M position and velocity covariance at handover is computed by the transformation

$$\underline{P}_{M,L,pv} = \underline{C}_{M,L,pv}\underline{P}_G(\bar{t}_{HO})\underline{C}^T_{M,L,pv} \tag{A.337}$$

where $\underline{P}_G(\bar{t}_{HO})$ is calculated as described in the previous subsection. The transformation $\underline{C}_{M,L,pv}$ is defined in Figure A.16.

[29]The other three main results computed by the simulation are: the T position and velocity covariance at handover (considered in Subsection A.9.11), and the mean M and T positions and velocities also at handover (considered in Subsection A.9.6).

$$\left[\begin{array}{c|c|ccc|cc} \underline{0}_{3\times(\dim\{\underline{x}_M\}+12)} & \bar{v}_M(t_0)+\bar{\tau}_{a,c}\bar{a}_c & \frac{1}{2}\bar{\tau}_{a,c}^2 & 0 & 0 & \underline{I}_{3\times3} & \underline{0}_{3\times3} \\ & & 0 & \frac{1}{2}\bar{\tau}_{a,c}^2 & 0 & & \\ & & 0 & 0 & \frac{1}{2}\bar{\tau}_{a,c}^2 & & \\ \hline \underline{0}_{3\times(\dim\{\underline{x}_M\}+12)} & \bar{a}_c & \bar{\tau}_{a,c} & 0 & 0 & \underline{0}_{3\times3} & \underline{I}_{3\times3} \\ & & 0 & \bar{\tau}_{a,c} & 0 & & \\ & & 0 & 0 & \bar{\tau}_{a,c} & & \end{array}\right]$$

Figure A.16: Matrix $\underline{C}_{M,L,pv}$

Discussion of Equation A.337 — From Equation A.337 and Figure A.16 the following expression is obtained for the deviation in M position from the mean at handover:

$$\delta p_{M,L}(\hat{t}_{HO}) = \delta\tau_{a,c}\,\bar{v}_M(t_0) + \frac{1}{2}\bar{\tau}_{a,c}^2\,\delta a_c + \bar{\tau}_{a,c}\,\delta\tau_{a,c}\,\bar{a}_c + \delta p_{M,L,d}(\bar{t}_{HO}) \tag{A.338}$$

The terms in the right-side of this equation are as follows:

- $\delta\tau_{a,c}\,\bar{v}_M(t_0)$ and $\bar{\tau}_{a,c}\,\delta\tau_{a,c}\,\bar{a}_c$ represent the effect of integrating the velocity at $t_0$ and the acceleration applied through an interval that is in error by $\delta\tau_{a,c}$
- $\frac{1}{2}\bar{\tau}_{a,c}^2\,\delta a_c$ represents the effect of errors in the computed acceleration
- $\delta p_{M,L,d}$ represents the effect of M INS attitude errors on the application of the computed acceleration.

Similarly, the following expression is obtained for the deviation in M velocity from the mean at handover:

$$\delta v_{M,L}(\hat{t}_{HO}) = \delta\tau_{a,c}\,\bar{a}_c + \bar{\tau}_{a,c}\,\delta a_c + \delta v_{M,L,d}(\bar{t}_{HO}) \tag{A.339}$$

The terms in the right-side of this equation are as follows:

- $\delta\tau_{a,c}\,\bar{a}_c$ represent the effect of integrating the acceleration applied through an interval that is in error by $\delta\tau_{a,c}$
- $\bar{\tau}_{a,c}\,\delta a_c$ represents the effect of errors in the computed acceleration
- $\delta v_{M,L,d}$ represents the effect of M INS attitude errors on the application of the computed acceleration.

## A.9.11 Compute T Location Covariance

The seventh step in the guidance algorithm is the computation of the T position and velocity covariance at handover,

$$\underline{P}_{T,L,pv}(\bar{t}_{HO}) \triangleq E\{\begin{bmatrix} \delta p_{T,L}(\hat{t}_{HO}) \\ \delta v_{T,L}(\hat{t}_{HO}) \end{bmatrix}\begin{bmatrix} \delta p_{T,L}(\hat{t}_{HO}) \\ \delta v_{T,L}(\hat{t}_{HO}) \end{bmatrix}^T\}. \tag{A.340}$$

This covariance is one of the four main results computed in the simulation: it characterizes the T position ($\delta p_{T,L}$) and velocity ($\delta v_{T,L}$) deviations from the mean at handover.

$\underline{P}_{T,L,pv}(\bar{t}_{HO})$ is computed from the Singer covariance ($\underline{P}_{T,L}(\bar{t}_{HO})$ in Equation A.10 of Subsection A.1.2):

$$\underline{P}_{T,L,pv} = \underline{C}_{T,L,pv}\underline{P}_{T,L}(\bar{t}_{HO})\underline{C}^{T}_{T,L,pv} \tag{A.341}$$

where the transformation $\underline{C}_{T,L}$ is defined in Figure A.17. The figure shows how the transformation chooses the appropriate position and velocity entries from the Singer state vector defined in Subsection A.1.2.

$$\left[\begin{array}{ccc|ccc|ccc} 1 & 0 & 0 & 0 & 0 & 0 & 0 & 0 & 0 \\ 0 & 0 & 0 & 1 & 0 & 0 & 0 & 0 & 0 \\ 0 & 0 & 0 & 0 & 0 & 0 & 1 & 0 & 0 \\ \hline 0 & 1 & 0 & 0 & 0 & 0 & 0 & 0 & 0 \\ 0 & 0 & 0 & 0 & 1 & 0 & 0 & 0 & 0 \\ 0 & 0 & 0 & 0 & 0 & 0 & 0 & 1 & 0 \end{array}\right]$$

Figure A.17: Matrix $\underline{C}_{T,L,pv}$

# A.10 SP Radar Model

## A.10.1 Background

This section presents a back-of-the-envelope radar accuracy model for an airborne surveillance platform such as the E-3 AWACS. The model is "back-of-the-envelope" because all accuracies are characterized by simple one-line formulas. A more detailed accuracy characterization can be developed but is beyond the scope of the present study. While the model is addressed to airborne early-warning radars such as that aboard the AWACS surveillance platform, the model is completely based on unclassified information.

All radar measurement accuracies (range, azimuth, elevation, and range-rate) can be characterized as the root-sum-square of a range-dependent (RD) term and a range-independent (RI) term:

$$\sigma_{\text{TOTAL}} = \sqrt{\sigma^2_{\text{RD}} + \sigma^2_{\text{RI}}}. \tag{A.342}$$

The RI term characterizes the physical limits of the radar: no matter how close the target is to the radar, the measurement accuracy is corrupted by factors such as vibration, deformation of the air frame, resolver accuracy, etc. The RD term represents the effect of signal-to-noise ratio (SNR) on the measurement accuracy:

- Accuracy improves with a stronger received signal power level (such as results from a larger target, a shorter distance to the target, or a more powerful radar)
- Accuracy deteriorates from a stronger noise power level (such as results from less expensive radar equipment or from the presence of jamming).

In Subsection A.10.3 expressions are given for both the RD and RI accuracies. These expressions are based on the assumptions listed in Subsection A.10.2.

## A.10.2 Assumptions

Model assumptions are divided into three categories: fundamental assumptions, radar parameter assumptions, and miscellaneous assumptions.

Fundamental Assumptions:

- All RD accuracies (range, range-rate, azimuth, and elevation accuracies) are expressed in terms of the azimuth accuracy (standard deviation of error) under *nominal conditions*, $\sigma^*_{RD,az}$. I.e., the "quality" of the radar is parameterized by $\sigma^*_{RD,az}$ A typical value of $\sigma^*_{RD,az}$ is

$$\sigma^*_{RD,az} = 1.5 \text{ deg.} \tag{A.343}$$

  To consider radars which are "better", values of $\sigma^*_{RD,az}$ smaller than 1.5 deg are assumed; and conversely for "worse" radars

- *Nominal conditions* are defined as follows:
  - Range to the target is 300 km
  - The target has RCS of 4 $m^2$ (corresponding to a typical fighter aircraft[30])
  - The radar has parameters as listed below.

Radar Parameter Assumptions: The following assumptions are based on the parameters of the AWACS E3 surveillance radar as reported in the unclassified literature ([Morchin, 1990]):

$$\begin{aligned} \lambda &= \text{Wavelength} \\ &= 10 \text{ cm (S-band)} && \text{(A.344)} \\ l_{az} &= \text{Horizontal dimension of antenna} \\ &= 7.5 \text{ m} && \text{(A.345)} \\ l_{el} &= \text{Vertical dimension of antenna} \\ &= 1.5 \text{ m.} && \text{(A.346)} \end{aligned}$$

The following additional assumptions are made:

$$\begin{aligned} \tau &= \text{Compressed pulse width} \\ &= 0.05 \ \mu \text{ sec} && \text{(A.347)} \\ \Delta f &= \text{Doppler filter bandwidth} \\ &= 300 \text{ Hz.} && \text{(A.348)} \end{aligned}$$

Miscellaneous assumptions:

[30]The radar cross section (RCS) measured in $m^2$, is roughly proportional to the size of the target.

- The radar measures range, range-rate, azimuth, and elevation
- All measurement noises are uncorrelated
- SNR is proportional to the RCS ($\sigma$) and inversely proportional to the fourth power of the distance to the target ($R$), so that

$$\text{SNR} = K_R \frac{\sigma}{R^4} \tag{A.349}$$

The constant $K_R$ depends on the transmitted power, system losses, and other factors according to the *radar equation* ([Skolnik, 1980]).

- All RD accuracies (e.g., [Hovanessian, 1988]) are inversely proportional to SNR according to ($c$ is the speed of light, $3 \times 10^8$ m/sec):

$$\begin{aligned}
\sigma_{RD,R} &= \text{RD range standard deviation (m)} \\
&= \frac{c\tau}{4\sqrt{\text{SNR}}} && \text{(A.350)} \\
\sigma_{RD,\dot{R}} &= \text{RD range-rate standard deviation (m/sec)} \\
&= \frac{\lambda \Delta f}{4\sqrt{\text{SNR}}} && \text{(A.351)} \\
\sigma_{RD,az} &= \text{RD azimuth standard deviation (deg)} \\
&= \frac{\lambda}{2l_{az}\sqrt{\text{SNR}}} \frac{180}{\pi} && \text{(A.352)} \\
\sigma_{RD,el} &= \text{RD elevation standard deviation (deg)} \\
&= \frac{\lambda}{2l_{el}\sqrt{\text{SNR}}} \frac{180}{\pi}. && \text{(A.353)}
\end{aligned}$$

## A.10.3 Accuracy Model

The accuracy model for the RD component is given by the following equations:

$$\begin{aligned}
\sigma_{RD,R} &= 2.23 \times 10^{-10}\, \sigma^*_{RD,az} \frac{R^2}{\sqrt{\sigma}} && \text{(m)} && \text{(A.354)} \\
\sigma_{RD,\dot{R}} &= 4.46 \times 10^{-10}\, \sigma^*_{RD,az} \frac{R^2}{\sqrt{\sigma}} && \text{(m/sec)} && \text{(A.355)} \\
\sigma_{RD,az} &= 2.22 \times 10^{-11}\, \sigma^*_{RD,az} \frac{R^2}{\sqrt{\sigma}} && \text{(deg)} && \text{(A.356)} \\
\sigma_{RD,el} &= 1.11 \times 10^{-10}\, \sigma^*_{RD,az} \frac{R^2}{\sqrt{\sigma}} && \text{(deg).} && \text{(A.357)}
\end{aligned}$$

These equations are obtained by solving Equation A.352 for $K_R$ (using Equation A.349) as a function of $\sigma^*_{RD,az}$ under nominal conditions. The resulting expression for SNR is then substituted in Equations A.350 to A.353 for the range, range-rate, azimuth, and elevation standard deviations.

The error model for the RI components are specified by constant standard deviations:

$$\sigma_{RI,R} = 5 \text{ m} \quad \text{(A.358)}$$

$$\sigma_{RI,\dot{R}} = 10 \text{ m/sec} \quad \text{(A.359)}$$

$$\sigma_{RI,az} = 1 \text{ deg} \quad \text{(A.360)}$$

$$\sigma_{RI,el} = 2 \text{ deg.} \quad \text{(A.361)}$$

The total error is obtained by rss'ing the RD and RI components:

$$\sigma_{\text{TOTAL},R} = \sqrt{\sigma^2_{RD,R} + \sigma^2_{RI,R}} \quad \text{(A.362)}$$

$$\sigma_{\text{TOTAL},\dot{R}} = \sqrt{\sigma^2_{RD,\dot{R}} + \sigma^2_{RI,\dot{R}}} \quad \text{(A.363)}$$

$$\sigma_{\text{TOTAL},az} = \sqrt{\sigma^2_{RD,az} + \sigma^2_{RI,az}} \quad \text{(A.364)}$$

$$\sigma_{\text{TOTAL},el} = \sqrt{\sigma^2_{RD,el} + \sigma^2_{RI,el}}. \quad \text{(A.365)}$$

An example of the computation of radar errors is shown in Table A.16. The table lists errors under nominal conditions for $\sigma^*_{RD,az} = 1.5$ deg.

Table A.16: RADAR ERROR STANDARD DEVIATIONS FOR $\sigma^*_{RD,az} = 1.5$ deg

| MEASUREMENT | RD ERROR | RI ERROR | TOTAL ERROR |
|---|---|---|---|
| Range (m) | 15 | 5 | 16 |
| Range-Rate (m/sec) | 30 | 10 | 32 |
| Azimuth (deg) | 1.5 | 1 | 2 |
| Elevation (deg) | 7.5 | 2 | 8 |

# A.11 SP Tracking Filter Model

## A.11.1 Background

The objective of the SP tracking filter model is the computation of the position and velocity estimation error covariance matrix at time $t_0$ (time $t_0$ is the time at which the M has achieved its cruising speed, Subsection A.9.4). This covariance matrix is defined by

$$\underline{P}_{TR,pv}(t_0) = E\{\begin{bmatrix} \delta p_T(t_0) \\ \delta v_T(t_0) \end{bmatrix} \begin{bmatrix} \delta p_T(t_0) \\ \delta v_T(t_0) \end{bmatrix}^T\}, \quad \text{(A.366)}$$

where $\delta p_T(t_0)$ and $\delta v_T(t_0)$ are the errors in estimating the target's *unperturbed*[31] position and velocity vectors in the $t$-frame.[32]

The matrix $\underline{P}_{TR,pv}(t_0)$ is obtained via a Kalman update and a Kalman propagation. The top-level of the update and propagate is given in Subsection A.11.2. The formulas for the matrices which define the update and propagate ( $\underline{H}_{TR}$, $\underline{R}_{TR}$, $\underline{F}_{TR}$, and $\underline{Q}_{TR}$) are given in Subsection A.11.3.

[31] "Unperturbed" means without the Singer perturbation (i.e., the *straight-line* T trajectory).

[32] The superscript $t$ indicating the $t$-frame is omitted in this section.

### A.11.2 Tracking Filter Top Level

The Kalman update and propagate procedure leading to the computation of $\underline{P}_{TR,pv}(t_0)$ is divided into four steps as follows:

- Computation of the covariance before the update (at $t^-_{LAUNCH}$)
- Computation of the covariance after the update (at $t^+_{LAUNCH}$)
- Propagation from $t^+_{LAUNCH}$ to $t_0$
- Computation of $\underline{P}_{TR,pv}(t_0)$.

*1. Computation of covariance before the update (at $t^-_{LAUNCH}$):* The state vector of the tracking filter is as defined in Table 3.7:

$$\underline{x}_{TR} = \left[\begin{array}{c} \delta p_{SP} \\ \delta v_{SP} \\ \delta\theta_{SP,az} \\ \hline \underline{x}_T \\ \hline \delta p_{\mathrm{Tx\ BIAS}} \\ \delta v_{\mathrm{Tx\ BIAS}} \\ \delta p_{\mathrm{Ty\ BIAS}} \\ \delta v_{\mathrm{Ty\ BIAS}} \\ \delta p_{\mathrm{Tz\ BIAS}} \\ \delta v_{\mathrm{Tz\ BIAS}} \end{array}\right]. \tag{A.367}$$

Because the three parts of $\underline{x}_{TR}$ are uncorrelated, the covariance of the state vector is a block-diagonal matrix:

$$\underline{P}_{TR}(t^-_{\mathrm{LAUNCH}}) = E\{\underline{x}_{TR}(t^-_{\mathrm{LAUNCH}})\underline{x}_{TR}(t^-_{\mathrm{LAUNCH}})^T\} \tag{A.368}$$

$$= \left[\begin{array}{ccc} \underline{P}_{SP,pva} & \underline{0}_{7\times9} & \underline{0}_{7\times6} \\ \underline{0}_{9\times7} & \underline{P}_{T,L} & \underline{0}_{9\times6} \\ \underline{0}_{6\times7} & \underline{0}_{6\times9} & \underline{P}_{T,bias} \end{array}\right]. \tag{A.369}$$

Expressions for the diagonal blocks follow.

The covariance $\underline{P}_{SP,pva}$ models the uncertainty in the position, velocity, and azimuth read-out of the SP INS. This covariance is given by a transformation of the covariance ($\underline{P}_{SP}$) of the SP INS,

$$\underline{P}_{SP,pva} = \underline{C}_{SP,pva}\underline{P}_{SP}\underline{C}^T_{SP,pva} \tag{A.370}$$

where the $\underline{C}_{SP,pva}$ is as shown in Figure A.18.

The covariance $\underline{P}_{T,L}$ models the uncertainty in the trajectory of the T as given by the Singer model described in Subsection A.1.2. The covariance is as defined in Equation A.10 and is computed by propagating the covariance according to Equation A.4 for the $x$-component and identical equations for the $y$- and $z$-components.

$$\left[\begin{array}{ccc|ccc|ccc|c}
0 & 0 & 0 & 0 & 0 & 0 & R_\oplus & 0 & L & \\
0 & 0 & 0 & 0 & 0 & 0 & -R_\oplus \ell \sin L & R_\oplus \cos L & \ell \cos L & \underline{0}_{3\times(\dim\{\underline{x}_{SP}\}-9)} \\
0 & 0 & 0 & 0 & 0 & 0 & 0 & 0 & -1 & \\
\hline
0 & 0 & 0 & R_\oplus & 0 & 0 & 0 & 0 & \frac{v_N}{R_\oplus} & \\
0 & 0 & 0 & 0 & R_\oplus \cos L & 0 & -v_E \tan L & 0 & \frac{v_E}{R_\oplus} & \underline{0}_{3\times(\dim\{\underline{x}_{SP}\}-9)} \\
0 & 0 & 0 & 0 & 0 & -1 & 0 & 0 & 0 & \\
\hline
0 & 0 & 1 & 0 & 0 & 0 & 0 & 0 & 0 & \underline{0}_{1\times(\dim\{\underline{x}_{SP}\}-9)}
\end{array}\right]$$

Figure A.18: Matrix $\underline{C}_{SP,pva}$

The covariance $\underline{P}_{T,bias}$ of the bias part of the state,

$$\underline{b}_{TR} = \begin{bmatrix} \delta p_{\mathrm{Tx\ BIAS}} \\ \delta v_{\mathrm{Tx\ BIAS}} \\ \delta p_{\mathrm{Ty\ BIAS}} \\ \delta v_{\mathrm{Ty\ BIAS}} \\ \delta p_{\mathrm{Tz\ BIAS}} \\ \delta v_{\mathrm{Tz\ BIAS}} \end{bmatrix} \tag{A.371}$$

represent the uncertainty in the location of the straight-line trajectory of the target before the radar measurement is processed. Because this uncertainty is "infinite" (T trajectory is unknown), the covariance is a diagonal matrix with large diagonal entries:

$$\underline{P}_{T,b} = \begin{bmatrix} (100\,\mathrm{km})^2 & 0 & 0 & 0 & 0 & 0 \\ 0 & (300\,\mathrm{m/sec})^2 & 0 & 0 & 0 & 0 \\ 0 & 0 & (100\,\mathrm{km})^2 & 0 & 0 & 0 \\ 0 & 0 & 0 & (300\,\mathrm{m/sec})^2 & 0 & 0 \\ 0 & 0 & 0 & 0 & (100\,\mathrm{km})^2 & 0 \\ 0 & 0 & 0 & 0 & 0 & (300\,\mathrm{m/sec})^2 \end{bmatrix}. \tag{A.372}$$

*2. Computation of covariance after the update (at $t^+_{LAUNCH}$):* The covariance after the update, $\underline{P}_{TR}(t^+_{\mathrm{LAUNCH}})$, is obtained by performing a Kalman update on the covariance $\underline{P}_{TR}(t^-_{\mathrm{LAUNCH}})$. The Kalman update is specified by the matrices $\underline{H}_{TR}$ and $\underline{R}_{TR}$ defined in Subsection A.11.3. These matrices model the linearized measurement equation

$$\underline{z}_{TR} = \underline{H}_{TR}\underline{\mathcal{E}}_{TR} + \underline{v}_{TR} \tag{A.373}$$

where the vector $\underline{z}_{TR}$ is the measurement of errors in range, range-rate, azimuth, and elevation, and all quantities are evaluated at $t_{LAUNCH}$.

*3. Propagation from $t^+_{LAUNCH}$ to $t_0$:* The covariance $\underline{P}_{TR}(t^+_{\mathrm{LAUNCH}})$ is propagated from $t^+_{LAUNCH}$ to $t_0$ according to the state equations

$$\dot{\underline{x}}_{TR} = \underline{F}_{TR}\underline{x}_{TR} + \underline{w}_{TR} \ . \tag{A.374}$$

This propagation is defined by the dynamics matrix $\underline{F}_{TR}$ and the white noise spectral density matrix $\underline{Q}_{TR}$ ([Gelb, 1974]). Expressions for these matrices are provided in Subsection A.11.3. The propagation produces $\underline{P}_{TR}(t_0)$.

*4. Computation of $\underline{P}_{TR,pv}(t_0)$:* The matrix $\underline{P}_{TR,pv}(t_0)$, defined by Equation A.366, is obtained from $\underline{P}_{TR}(t_0)$ by the transformation

$$\underline{P}_{TR,pv}(t_0) = \underline{C}_{TR}\underline{P}_{TR}(t_0)\underline{C}^T_{TR}, \tag{A.375}$$

where

$$\underline{C}_{TR} = \left[\begin{array}{c|cccccc} & 1 & 0 & 0 & 0 & 0 & 0 \\ \underline{0}_{3\times 16} & 0 & 0 & 1 & 0 & 0 & 0 \\ & 0 & 0 & 0 & 0 & 1 & 0 \\ \hline & 0 & 1 & 0 & 0 & 0 & 0 \\ \underline{0}_{3\times 16} & 0 & 0 & 0 & 1 & 0 & 0 \\ & 0 & 0 & 0 & 0 & 0 & 1 \end{array}\right] . \tag{A.376}$$

The transformation $\underline{C}_{TR}$ includes only the errors in estimating the bias states because the M guidance computations are based on the straight-line unperturbed T trajectory, excluding the short-term Singer perturbations. The bias states, however, are observed in the presence of the Singer perturbations as modeled by the $\underline{H}_{TR}$ matrix defined below.

## A.11.3 Computation of $\underline{H}_{TR}$ $\underline{R}_{TR}$ $\underline{F}_{TR}$, and $\underline{Q}_{TR}$

*Matrix $\underline{H}_{TR}$:* The matrix $\underline{H}_{TR}$ appearing in the linearized measurement equation (Equation A.373) has four rows corresponding to the four radar measurements:

$$\underline{H}_{TR} = \left[\begin{array}{c} \underline{H}_1 \\ \underline{H}_2 \\ \underline{H}_3 \\ \underline{H}_4 \end{array}\right] . \tag{A.377}$$

In this equation, the $\underline{H}_i$ are $1 \times 22$ row matrices:

$$\underline{H}_1 = \frac{\partial R}{\partial \underline{x}_{TR}} \tag{A.378}$$

$$\underline{H}_2 = \frac{\partial \dot{R}}{\partial \underline{x}_{TR}} \tag{A.379}$$

$$\underline{H}_3 = \frac{\partial a}{\partial \underline{x}_{TR}} \tag{A.380}$$

$$\underline{H}_4 = \frac{\partial e}{\partial \underline{x}_{TR}} \tag{A.381}$$

where

$R$ = True range
$\dot{R}$ = True range-rate
$a$ = True azimuth
$e$ = True elevation
$\underline{x}_{TR}$ = Tracking state vector defined in Equation A.367.

The entries in $\underline{x}_{TR}$ are given in Figure A.19 ($x$, $y$, and $z$ correspond to North, East, and Down).

$$\left[ \delta x_S \quad \delta y_S \quad \delta z_S \,\middle|\, \delta v_{Sx} \quad \delta v_{Sy} \quad \delta v_{Sz} \,\middle|\, \delta\theta_{SP,az} \,\middle|\, p_{Tx} \quad v_{Tx} \quad a_{Tx} \,\middle|\, p_{Ty} \quad v_{Ty} \quad a_{Ty} \,\middle|\, p_{Tz} \quad v_{Tz} \quad a_{Tz} \,\middle|\right.$$

$$\left. \delta p_{\mathrm{Tx\ BIAS}} \quad \delta v_{\mathrm{Tx\ BIAS}} \quad \delta p_{\mathrm{Ty\ BIAS}} \quad \delta v_{\mathrm{Ty\ BIAS}} \quad \delta p_{\mathrm{Tz\ BIAS}} \quad \delta v_{\mathrm{Tz\ BIAS}} \right]$$

Figure A.19: Entries in State Vector $\underline{x}_{TR}$

Expressions for the row matrices $\underline{H}_i$ are given in Figures A.20 to A.23. Expressions for the partials appearing in these figures are given in Tables A.17 to A.20. All quantities appearing in these figures and tables are evaluated at the update time, $t_{LAUNCH}$.

$$\left[ \frac{\partial R}{\partial \delta x_S} \quad \frac{\partial R}{\partial \delta y_S} \quad \frac{\partial R}{\partial \delta z_S} \,\middle|\, 0 \quad 0 \quad 0 \,\middle|\, 0 \,\middle|\, \frac{\partial R}{\partial p_{Tx}} \quad 0 \quad 0 \,\middle|\, \frac{\partial R}{\partial p_{Ty}} \quad 0 \quad 0 \,\middle|\, \frac{\partial R}{\partial p_{Tz}} \quad 0 \quad 0 \,\middle|\right.$$

$$\left. \frac{\partial R}{\partial \delta p_{\mathrm{Tx\ BIAS}}} \quad 0 \quad \frac{\partial R}{\partial \delta p_{\mathrm{Ty\ BIAS}}} \quad 0 \quad \frac{\partial R}{\partial \delta p_{\mathrm{Tz\ BIAS}}} \quad 0 \right]$$

Figure A.20: Row Matrix $\underline{H}_1$

$$\left[ 0 \quad 0 \quad 0 \,\middle|\, \frac{\partial \dot{R}}{\partial \delta v_{Sx}} \quad \frac{\partial \dot{R}}{\partial \delta v_{Sy}} \quad \frac{\partial \dot{R}}{\partial \delta v_{Sz}} \,\middle|\, 0 \,\middle|\, 0 \quad \frac{\partial \dot{R}}{\partial v_{Tx}} \quad 0 \,\middle|\, 0 \quad \frac{\partial \dot{R}}{\partial v_{Ty}} \quad 0 \,\middle|\, 0 \quad \frac{\partial \dot{R}}{\partial v_{Tz}} \quad 0 \,\middle|\right.$$

$$\left. 0 \quad \frac{\partial \dot{R}}{\partial \delta v_{\mathrm{Tx\ BIAS}}} \quad 0 \quad \frac{\partial \dot{R}}{\partial \delta v_{\mathrm{Ty\ BIAS}}} \quad 0 \quad \frac{\partial \dot{R}}{\partial \delta v_{\mathrm{Tz\ BIAS}}} \right]$$

Figure A.21: Row Matrix $\underline{H}_2$

*Matrix $\underline{R}_{TR}$:* The accuracy of the range, range-rate, azimuth, and elevation measurements are specified by the matrix

$$\underline{R}_{TR} = \begin{bmatrix} \sigma^2_{\mathrm{TOTAL},R} & 0 & 0 & 0 \\ 0 & \sigma^2_{\mathrm{TOTAL},\dot{R}} & 0 & 0 \\ 0 & 0 & \sigma^2_{\mathrm{TOTAL},az} & 0 \\ 0 & 0 & 0 & \sigma^2_{\mathrm{TOTAL},el} \end{bmatrix}. \qquad \text{(A.382)}$$

$$\left[ \frac{\partial a}{\partial \delta x_S} \quad \frac{\partial a}{\partial \delta y_S} \quad 0 \,\middle|\, 0 \quad 0 \quad 0 \,\middle|\, 1 \,\middle|\, \frac{\partial a}{\partial p_{Tx}} \quad 0 \quad 0 \,\middle|\, \frac{\partial a}{\partial p_{Ty}} \quad 0 \quad 0 \,\middle|\, 0 \quad 0 \quad 0 \,\middle|\right.$$

$$\left. \frac{\partial a}{\partial \delta p_{\mathrm{Tx\ BIAS}}} \quad 0 \quad \frac{\partial a}{\partial \delta p_{\mathrm{Ty\ BIAS}}} \quad 0 \quad 0 \quad 0 \right]$$

Figure A.22: Row Matrix $\underline{H}_3$

$$\left[ \frac{\partial e}{\partial \delta x_S} \quad \frac{\partial e}{\partial \delta y_S} \quad \frac{\partial e}{\partial \delta z_S} \,\middle|\, 0 \quad 0 \quad 0 \,\middle|\, 0 \,\middle|\, \frac{\partial e}{\partial p_{Tx}} \quad 0 \quad 0 \,\middle|\, \frac{\partial e}{\partial p_{Ty}} \quad 0 \quad 0 \,\middle|\, \frac{\partial e}{\partial p_{Tz}} \quad 0 \quad 0 \,\middle|\right.$$

$$\left. \frac{\partial e}{\partial \delta p_{\mathrm{Tx\ BIAS}}} \quad 0 \quad \frac{\partial e}{\partial \delta p_{\mathrm{Ty\ BIAS}}} \quad 0 \quad \frac{\partial e}{\partial \delta p_{\mathrm{Tz\ BIAS}}} \quad 0 \right]$$

Figure A.23: Row Matrix $\underline{H}_4$

Table A.17: PARTIAL DERIVATIVES OF $R$

$$\frac{\partial R}{\partial \delta x_S} = \frac{-(x_T - x_S)}{R}$$

$$\frac{\partial R}{\partial \delta y_S} = \frac{-(y_T - y_S)}{R}$$

$$\frac{\partial R}{\partial \delta z_S} = \frac{-(z_T - z_S)}{R}$$

$$\frac{\partial R}{\partial p_{Tx}} = \frac{\partial R}{\partial \delta p_{\mathrm{Tx\ BIAS}}} = \frac{x_T - x_S}{R}$$

$$\frac{\partial R}{\partial p_{Ty}} = \frac{\partial R}{\partial \delta p_{\mathrm{Ty\ BIAS}}} = \frac{y_T - y_S}{R}$$

$$\frac{\partial R}{\partial p_{Tz}} = \frac{\partial R}{\partial \delta p_{\mathrm{Tz\ BIAS}}} = \frac{z_T - z_S}{R}$$

where:

$$R = \sqrt{(x_T - x_S)^2 + (y_T - y_S)^2 + (z_T - z_S)^2}$$

$$[x_T \quad y_T \quad z_T]^T = p_T^t$$

$$[x_S \quad y_S \quad z_S]^T = p_{SP}^t$$

Table A.18: PARTIAL DERIVATIVES OF $\dot{R}$

$$\frac{\partial \dot{R}}{\partial \dot{x}_S} = \frac{-(\dot{x}_T - \dot{x}_S)}{\dot{R}}$$

$$\frac{\partial \dot{R}}{\partial \dot{y}_S} = \frac{-(\dot{y}_T - \dot{y}_S)}{\dot{R}}$$

$$\frac{\partial \dot{R}}{\partial \dot{z}_S} = \frac{-(\dot{z}_T - \dot{z}_S)}{\dot{R}}$$

$$\frac{\partial \dot{R}}{\partial \dot{x}_T} = \frac{\partial \dot{R}}{\partial \dot{x}_{T\,\mathrm{BIAS}}} = \frac{\dot{x}_T - \dot{x}_S}{\dot{R}}$$

$$\frac{\partial \dot{R}}{\partial \dot{y}_T} = \frac{\partial \dot{R}}{\partial \dot{y}_{T\,\mathrm{BIAS}}} = \frac{\dot{y}_T - \dot{y}_S}{\dot{R}}$$

$$\frac{\partial \dot{R}}{\partial \dot{z}_T} = \frac{\partial \dot{R}}{\partial \dot{z}_{T\,\mathrm{BIAS}}} = \frac{\dot{z}_T - \dot{z}_S}{\dot{R}}$$

where:

$$\dot{R} = \sqrt{(\dot{x}_T - \dot{x}_S)^2 + (\dot{y}_T - \dot{y}_S)^2 + (\dot{z}_T - \dot{z}_S)^2}$$

$$[\dot{x}_T \quad \dot{y}_T \quad \dot{z}_T]^T = v_T^t$$

$$[\dot{x}_S \quad \dot{y}_S \quad \dot{z}_S]^T = v_{SP}^t$$

Table A.19: PARTIAL DERIVATIVES OF $a$

$$\frac{\partial a}{\partial x_S} = \frac{1}{1+\xi^2}\frac{y_T - y_S}{(x_T - x_S)^2}$$

$$\frac{\partial a}{\partial y_S} = \frac{-1}{1+\xi^2}\frac{1}{x_T - x_S}$$

$$\frac{\partial a}{\partial p_{Tx}} = \frac{\partial a}{\partial p_{T\mathrm{x\ BIAS}}} = \frac{-1}{1+\xi^2}\frac{y_T - y_S}{(x_T - x_S)^2}$$

$$\frac{\partial a}{\partial p_{Ty}} = \frac{\partial a}{\partial p_{T\mathrm{y\ BIAS}}} = \frac{1}{1+\xi^2}\frac{1}{x_T - x_S}$$

where $\xi = \frac{y_T - y_S}{x_T - x_S}$

Table A.20: PARTIAL DERIVATIVES OF $\epsilon$

$$\frac{\partial \epsilon}{\partial \delta x_S} = \frac{-1}{\sqrt{1-\eta^2}} \frac{z_T - z_S}{R^2} \frac{\partial R}{\partial \delta x_S}$$

$$\frac{\partial \epsilon}{\partial \delta y_S} = \frac{-1}{\sqrt{1-\eta^2}} \frac{z_T - z_S}{R^2} \frac{\partial R}{\partial \delta y_S}$$

$$\frac{\partial \epsilon}{\partial \delta z_S} = \frac{-1}{\sqrt{1-\eta^2}} \left[ \frac{z_T - z_S}{R^2} \frac{\partial R}{\partial \delta z_S} + \frac{1}{R} \right]$$

$$\frac{\partial \epsilon}{\partial p_{Tx}} = \frac{\partial \epsilon}{\partial \delta p_{Tx\ BIAS}} = \frac{-1}{\sqrt{1-\eta^2}} \frac{z_T - z_S}{R^2} \frac{\partial R}{\partial p_{Tx}}$$

$$\frac{\partial \epsilon}{\partial p_{Ty}} = \frac{\partial \epsilon}{\partial \delta p_{Ty\ BIAS}} = \frac{-1}{\sqrt{1-\eta^2}} \frac{z_T - z_S}{R^2} \frac{\partial R}{\partial p_{Ty}}$$

$$\frac{\partial \epsilon}{\partial p_{Tz}} = \frac{\partial \epsilon}{\partial \delta p_{Tz\ BIAS}} = \frac{-1}{\sqrt{1-\eta^2}} \left[ \frac{z_T - z_S}{R^2} \frac{\partial R}{\partial p_{Tz}} - \frac{1}{R} \right]$$

where $\eta = \frac{z_T - z_S}{R}$

where the standard deviations along the diagonal are given in Equations A.362 to A.365 of Section A.10. These standard deviations are assumed to be indicative of both *measurement* accuracy (i.e., the accuracy of the measurement made during one scan) and *tracking* accuracy. This simplifying assumption is based on the uncertainty introduced by target motion from scan to scan.

*Matrix* $\underline{F}_{TR}$: The $F$-matrix for propagating the state $\underline{x}_{TR}$ (defined in Equation A.367) is shown in Figure A.24. The figure shows that: the first part of $\underline{x}_{TR}$ is time-invariant; the second part propagates according to the Singer dynamics (Equations A.2 and A.3); and the third part propagates according to "position is the integral of velocity".

*Matrix* $\underline{Q}_{TR}$: The matrix $\underline{Q}_{TR}$ is shown in Figure A.25. This matrix is zero except for the terms driving the Singer states which have entries $Q_{Tx}$, $Q_{Ty}$, and $Q_{Tz}$ defined by Equation A.5.

$$
\left[\begin{array}{c|ccc|cccccc}
\multicolumn{4}{c|}{\underline{0}_{7\times 22}} \\
\hline
\underline{0}_{9\times 7} & \underline{F}_{Tx} & \underline{0}_{3\times 3} & \underline{0}_{3\times 3} & \multicolumn{6}{c}{\multirow{3}{*}{$\underline{0}_{9\times 6}$}} \\
 & \underline{0}_{3\times 3} & \underline{F}_{Ty} & \underline{0}_{3\times 3} & & & & & & \\
 & \underline{0}_{3\times 3} & \underline{0}_{3\times 3} & \underline{F}_{Tz} & & & & & & \\
\hline
 & & & & 0 & 1 & 0 & 0 & 0 & 0 \\
 & & & & 0 & 0 & 0 & 0 & 0 & 0 \\
 & & & & 0 & 0 & 0 & 1 & 0 & 0 \\
\multicolumn{3}{c|}{\underline{0}_{6\times 16}} & & 0 & 0 & 0 & 0 & 0 & 0 \\
 & & & & 0 & 0 & 0 & 0 & 0 & 1 \\
 & & & & 0 & 0 & 0 & 0 & 0 & 0
\end{array}\right]
$$

Figure A.24: Matrix $\underline{F}_{TR}$

$$
\left[\begin{array}{c|ccc|c}
\multicolumn{4}{c|}{\underline{0}_{7\times 22}} \\
\hline
\underline{0}_{9\times 7} & \underline{Q}_{Tx} & \underline{0}_{3\times 3} & \underline{0}_{3\times 3} & \multirow{3}{*}{$\underline{0}_{9\times 6}$} \\
 & \underline{0}_{3\times 3} & \underline{Q}_{Ty} & \underline{0}_{3\times 3} & \\
 & \underline{0}_{3\times 3} & \underline{0}_{3\times 3} & \underline{Q}_{Tz} & \\
\hline
\multicolumn{4}{c}{\underline{0}_{6\times 22}}
\end{array}\right]
$$

Figure A.25: Matrix $\underline{Q}_{TR}$

# Appendix B

# GENERALIZED INS FULL-ORDER MODEL

[Britting, 1971] develops the notion of a "generalized" INS error model which applies, with only minor modifications, to all INS mechanizations. Following this development, error equations for both strapdown (M and LP) and local level (SP) mechanizations are given in this section. The error equations are represented in the state-space form

$$\frac{d}{dt}\begin{bmatrix} \underline{n} \\ \underline{\varepsilon} \\ \underline{\alpha} \\ \delta h_A \end{bmatrix} = \begin{bmatrix} \underline{F}_n & \underline{F}_{n\varepsilon} & \underline{F}_{n\alpha} & \underline{F}_{nh} \\ \underline{0} & \underline{F}_\varepsilon & \underline{0} & \underline{0} \\ \underline{0} & \underline{0} & \underline{F}_\alpha & \underline{0} \\ \underline{0} & \underline{0} & \underline{0} & F_h \end{bmatrix} \begin{bmatrix} \underline{n} \\ \underline{\varepsilon} \\ \underline{\alpha} \\ \delta h_A \end{bmatrix} + \begin{bmatrix} \underline{w}_n \\ \underline{w}_\varepsilon \\ \underline{w}_\alpha \\ w_h \end{bmatrix}. \tag{B.1}$$

The components of the state vector in this equation corresponds to the state variables listed in Tables 3.4, 3.6, and 3.8 as follows. The vector $\underline{n}$ corresponds to the first nine entries on these tables: attitude errors, position rate, and position. The vectors $\underline{\varepsilon}$ and $\underline{\alpha}$ and the scalar $\delta h_A$ correspond to gyro, accelerometer, and altimeter errors also listed in the tables. The structure of the state equation represents the effect of instrument errors ($\underline{\varepsilon}$, $\underline{\alpha}$, and $\delta h_A$) feeding the navigation states ($\underline{n}$).

The interaction between the navigation states and the instrument errors is specified by the blocks in the $F$-matrix. The following paragraphs describe these blocks and the white noise vectors ($\underline{w}_n$, $\underline{w}_\varepsilon$, $\underline{w}_\alpha$, and $\underline{w}_h$) based on the development presented in [Britting, 1971] and [Schmidt, 1978].

## B.1 Matrix $\underline{F}_n$

The matrix $\underline{F}_n$ is defined in Figure B.1. This matrix can be used to model any Schuler-tuned mechanization and consequently is applicable to both the strapdown and platform error models. The nomenclature used in Figure B.1 is:

$$\begin{aligned} R_p &= \text{Distance from the center of the Earth to the vehicle} \\ &= R_{sp} + h \\ R_{sp} &= \text{Radius of a spherical Earth (6378 km)} \end{aligned}$$

$\Omega_{\oplus}$ = Angular velocity of the Earth
$L$ = Latitude
$\lambda$ = Celestial longitude (relative to the vernal equinox)
$\ell$ = Terrestrial longitude (relative to Greenwich)
$h$ = Altitude
$f_N$ = Output of an accelerometer pointing North (specific force)
$f_E$ = Output of an accelerometer pointing East (specific force)
$f_D$ = Output of an accelerometer pointing Down (specific force)
$K_1, K_2$ = Gains for 2nd order altimeter loop
$\omega_s$ = Schuler frequency ($\sqrt{g/R_p}$)
$g$ = Gravity acceleration at the location of the vehicle.

The first three rows of $\underline{F}_n$ (Figure B.1) describe the dynamics of the errors in estimating the orientation of the platform relative to the local-level frame. These errors are produced by gyro errors introduced into the differential equation by the $\underline{F}_{n\epsilon}\underline{\varepsilon}$ term in Equation B.1. The middle three rows characterize how accelerometers errors ($\underline{F}_{n\alpha}\underline{\alpha}$ in Equation B.1) and attitude errors lead to errors in the estimated velocities (latitude rate, longitude rate, and altitude rate). The bottom three rows represent the integration of latitude rate, longitude rate, and altitude rate to obtain latitude, longitude, and altitude.

## B.2 Matrix $\underline{F}_\varepsilon$ and Vector $\underline{w}_\varepsilon$

The matrix $\underline{F}_\epsilon$ and vector $\underline{w}_\epsilon$ in Equation B.1 specify the state equations

$$\dot{\underline{\varepsilon}} = \underline{F}_\epsilon \underline{\varepsilon} + \underline{w}_\epsilon \tag{B.2}$$

for the vector of gyro errors $\underline{\varepsilon}$. Each of the entries in the vector $\underline{\varepsilon}$ models an error source for one of the three gyros ($x$, $y$, or $z$) of the INS.[1] The error sources can be classified into three groups as summarized in the first two columns of Table B.1:

- Gyro drift rate (top part of the table), a result of random drift of the gyro output axis
- Scale factor errors (middle part), a result of gyro torquer inaccuracies
- Misalignment errors (bottom part), a result of inaccuracies in mounting the gyros on the INS.

As indicated in the third column of the table, each error source in $\underline{\varepsilon}$ is modeled by either a bias, a first-order Markov, or a random walk, depending on the error source group. The parameters of these models define the entries in the matrix $\underline{F}_\epsilon$ and the vector $\underline{w}_\epsilon$ ([Gelb, 1974]). Parameters assumed for the M, LP, and SP gyros are given in Sections A.4, A.5, and A.6.

[1] For a platform INS, $x$ =North, $y$=East, and $z$ =Down. For a strapdown mechanization, $x$ =Roll, $y$ =Pitch, and $z$ =Yaw.

$$
\left[\begin{array}{c|c|c|c|c|c|c|c|c}
0 & -\dot{\lambda}\sin L & \dot{L} & 0 & \cos L & 0 & -\dot{\lambda}\sin L & 0 & 0 \\
\dot{\lambda}\sin L & 0 & \dot{\lambda}\cos L & -1 & 0 & 0 & 0 & 0 & 0 \\
-\dot{L} & -\dot{\lambda}\cos L & 0 & 0 & -\sin L & 0 & -\dot{\lambda}\cos L & 0 & 0 \\
\hline
0 & -\frac{f_D}{R_\oplus} & \frac{f_E}{R_\oplus} & -2\frac{\dot{h}}{R_\oplus} & -\dot{\lambda}\sin 2L & -2\frac{\dot{L}}{R_\oplus} & -\dot{\ell}(\dot{\ell}+2\Omega_\oplus)\cos 2L & 0 & -\frac{\ddot{L}}{R_\oplus} - \frac{\dot{\ell}(\dot{\ell}+2\Omega_\oplus)\sin 2L}{2R_\oplus} \\
\frac{f_D}{R_\oplus \cos L} & 0 & -\frac{f_N}{R_\oplus \cos L} & 2\dot{\lambda}\tan L & 2\left[\dot{L}\tan L - \frac{\dot{h}}{R_\oplus}\right] & -2\frac{\dot{\lambda}}{R_\oplus} & (\ddot{\ell}+2\frac{\dot{h}\dot{\lambda}}{R_\oplus})\tan L + 2\dot{L}\dot{\lambda} & 0 & \frac{2\dot{L}\dot{\lambda}\tan L - \ddot{l}}{R_\oplus} \\
f_E & -f_N & 0 & 2R_\oplus\dot{L} & 2R_\oplus\dot{\lambda}\cos^2 L & 0 & -R_\oplus\dot{\ell}(\dot{\ell}+2\Omega_\oplus)\sin 2L & 0 & \dot{L}^2 + \dot{\ell}(\dot{\ell}+2\Omega_\oplus)\cos^2 L + 2\omega_s^2 - K_2 \\
\hline
0 & 0 & 0 & 1 & 0 & 0 & 0 & 0 & 0 \\
0 & 0 & 0 & 0 & 1 & 0 & 0 & 0 & 0 \\
0 & 0 & 0 & 0 & 0 & 1 & 0 & 0 & -K_1
\end{array}\right]
$$

Figure B.1: $\underline{F}_n$ Matrix

Table B.1: COMPONENTS OF THE GYRO ERROR VECTOR, $\underline{\varepsilon}$

| SYMBOL | DEFINITION | MODEL TYPE |
|---|---|---|
| $\underline{\varepsilon}_x$ | $x$-gyro drift rate | Bias, R.W., Markov |
| $\underline{\varepsilon}_y$ | $y$-gyro drift rate | |
| $\underline{\varepsilon}_z$ | $z$-gyro drift rate | |
| $t_x$ | $x$-gyro scale factor error | Bias, Markov |
| $t_y$ | $y$-gyro scale factor error | |
| $t_z$ | $z$-gyro scale factor error | |
| $o_{xy}$ | $x$-gyro misalignment resulting from a rotation about $y$-axis | Bias |
| $o_{xz}$ | $x$-gyro misalignment resulting from a rotation about $z$-axis | |
| $o_{yx}$ | $y$-gyro misalignment resulting from a rotation about $x$-axis | |
| $o_{yz}$ | $y$-gyro misalignment resulting from a rotation about $z$-axis | |
| $o_{zx}$ | $z$-gyro misalignment resulting from a rotation about $x$-axis | |
| $o_{zy}$ | $z$-gyro misalignment resulting from a rotation about $y$-axis | |

## B.3 Matrix $\underline{F}_\alpha$ and Vector $\underline{w}_\alpha$

The matrix $\underline{F}_\alpha$ and vector $\underline{w}_\alpha$ specify the state equations

$$\dot{\underline{\alpha}} = \underline{F}_\alpha \underline{\alpha} + \underline{w}_\alpha \tag{B.3}$$

for the vector of acceleration, $\underline{\alpha}$. The entries in this vector include three groups analogous to those of the gyro errors (random acceleration error, scale factor error, and misalignments) as shown in Table B.2. In addition, a fourth group modeling gravity uncertainty errors, is also included in the vector $\underline{\alpha}$. Parameters assumed for the acceleration errors driving the M, LP, and SP INSs are given in Sections A.4, A.5, and A.6.

Table B.2: COMPONENTS OF THE ACCELERATION VECTOR, $\underline{\alpha}$

| SYMBOL | DEFINITION | MODEL TYPE |
|---|---|---|
| $\underline{\alpha}_x$ | $x$-accelerometer random error | Bias, R.W., Markov |
| $\underline{\alpha}_y$ | $y$-accelerometer random error | |
| $\underline{\alpha}_z$ | $z$-accelerometer random error | |
| $a_x$ | $x$-accelerometer scale factor error | Bias, Markov |
| $a_y$ | $y$-accelerometer scale factor error | |
| $a_z$ | $z$-accelerometer scale factor error | |
| $\theta xy$ | $x$-accelerometer misalignment (analogous to $\phi_{xy}$) | Bias |
| $\theta_{xz}$ | $x$-accelerometer misalignment (analogous to $\phi_{xz}$) | |
| $\theta_{yx}$ | $y$-accelerometer misalignment (analogous to $\phi_{yx}$) | |
| $\theta_{yz}$ | $y$-accelerometer misalignment (analogous to $\phi_{yz}$) | |
| $\theta_{zx}$ | $z$-accelerometer misalignment (analogous to $\phi_{zx}$) | |
| $\theta_{zy}$ | $z$-accelerometer misalignment (analogous to $\phi_{zy}$) | |
| $\eta$ | Vertical deflection about East axis | Bias, Markov |
| $\xi$ | Vertical deflection about North axis | |
| $\delta g$ | Gravity anomaly | |

## B.4 Scalars $F_h$ and $w_h$

The vertical channels of the three INSs under consideration are assumed to be damped by an altimeter having errors characterized by a first-order Markov,

$$\delta\dot{h}_a = F_h\,\delta h_{\rm A} + w_h \quad . \tag{B.4}$$

Parameters for these Markovs are given in Sections A.4, A.5, and A.6.

## B.5 Matrix $\underline{F}_{n\varepsilon}$

The matrix $\underline{F}_{n\varepsilon}$ is given by

$$\underline{F}_{n\varepsilon} = \left[\begin{array}{c} \underline{C}_p^n \underline{F}_{n\varepsilon 1} \\ \hline \underline{0}_{3\times\dim\{\underline{\varepsilon}\}} \\ \hline \underline{0}_{3\times\dim\{\underline{\varepsilon}\}} \end{array}\right] \quad . \tag{B.5}$$

The notation in this equation is as follows: $\underline{C}_p^n$ is the direction cosine transformation between the platform frame[2] and the navigation (also called local-level or geographic) frame ([Britting, 1971]); $\underline{F}_{n\varepsilon 1}$ is a matrix specified below; and $\underline{0}_{3\times\dim\{\underline{\varepsilon}\}}$ is the zero matrix having the indicated dimension.

Equations B.5 and B.1 show that the effect of the matrix $\underline{F}_{n\varepsilon}$ is to transform the vector of gyro errors, $\underline{\varepsilon}$, into quantities that drive the attitude error states (all other states are not directly affected as indicated by the zero matrices). This transformation is a two step process. First, the vector $\underline{\varepsilon}$ is multiplied by the matrix $\underline{F}_{n\varepsilon 1}$ shown in Figure B.2. This

$$\left[\begin{array}{ccc|ccc|cccccc} 1\ldots1 & 0\ldots0 & 0\ldots0 & \omega_x & 0 & 0 & \omega_z & -\omega_y & 0 & 0 & 0 & 0 \\ 0\ldots0 & 1\ldots1 & 0\ldots0 & 0 & \omega_y & 0 & 0 & 0 & -\omega_z & \omega_x & 0 & 0 \\ 0\ldots0 & 0\ldots0 & 1\ldots1 & 0 & 0 & \omega_z & 0 & 0 & 0 & 0 & \omega_y & -\omega_x \end{array}\right]$$

Figure B.2: Matrix $\underline{F}_{n\varepsilon 1}$

transformation "adds-up" the gyro errors from the three groups (random drift rate, scale factor, and misalignments) in each dimension of the platform frame. The weights $\omega_x$, $\omega_y$, and $\omega_z$, multiplying the scale factor and misalignment errors, are the angular rates experienced by the $x$, $y$, and $z$ gyros.

[2]For a strapdown INS, the "platform" frame is the body frame; for a platform INS, it is the local-level frame.

The second step is the transformation of the total error in each dimension from the platform frame to the local-level frame to drive the attitude states. This step is implemented with the direction cosine matrix $C_p^n$ which is defined by ([Farrell, 1976])

$$\underline{C}_p^n = \begin{bmatrix} \vec{i}_n \cdot \vec{i}_p & \vec{i}_n \cdot \vec{j}_p & \vec{i}_n \cdot \vec{k}_p \\ \vec{j}_n \cdot \vec{i}_p & \vec{j}_n \cdot \vec{j}_p & \vec{j}_n \cdot \vec{k}_p \\ \vec{k}_n \cdot \vec{i}_p & \vec{k}_n \cdot \vec{j}_p & \vec{k}_n \cdot \vec{k}_p \end{bmatrix}. \tag{B.6}$$

In this equation $(\vec{i}_n, \vec{j}_n, \vec{k}_n)$ and $(\vec{i}_p, \vec{j}_p, \vec{k}_p)$ are unit vectors along the $n$ and $p$ frames, and "$\cdot$" indicates the dot product. The formulas for computing $C_p^n$ are as follows:

- For the SP (in fact, for any local-level INS), the $p$ frame is the $n$ frame so that

$$\underline{C}_p^n = \underline{I}. \tag{B.7}$$

- For the LP, $C_p^n$ is computed from the assumed trajectory as given in Section A.3
- For the M, $C_p^n$ is computed from the guidance commands using the formulas given in Section A.9.

## B.6 Matrix $\underline{F}_{n\alpha}$

The matrix $\underline{F}_{n\alpha}$ is given by

$$\underline{F}_{n\alpha} = \left[\begin{array}{c} \underline{0}_{3\times\dim\{\underline{\alpha}\}} \\ \hline \underline{D}\,\underline{C}_p^n\underline{F}_{n\alpha 1} \mid \underline{F}_{n\alpha 2} \\ \hline \underline{0}_{3\times\dim\{\underline{\alpha}\}} \end{array}\right]. \tag{B.8}$$

The notation in this equation is as follows. The matrix $\underline{D}$, given by

$$\underline{D} = \begin{bmatrix} \frac{1}{R_p} & 0 & 0 \\ 0 & \frac{1}{R_p \cos L} & 0 \\ 0 & 0 & -1 \end{bmatrix}, \tag{B.9}$$

transforms velocities from the linear scale ($v_{\text{North}}$, $v_{\text{East}}$, and $v_{\text{Down}}$) to an angular rates scales (latitude, longitude, and altitude rates). The direction cosine matrix $\underline{C}_p^n$, transforming the $p$-frame to the $n$-frame, is as defined in Equation B.6. The matrices $\underline{F}_{n\alpha 1}$ and $\underline{F}_{n\alpha 2}$ are defined below.

Equations B.8 and B.1 show that the effect of the matrix $\underline{F}_{n\alpha}$ is to transform the vector of acceleration *and* gravity errors, $\underline{\alpha}$, into quantities that drive the velocity error states

(latitude rate error, longitude rate error, and altitude rate error). This transformation involves the addition of two terms: errors due to acceleremoter uncertainties and errors due to gravity uncertainties.

Errors due to accelerometer uncertainties are modeled by the product of $\underline{D}\,\underline{C}_p^n\underline{F}_{n\alpha 1}$ times the first three parts of $\alpha$ shown in Table B.2 containing accelerometer errors. The matrix $\underline{F}_{n\alpha 1}$, shown in Figure B.3, "adds-up" the three groups of accelerometer errors (random drift rate, scale factor, and misalignments) in each dimension of the platform frame. The resulting total error is then converted from the platform to the navigation frame by $\underline{C}_p^n$, and from the linear to the angular rate scale by $\underline{D}$. The weights $f_x$, $f_y$, and $f_z$ multiplying the scale factor and misalignment errors are the specific force experienced by the $x$, $y$, and $z$ accelerometers.

$$\left[\begin{array}{ccc|ccc|cccccc} 1\ldots1 & 0\ldots0 & 0\ldots0 & f_x & 0 & 0 & -f_z & f_y & 0 & 0 & 0 & 0 \\ 0\ldots0 & 1\ldots1 & 0\ldots0 & 0 & f_y & 0 & 0 & 0 & f_z & -f_x & 0 & 0 \\ 0\ldots0 & 0\ldots0 & 1\ldots1 & 0 & 0 & f_z & 0 & 0 & 0 & 0 & -f_y & f_x \end{array}\right]$$

Figure B.3: Matrix $\underline{F}_{n\alpha 1}$

Errors due to gravity uncertainties are introduced by the product $\underline{F}_{n\alpha 2}$ times the last three states in $\alpha$. The matrix $\underline{F}_{n\alpha 2}$ is given by

$$\underline{D} = \begin{bmatrix} \frac{-g}{R_p} & 0 & 0 \\ 0 & \frac{g}{R_p \cos L} & 0 \\ 0 & 0 & 1 \end{bmatrix}. \qquad \text{(B.10)}$$

This matrix models the effect of the vertical deflections about East and North on the time derivatives of latitude and longitude rates, and also the effect of the gravity anomaly on altitude acceleration .

## B.7 Matrix $\underline{F}_{nh}$

The matrix $\underline{F}_{nh}$ is given by

$$\underline{F}_{nh} = \left[\begin{array}{c} \underline{0}_{3\times 1} \\ \hline \begin{bmatrix} 0 \\ 0 \\ K_2 \end{bmatrix} \\ \hline \begin{bmatrix} 0 \\ 0 \\ K_1 \end{bmatrix} \end{array}\right] . \tag{B.11}$$

The constants $K_1$ and $K_2$ appearing in $\underline{F}_{nh}$ and in the last column of $\underline{F}_n$ (Figure B.1) define a second-order loop used to damp the vertical channel of the INS ([Kayton, 1969] and [Schmidt, 1978]). The transfer function for this loop is given by

$$\delta h(s) = \frac{-1}{s^2 + K_1 s + (K_2 - \frac{2g_0}{R_p})} \delta f_D(s) + \frac{K_2 + K_1 s}{s^2 + K_1 s + (K_2 - \frac{2g_0}{R_p})} \delta h_{\mathrm{A}}. \tag{B.12}$$

In this equation, $\delta h(s)$ is the altitude error ($\delta h_{\mathrm{M}}$ for M, $\delta h_{\mathrm{S}}$ for SP, or $\delta h_{\mathrm{L}}$ for LP); $\delta h_{\mathrm{A}}$ is the altimeter error ($\delta h_{\mathrm{MA}}$ for M, $\delta h_{\mathrm{SA}}$ for SP, or $\delta h_{\mathrm{LA}}$ for LP); $\delta f_D$ is the total specific force error in the Down direction; and $K_1$ and $K_2$ are the damping constants.

The remainder of this subsection is addressed at the selection of the damping constants $K_1$ and $K_2$ for the M, LP, and SP INSs. The constant $K_2$ is set to

$$K_2 = \frac{K_1^2}{4} + \frac{2g_0}{R_p} \tag{B.13}$$

to achieve critical damping which prevents "ringing" (oscillations) in the loop response ([Van Valkenburg, 1964]). For critical damping, the transfer function in Equation B.12 becomes

$$\delta h(s) = \frac{-\left[\frac{2}{K_1}\right]^2}{(1 + sT_1)^2} \delta f_D(s) + \frac{\left[1 + \frac{8g_0}{R_p K_1^2}\right](1 + sT_2)}{(1 + sT_1)^2} \delta h_{\mathrm{A}} \tag{B.14}$$

where

$$T_1 = \frac{2}{K_1} \tag{B.15}$$

$$T_2 = \frac{K_1}{\left(\frac{K_1^2}{4} + \frac{2g_0}{R_p}\right)}. \tag{B.16}$$

The constants $T_1$ and $T_2$ specify the break frequencies $\omega_1$ and $\omega_2$ of the associated Bode plot ([Van Valkenburg, 1964]):

$$\omega_1 = \frac{1}{T_1} = \frac{K_1}{2} \tag{B.17}$$

$$\omega_2 = \frac{1}{T_2} = \frac{K_1}{4} + \frac{2g_0}{R_p K_1}. \tag{B.18}$$

What remains now is the selection of the constant $K_1$ which determines the characteristics of the altitude error $\delta h$, as evident from Equations B.14 to B.16. The constant is thus set to achieve a "satisfactory" $\delta h$ according to the following three criteria:

1. Set $K_1$ so that the loop damps-out errors quickly
2. Minimize the effect of the errors introduced by the accelerometer errors, $\delta f_D$, via Equation B.14
3. Minimize the effect of the errors introduced by the altimeter errors, $\delta h_A$, via Equation B.14.

These three criteria are considered in the following three paragraphs.

The response time of a critically damped second-order loop, defined here as the time required for the step response to achieve 90% of its final value, is given by $\tau_{90} = 4/\omega_n$ where $\omega_n$ is the natural frequency of the loop ([Kuo, 1962]). In Equation B.14 $\omega_n = \omega_1$ so that

$$\tau_{90} = \frac{4}{\omega_1} \tag{B.19}$$

where $\omega_1 = K_1/2$. Consequently, to obtain quick damping of altitude errors $\omega_1$ must be sufficiently *large*.

The effect of accelerometer errors (first term on the right side of Equation B.14) can be divided into two components: low-frequency and high-frequency accelerometer errors. High-frequency errors are attenuated by making $\omega_1$ as *small* as possible. The effect of low-frequency errors can be measured from the steady-state altitude error produced by the accelerometer bias, $\delta h_{ssa}$, which from the final value theorem ([Kuo, 1962]) is given by

$$\delta h_{ssa} = \frac{4\delta A}{K_1^2} = \frac{\delta A}{\omega_1^2}, \tag{B.20}$$

where $\delta A$ is the magnitude of a step acceleration error. Consequently to obtain a satisfactory low-frequency response to accelerometer errors, $\omega_1$ must be made *large*.

The effect of the errors introduced by the altimeter (second term on the right side of Equation B.14) is reduced by (1) making $\omega_1$ as *small* as possible to filter-out high-frequency errors, and (2) making $\omega_2$ large to avoid amplification of higher frequency errors by the lead factor of the second term in Equation B.14. The value of $\omega_2$, however, is given by (from Equations B.17 and B.18)

$$\omega_2 = \frac{\omega_1}{2} + \frac{g_0}{R_p \omega_1} \tag{B.21}$$

for critical damping. This equation indicates that the effect of altimeter error on altitude error is not a monotonic function of $\omega_1$ (i.e., it is not a simple matter of making $\omega_1$ small or large).

Consequently, it is necessary to obtain an exact equation for the RMS value of $\delta h$ produced by $\delta h_A$. Assuming a first-order Markov for $\delta h_A$, the transfer function relating $\delta h$ and $\delta h_A$ is obtained from Equations B.14 to B.16 (setting $\delta f_D = 0$):

$$\delta h_{\text{due to altimeter}} = \frac{K_1 s + \left[\frac{K_1^2}{4} + \frac{2g_0}{R_p}\right]}{(s + \frac{K_1}{2})^2} \frac{\sigma\sqrt{2\beta}}{s + \beta} \tag{B.22}$$

where $\sigma$ and $\beta$ are the RMS value and inverse correlation time of the Markov process. From this transfer function, an expression for the RMS value of $\delta h$ is obtained following the procedure in [Newton, Gould, and Kaiser, 1957]:

$$\sigma_{\delta h,\ \text{due to altimeter}} = \frac{c_2^2 d_0 d_1 + (c_1^2 - 2c_0 c_2) d_0 d_3 + c_0^2 d_2 d_3}{2 d_0 d_3 (d_1 d_2 - d_0 d_3)}. \tag{B.23}$$

The terms in this equation are given by:

$$\begin{aligned}
c_2 &= 0 \\
c_1 &= K_1 \sigma \sqrt{2\beta} \\
c_0 &= \sigma\sqrt{2\beta}\left[\frac{K_1^2}{4} + \frac{2g_0}{R_p}\right] \\
d_3 &= 1 \\
d_2 &= K_1 + \beta \\
d_1 &= \frac{K_1^2}{4} + \beta K_1 \\
d_0 &= \beta\frac{K_1^2}{4}.
\end{aligned}$$

In summary, the three criteria listed above for a satisfactory vertical channel damping response lead to conflicting (large/small) requirements on $\omega_1$. To obtain a satisfactory compromise value for $K_1$, five variables were evaluated as a function of $K_1$ using a program coded in the BASIC language:

- $\omega_1$ from Equation B.17
- $\tau_{90}$ from Equation B.19
- $\omega_2$ from Equation B.18
- $\delta h_{sat}$ from Equation B.20
- $\sigma_{\delta h,\ \text{due to altimeter}}$ from Equation B.23.

These five variables were evaluated for the altimeter and accelerometer error models of the M, LP, and SP listed in Tables A.3, A.4, and A.5.

Based on these calculations, the $K_1$ and $K_2$ values shown in Table B.3 are selected as damping constants for the vertical channels of the M, LP, and SP. The bases of these selections are as follows:

**M INS:** (Calculations summarized in Table B.4)

- Initial vertical channel errors are damped within mission time ($\tau_{90} = 80$ sec)
- $\omega_1$ is small, resulting in a reduction of the high-frequency errors introduced by the low-quality accelerometers
- $\omega_2$ is sufficiently large to prevent amplification of altimeter errors ($\sigma_{\delta h,\text{ due to altimeter}} = 150$ m)
- $\delta h_{ssa}$ is small (5.9 m).

**LP INS:** (Calculations summarized in Table B.5)

- $\delta h_{ssa}$ is negligible (0.6 m).
- $\omega_1$ is small, resulting in a reduction of the high-frequency accelerometers errors.
- $\omega_2$ is sufficiently large to prevent amplification of altimeter errors ($\sigma_{\delta h,\text{ due to altimeter}} = 150$ m)

**SP INS:** (Calculations summarized in Table B.6)

- $\omega_1$ is large enough to make $\delta h_{ssa}$ negligible (0.1 m)
- $\omega_1$ is small, resulting in a reduction of the high-frequency errors introduced by the low-quality accelerometers
- $\omega_2$ is sufficiently large to make $\sigma_{\delta h,\text{ due to altimeter}}$ within 3 m of its minimum value (which is obtained for $K_1 = 0.03$).

Table B.3: DAMPING CONSTANTS FOR THE M, LP, AND SP INS

| INS | $K_1$ | $K_2$ |
|---|---|---|
| M | 0.10 | $2.50 \times 10^{-3}$ |
| LP | 0.08 | $1.60 \times 10^{-3}$ |
| SP | 0.06 | $9.03 \times 10^{-4}$ |

Table B.4: SELECTION OF $K_1$ FOR M INS[3]

| $K_1$ | $\omega_1$ (rad/sec) | $\tau_{90}$ (sec) | $\omega_2$ (rad/sec) | $\delta h_{ssa}$ (m) | $\sigma_{\delta h,\text{ due to altimeter}}$ (m) |
|---|---|---|---|---|---|
| 0.001 | $5.0 \times 10^{-4}$ | 8000 | $3.32 \times 10^{-3}$ | 58800 | 800 |
| 0.01 | $5.0 \times 10^{-3}$ | 800 | $2.80 \times 10^{-3}$ | 588 | 165 |
| 0.1 | $5.0 \times 10^{-2}$ | 80 | $2.50 \times 10^{-2}$ | 5.88 | 151 |
| 1.0 | 0.5 | 8 | 0.25 | 0.06 | 150 |
| 10.0 | 5.0 | 0.8 | 2.5 | $\approx 0$ | 150 |

Table B.5: SELECTION OF $K_1$ FOR LP INS[4]

| $K_1$ | $\omega_1$ (rad/sec) | $\tau_{\omega 0}$ (sec) | $\omega_2$ (rad/sec) | $\delta h_{ssa}$ (m) | $\sigma_{\delta h}$ due to altimeter (m) |
|---|---|---|---|---|---|
| 0.001 | $5.0 \times 10^{-4}$ | 8000 | $3.32 \times 10^{-3}$ | 3920 | 1150 |
| 0.01 | $5.0 \times 10^{-3}$ | 800 | $2.80 \times 10^{-3}$ | 39 | 168 |
| 0.08 | $4.0 \times 10^{-2}$ | 100 | $2.00 \times 10^{-2}$ | 0.6 | 150 |
| 0.1 | $5.0 \times 10^{-2}$ | 80 | $2.50 \times 10^{-2}$ | 0.4 | 150 |
| 1.0 | 0.5 | 8 | 0.25 | $\approx 0$ | 150 |
| 10.0 | 5.0 | 0.8 | 2.5 | $\approx 0$ | 150 |

Table B.6: SELECTION OF $K_1$ FOR SP INS[5]

| $K_1$ | $\omega_1$ (rad/sec) | $\tau_{\omega 0}$ (sec) | $\omega_2$ (rad/sec) | $\delta h_{ssa}$ (m) | $\sigma_{\delta h}$ due to altimeter (m) |
|---|---|---|---|---|---|
| 0.001 | $5.0 \times 10^{-4}$ | 8000 | $3.32 \times 10^{-3}$ | 392 | 7 |
| 0.003 | $1.5 \times 10^{-3}$ | 2660 | $1.77 \times 10^{-3}$ | 44 | 2.7 |
| 0.01 | $5.0 \times 10^{-3}$ | 800 | $2.80 \times 10^{-3}$ | 4 | 3 |
| 0.06 | $3.0 \times 10^{-2}$ | 133 | $1.50 \times 10^{-2}$ | 0.1 | 6 |
| 0.1 | $5.0 \times 10^{-2}$ | 89 | $2.50 \times 10^{-2}$ | $\approx 0$ | 6 |
| 1.0 | 0.5 | 8 | 0.25 | $\approx 0$ | 6 |
| 10.0 | 5.0 | 0.8 | 2.5 | $\approx 0$ | 6 |

## B.8 White Noise Vector, $\underline{w}_n$

The vector $\underline{w}_n$ in Equation B.1 can be used to model the white noise component of gyro drift rate present in the laser gyros assumed for the M and LP INS. By thus modeling this component, three states are "saved", resulting in a state vector of smaller dimension.

This modeling technique is not used in the model described in this memo because it introduces complications in the simulation of transfer alignment (Subsection A.8). Consequently, in all cases considered here

$$\underline{w}_n = \underline{0}. \tag{B.24}$$

To model the white noise component present in the laser gyros, a first-order Markov error source is included in the vector $\underline{\varepsilon}$ of Equation B.1. The parameters for this Markov model are defined in the footnotes to Tables A.3 and A.4 which list the parameters for the M and LP INS error models.

[3]Conditions: Accelerometer bias = 1500 $\mu$g; Altimeter RMS level = 150 m; Altimeter Markov correlation time = 11 min at 2 Mach M velocity.

[4]Conditions: Accelerometer bias = 100 $\mu$g; Altimeter RMS level = 150 m; Altimeter Markov correlation time = 28 min at 0.8 Mach LP velocity.

[5]Conditions: Accelerometer bias = 10 $\mu$g; Altimeter RMS level = 6 m; Altimeter Markov correlation time = 30 sec.

# Appendix C

# REFERENCES

**Anderson, J.D., 1989.** Introduction to Flight, McGraw-Hill, New York, 1989.

**Barton, 1984.** Handbook of Radar Measurement, Artech House, Norwood, MA, 1984.

**Baziw, J., and Leondes, C.T., 1972a.** "In-Flight Alignment and Calibration of Inertial Measurement Units—Part I: General Formulation," IEEE Transactions on Aerospace and Electronic Systems, Vol. AES-8, No. 4, July 1972, pp. 439-449.

**Baziw, J., and Leondes, C.T., 1972b.** "In-Flight Alignment and Calibration of Inertial Measurement Units—Part II: Experimental Results," IEEE Transactions on Aerospace and Electronic Systems, Vol. AES-8, No. 4, July 1972, pp. 456-465.

**Britting, K.R., 1971.** Inertial Navigation Systems Analysis, Wiley, New York, 1971.

**Dole, C.E., 1981.** Flight Theory and Aerodynamics, Wiley, New York, 1981.

**Etkin, B., 1972.** Dynamics of Atmospheric Flight, Wiley, New York, 1972.

**Farrell, J.L., 1976.** Integrated Aircraft Navigation, Academic Press, New York, 1976.

**Foster, J.A., 1987.** Airborne Bistatic Radar Applications, M.S. Thesis, Department of Electrical and Electronic Engineering, Loughborough University of Technology, R.A.F. College Cranwell, U.K., 1987.

**Gelb, A., 1974.** Applied Optimal Estimation, M.I.T. Press, Cambridge, MA, 1974.

**Hovanessian, S.A., 1988.** Introduction to Sensor Systems, Artech House, Norwood, MA, 1988.

**Kayton, M., 1969.** "Inertial Navigation," in Kayton, M., and Fried, W.R., eds., Avionics Navigation Systems, Wiley, New York, 1969.

**Kuo, B.C., 1962.** Automatic Control Systems, Prentice-Hall, Englewood Cliffs, N.J., 1962.

**Levinson, E., 1978.** "Strapdown Inertial System Applications," in Schmidt, G.T., ed., North Atlantic Treaty Organization Advisory Group for Aerospace Research and Development, AGARD Lecture Series No. 95, June, 1978.

**Maybeck, P.S., 1976.** "Covariance Analysis of a Kalman Filter for a Conventional-Gyro Strapdown INS/Radiometric Area Correlator Guidance System," Air Force Institute of Technology Report AFIT-TR-76-14, July, 1976.

**Maybeck, P.S., 1977.** "Analysis of a Kalman Filter for a Strapdown Inertial/Radiometric Area Correlator Guidance System," Proceedings of the IEEE 1977 National Aerospace and Electronics Conference, NAECON '77, Dayton, OH, May 17-19, 1977, pp. 751-757.

**McCormick, B.W., 1979.** Aerodynamics, Aeronautics, and Flight Mechanics, Wiley, New York, 1979.

**Morchin, W.C., 1990.** Airborne Early Warning Radar Artech House, Norwood, MA, 1990.

**Morrison, R.F., and Levinson, E., 1977.** "The SLIC-7 Laser Gyro Inertial Guidance System," Proceedings of the IEEE 1977 National Aerospace and Electronics Conference, NAECON '77, Dayton, OH, May 17-19, 1977, pp. 1045ff.

**Mueller, C.E., Phelps, R.K., Scheidenhelm, R., 1977.** "Tactical Guidance Requirements for Strapdown Inertial," Proceedings of the IEEE 1977 National Aerospace and Electronics Conference, NAECON '77, Dayton, OH, May 17-19, 1977, pp. 433-440.

**Newton, G.C., Gould, L.A., and Kaiser, J.F., 1957.** Analytical Design of Linear Feedback Controls, Wiley, New York, 1957.

**Perlmutter, L.D., Kraemer, J.W., and Roessler, N.J., 1977.** "Strapdown Inertial Sensor Requirements for Tactical Guidance," Proceedings of the IEEE 1977 National Aerospace and Electronics Conference, NAECON '77, Dayton, OH, May 17-19, 1977, pp. 424-432.

**San Giovanni, C., 1977.** "Performance of a Differential Omega-Ring Laser Strapdown Aircraft Navigator," Proceedings of the IEEE 1977 National Aerospace and Electronics Conference, NAECON '77, Dayton, OH, May 17-19, 1977, pp. 1031-1043.

**Schmidt, G.T., 1978.** "Strapdown Inertial Systems—Theory and Applications Introduction and Overview," in Schmidt, G.T., ed., North Atlantic Treaty Organization Advisory Group for Aerospace Research and Development, AGARD Lecture Series No. 95, June, 1978.

**Singer, R.A., 1969.** "Estimating Optimal Tracking Filter Performance for Manned Maneuvering Targets," IEEE Transactions on Aerospace and Electronic Systems, Vol. AES-6, No. 4, July 1970.

**Skolnik, M.I., 1980.** Introduction to Radar Systems, McGraw-Hill, New York, 1980.

**Van Valkenburg, M.E., 1964.** Network Analysis, Prentice-Hall, Englewood Cliffs, N.J., 1964.